AD_____

GRANT NUMBER DAMD17-96-1-6047

TITLE: Macrocyclic Radiochelates for Antibody Imaging and Therapy of Breast Cancer

PRINCIPAL INVESTIGATOR: Michael R. Lewis, Ph.D.

CONTRACTING ORGANIZATION: Beckman Research Institute of the
City of Hope
Duarte, California 91010

REPORT DATE: June 1998

TYPE OF REPORT: Final

PREPARED FOR: Commander
U.S. Army Medical Research and Materiel Command
Fort Detrick, Frederick, Maryland 21702-5012

DISTRIBUTION STATEMENT: Approved for public release;
distribution unlimited

The views, opinions and/or findings contained in this report are those of the author(s) and should not be construed as an official Department of the Army position, policy or decision unless so designated by other documentation.

REPORT DOCUMENTATION PAGE

Form Approved
OMB No. 0704-0188

1. AGENCY USE ONLY *(Leave blank)*	2. REPORT DATE June 1998	3. REPORT TYPE AND DATES COVERED Final (1 Jun 96 – 31 May 98)

4. TITLE AND SUBTITLE
Macrocyclic Radiochelates for Antibody Imaging and Therapy of Breast Cancer

5. FUNDING NUMBERS
DAMD17-96-1-6047

6. AUTHOR(S)
Michael R. Lewis, Ph.D.

7. PERFORMING ORGANIZATION NAME(S) AND ADDRESS(ES)
Beckman Research Institute of the City of Hope
Duarte, California 91010

8. PERFORMING ORGANIZATION REPORT NUMBER

9. SPONSORING/MONITORING AGENCY NAME(S) AND ADDRESS(ES)
Commander
U.S. Army Medical Research and Materiel Command
Fort Detrick, Frederick, MD 21702-5012

10. SPONSORING/MONITORING AGENCY REPORT NUMBER

11. SUPPLEMENTARY NOTES

12a. DISTRIBUTION / AVAILABILITY STATEMENT
Approved for public release; distribution unlimited

12b. DISTRIBUTION CODE

13. ABSTRACT *(Maximum 200)*

See abstract in text, page iii.

19980722 074

14. SUBJECT TERMS Breast Cancer
Chelate Radiometal Antibody Radioimaging
Radioimmunotherapy Carcinoembryonic antigen

15. NUMBER OF PAGES
113

16. PRICE CODE

17. SECURITY CLASSIFICATION OF REPORT	18. SECURITY CLASSIFICATION OF THIS PAGE	19. SECURITY CLASSIFICATION OF ABSTRACT	20. LIMITATION OF ABSTRACT
Unclassified	Unclassified	Unclassified	Unlimited

Standard Form 298 (Rev. 2-89)
Prescribed by ANSI Std. Z39-18

ABSTRACT

Conjugation of bifunctional chelating agents allows monoclonal antibodies (mAbs) to be labeled with radiometals for delivery of diagnostic or therapeutic radiation to primary breast tumors or metastatic disease. Physiologically stable radiometal chelates, such as those of 1,4,7,10-tetraazacyclododecane N,N',N'',N'''-tetraacetic acid (DOTA), are desirable to reduce dose-limiting radiation toxicity to normal tissues. Two new classes of DOTA derivatives, maleimidocysteineamido-DOTA derivatives and hydrazido-DOTA derivatives, were synthesized and conjugated, respectively, to reduced interchain disulfide bonds and oxidized carbohydrate residues of the anti-carcinoembryonic antigen mAbs cT84.66 and ZCE025. Conjugates of cT84.66 prepared with maleimide derivatives of DOTA exhibited near-quantitative labeling with the imaging radiometal ^{111}In and the therapy radiometal ^{90}Y, quantitative immunoreactivity, and linker-specific cleavage reactions which were considerably faster at pH 7.4 than at pH 5.4. Biodistribution studies demonstrated that this property imparted favorable tumor uptake and normal tissue clearance to radiolabeled cT84.66. Conjugation of oxidized cT84.66 with hydrazido-DOTA resulted in extensive antibody aggregation and low radiometal labeling yields. Conjugation of oxidized ZCE025 with hydrazido-DOTA, carbohydrazido-DOTA, and hydrazidocysteineamido-DOTA was also unsuccessful. It is possible that modification of the ZCE025 conjugation procedure or use of a cT84.66 construct with a genetically engineered oligosaccharide will allow successful attachment and radiometal labeling of the hydrazido-DOTA derivatives.

FOREWORD

Opinions, interpretations, conclusions and recommendations are those of the author and are not necessarily endorsed by the U.S. Army.

_____ Where copyrighted material is quoted, permission has been obtained to use such material.

_____ Where material from documents designated for limited distribution is quoted, permission has been obtained to use the material.

_____ Citations of commercial organizations and trade names in this report do not constitute an official Department of Army endorsement or approval of the products or services of these organizations.

_____ In conducting research using animals, the investigator(s) adhered to the "Guide for the Care and Use of Laboratory Animals," prepared by the Committee on Care and use of Laboratory Animals of the Institute of Laboratory Resources, national Research Council (NIH Publication No. 86-23, Revised 1985).

_____ For the protection of human subjects, the investigator(s) adhered to policies of applicable Federal Law 45 CFR 46.

_____ In conducting research utilizing recombinant DNA technology, the investigator(s) adhered to current guidelines promulgated by the National Institutes of Health.

_____ In the conduct of research utilizing recombinant DNA, the investigator(s) adhered to the NIH Guidelines for Research Involving Recombinant DNA Molecules.

_____ In the conduct of research involving hazardous organisms, the investigator(s) adhered to the CDC-NIH Guide for Biosafety in Microbiological and Biomedical Laboratories.

PI - Signature   7 May 1998
                                                    Date

TABLE OF CONTENTS

INTRODUCTION

Radioimmunoconjugates are monoclonal antibodies (mAbs) that target tumor-associated antigens and are modified chemically to carry medically useful radionuclides for imaging and therapy of malignant disease (*1*). Although a large number of radionuclides are available for antibody labeling, most efforts to date have focused on the use of radioiodines such as ^{131}I. However, the utility of ^{131}I is limited by its metabolism and emission characteristics. Most radionuclides are metals, and the conjugation of radiometal complexes to antibodies represents a more versatile strategy for selective delivery of appropriate diagnostic or therapeutic radiation to primary tumors or metastatic disease. This versatility stems from the variety of metallic radionuclides available, encompassing a range of coordination chemistries, half-lives, and radioemissions suitable for both imaging and therapy. Generally, pure photon emitters are favored for imaging and pure particulate emitters are favored for therapy. Radiometals such as ^{111}In(III), ^{67}Ga(III), and ^{99m}Tc(V) have physical properties which are well suited for tumor imaging with mAbs, while ^{90}Y(III), ^{67}Cu(II), ^{186}Re(V), and ^{177}Lu(III) have cytotoxic properties which can be exploited for therapy by antibody-directed tumor targeting (*2-6*).

Labeling of monoclonal antibodies with radioactive metals has typically been accomplished by the use of bifunctional chelating agents (BCAs), which contain both a reactive functionality for covalent attachment to proteins and a multidentate metal-binding ligand (*2, 3, 7*). The metal-binding chelating agent is composed of oxygen, nitrogen, or sulfur atoms that coordinate to metal ions in extremely stable complexes. The second functional component is designed to react with endogenous or introduced functional sites on the mAb.

Chelating agents which form physiologically stable complexes are desirable for radioimmunoscintigraphy (RIS) and radioimmunotherapy (RIT) in order to reduce radiation damage and toxicity to normal organs and tissues attributable to uptake of the free radiometal (*8*). For example, ^{90}Y localizes to bone by an unknown mechanism. Uptake of ^{90}Y approaching 20% of the injected dose per gram (% ID/g) of bone was seen when the ionic form was administered to

1

mice (9). Since bone marrow is an organ at risk in cancer radiotherapy, the dissociation of the radiometal ion from the antibody-conjugated chelate must be evaluated *in vitro* under physiological conditions and *in vivo* in animal models prior to the initiation of human clinical trials. The stability of the conjugated radiometal complex will depend upon the type of BCA used. In addition, the versatility of chelate conjugation chemistry introduces the potential of optimizing several other important properties in the resulting mAb conjugates, including radiolabeling efficiency, specific activity, immunoreactivity, and immunogenicity.

Considerable progress has been made in the conjugation of bifunctional chelating agents to antibodies, beginning with ethylenediaminetetraacetic acid (EDTA) derivatives (*10*) and leading to progressively more stable mAb-radiometal conjugates modified with derivatives of diethylenetriaminepentaacetic acid (DTPA) (*11-17*) and polyazamacrocyclic chelating agents (*18-37*). Each generation of improvements has produced bifunctional radiometal chelates with greater thermodynamic, kinetic, and physiological stability, as well as more versatile chemistry for attachment to antibodies. However, the costs of these improvements have been progressively elaborate synthetic schemes to generate BCAs and increased difficulty in labeling the resulting mAb conjugates with radiometals.

Radionuclides for Tumor Imaging and Therapy

A primary consideration for choosing suitable radionuclides for imaging and therapy is their availability. Because many radionuclides are not available with the appropriate purity, specific activity, or attachment chemistry, it is not surprising that the earliest work in this field focused on radiolabeling antibodies with iodine isotopes such as [131]I. Complications in the use of radioiodinated antibodies include their rapid metabolism by certain tissues, including the liver, and the resulting rapid redistribution or elimination of radioiodine. In addition, dehalogenation in the tumor leads to lower accumulations of radioactivity in the tumor. Therefore, therapeutic amounts

of ^{131}I must be in a range posing considerable hazard to personnel, and these problems have prompted a search for other radionuclides with more desirable properties.

Selection criteria for radionuclides used in antibody-directed tumor imaging and therapy are based on their half-lives, radioemissions, availability, chemical and biological stability, and ease of attachment to the mAb (2-5). The physical half-life of the radionuclide should correspond to the biological half-life of the antibody. Whole antibodies typically have a biological half-life of 24-48 h; therefore, radionuclides with 24-72 h half-lives have been popular for mAb applications. Smaller antibody fragments are often cleared with *in vivo* half-lives of 2-12 h, and radionuclides with shorter half-lives (6-14 h) can be used in those cases.

For tumor imaging, radionuclides with gamma or positron emissions only are preferred, while for tumor therapy, beta-emitting radionuclides are commonly employed. In the case of clinical RIT, an imageable photon must be emitted along with the particulate radiation in order that absorbed dose be estimated. Thus, two radiolabels are used for RIT in many situations. One gamma- or positron-emitting label must be suitable for the imaging or therapy planning situation, and the second, essentially of a particulate type, provided for the subsequent treatment(s). If the particulate emitter has no associated photon suitable for imaging, the provision of a imaging label becomes a necessity for dose estimation.

Given that two labels must be used for RIT with pure particulate emitters, it is important to demonstrate that variation of the radionuclide has minimal and predictable impact upon the pharmacokinetics of the radiolabeled mAb. Once this has been demonstrated, an imaging sequence can be used to plan and document patient RIT treatments. Biodistributions in an animal model of human cancer can be used to show the variation of organ uptake with a change in the radionuclide coupled to the mAb. Radiometals offer a versatile approach to the use of dual labels for imaging/dosimetry and therapy, respectively. The wide variety of metallic radionuclides has provoked widespread interest in identifying radiometals with useful imaging and therapeutic properties.

From the earliest discussions of therapeutic efficacy, ^{90}Y(III) has been described as a possible RIT radionuclide (*4*). Its pure, high energy beta (range 1.1 cm) leads to the clinical advantage of cross-fire capability, which is the ability to treat tumor cells distant from those to which the radioimmunoconjugate has localized. Generally the corresponding gamma-emitter ^{111}In(III) has been used for imaging and dosimetry applications in ^{90}Y therapy. Both trivalent metals can be attached to mAbs using the same bifunctional chelating agent. Indium-111 emits two gamma photons at 171 and 247 keV, energies that are efficiently detected with commercial Anger cameras.

Radiometal Ion Complexes for Antibody Conjugation

Derivatives of the macrocyclic chelating agent 1,4,7,10-tetraazacyclododecane *N,N',N'',N'''*-tetraacetic acid (DOTA) are attractive candidates for RIS and RIT applications. DOTA possesses a relatively rigid, preorganized cavity which enables it to bind a large number of main group and transition metal ions with extremely high stability constants (*38-43*). However, the adverse consequences of this structural property are the slow rate of incorporation of the metal ion into the chelate complex (*44*) and effective competition for the ligand by trace metals (*41*). The use of radiometal labeling procedures which have been established for mAbs conjugated to other chelating agents often results in low radiochemical yields when applied to mAb-DOTA conjugates (*45*). For example, Meares reports 50% incorporation of ^{88}Y(III) (a pure gamma-emitting isotope) into an antibody-DOTA conjugate after a 2 h incubation at room temperature (*25*), a result which at the time represented the highest efficiency Y(III) radiolabeling of a macrocycle-antibody conjugate. In order to utilize carrier-free radiometal solutions and minimize radiation damage to the protein, the formation of the radiolabeled immunoconjugate should be rapid and efficient.

Physical studies on the mechanism of chelation by DOTA have shown that for many metals the process proceeds by two steps (*46, 47*). The first step is the rapid, reversible formation of a loosely associated ligand-metal adduct (a type I complex, $K_{eq} = 10^2$-10^3 M^{-1}). The second step is a

slower, essentially irreversible incorporation of the metal ion into the final chelate structure (type II complex, $k_f = 10^{-3}$-10^2 s^{-1}; $k_{obs} = 10^{-1}$-10^5 M^{-1}s^{-1}). Elaborating on this concept, the low radiochemical yields observed for labeling of mAb-DOTA conjugates, compared to free ligand, may be a result of competition between nonspecific metal-binding sites on the protein surface and formation of the type I complex, making this the rate-limiting step in the radiolabeling reaction.

At least four strategies are available to improve the formation of type I complexes in the radiometal labeling of antibody-DOTA conjugates. The strategies are: 1) to use linkers to space the chelating agent away from the protein surface, 2) to optimize several important radiometal labeling parameters such as temperature, pH, and buffer conditions, 3) to augment or replace the carboxyl groups of DOTA with functional groups that promote the formation of tighter type I complexes, and 4) to attach the chelator to a specific hydrophilic and/or solvent-accessible domain of the protein. Individually or in conjunction, these strategies may allow the chelator to be exposed to a higher local concentration of radiometal, shifting the equilibrium toward formation of the type I complex. All strategies retain the macrocyclic structure of DOTA, which preserves the extremely high *in vivo* stability of the type II complex.

Chelate-Antibody Linker Systems

The major normal tissues which usually show considerable uptake of radiolabeled antibodies are blood (which contributes to dose-limiting bone marrow toxicity), liver, and, in the case of mAb fragments, kidney (*48, 49*). In efforts to improve the biodistribution and normal tissue uptake properties of radioimmunoconjugates, several groups have inserted linkers with biochemical and/or metabolic activity between the radiometal chelate and the antibody. To date, most of these "metabolizable" linkers have contained disulfide, ester, or oligopeptide groups. This strategy generally requires that the radiolabeled mAb be internalized into normal cells, such as liver or kidney, so that the metabolically active linker can be degraded in the lysosomal compartment. It

is anticipated that the released radiometal chelate will clear rapidly from these tissues, and subsequently the body, through the biliary or renal systems.

In order for improvements to be made in tumor to normal tissue ratios, some difference in uptake and/or metabolism between the two tissues must be exploited. When BCAs are coupled to mAbs through an amide linkage, proteolysis in the lysosomal compartment usually results in the generation of an adduct of a single amino acid and the radiometal chelate as the final metabolite (50-52). Often this type of metabolite is not recognized by amino acid transporter mechanisms and is released very slowly from cells (53, 54). Typically it is recovered intact in urine and feces. Thus, for a metabolically labile linker to be useful in decreasing normal tissue uptake, it must not only be released quickly from the mAb, but also must generate a metabolite that is cleared rapidly from normal cells.

Differential effects on biodistribution have been observed when different linkers have been inserted between the radiometal chelate and the antibody. Meares *et al.* (55) obtained increased whole body clearance and reduced liver accumulation of ^{111}In in BALB/c mice using an EDTA derivative conjugated to the anti-lymphoma mAb Lym-1 via a disulfide linkage. More recently, Li and Meares reported the conjugation of a peptide-linked DOTA derivative to Lym-1 (35). The peptide linker in this conjugate was designed to be a substrate for the liver enzymes cathepsin B and cathepsin D. Cathepsin B cleaved the [114m]In chelate from the antibody efficiently *in vitro* by hydrolyzing the peptide bond before the phenylalanine residue in the linker. However, no cleavage of the peptide linker was observed upon incubation with cathepsin D for 7 days. It was concluded from these studies that this peptide linker was not an optimal substrate for the cathepsins, prompting a search for sequence-specific linkers with high cathepsin activity.

Paik *et al.* (56) used the diester ethyleneglycol*bis*(succinimidylsuccinate) to attach DTPA to the anti-melanoma mAb 96.5. Compared to the conjugate containing an amide linkage to DTPA, this derivative produced faster blood, liver, kidney, spleen, and whole body clearance of the ^{111}In-labeled mAb in a nude mouse xenograft model. Tumor uptake was retained for the conjugate with the metabolizable linker, and a 2- to 3-fold increase in tumor to normal tissue ratios was observed

6

at 48 h. The use of ester-containing linkers may have even more important effects on uptake of antibody fragments. Weber *et al.* (*57*) obtained a 2-fold increase in kidney clearance, compared to an amide-linked BCA, for a ^{99m}Tc-labeled Fab' conjugate. However, Arano and coworkers (*58*), using a stable ^{131}I label conjugated to a Fab fragment via a labile ester linkage, had a less satisfactory result. These authors concluded that tumor uptake and radioimmunotherapy would be hindered because cleavage of the ester bond in plasma and blood clearance were too rapid, resulting in decreased tumor uptake.

Carcinoembryonic Antigen as a Target for Radiolabeled Antibody-Mediated Breast Tumor Imaging and Therapy

For targeting purposes, the ideal tumor-associated antigen is expressed to a high degree of probability and density on the surface of tumor cells, in contrast with low expression or accessibility in normal tissue. Furthermore, the tumor antigen should not be released into circulation. The monoclonal antibody that targets this antigen should display high affinity ($>10^8$ M^{-1}), rapid *in vivo* distribution, and high levels of tumor accretion, without crossreactivity in normal tissue. Effective tumor penetration, an optimum rate of blood clearance sufficient for high tumor uptake, and internalization into tumor cells upon antigen binding are also desirable properties for an antitumor antibody.

Carcinoembryonic antigen (CEA) is one of the best characterized antigens associated with solid tumors, and anti-CEA antibodies have been widely and successfully used for cancer diagnosis, tumor imaging, and tumor therapy. CEA was first described by Gold and Freedman in 1965 (*59*) as a 180 kDa antigen expressed in the fetal colon and colonic cancer. It was subsequently demonstrated that CEA is expressed and found only in low levels in a limited number of normal adult tissues and in serum. In the normal colon, CEA is expressed only on the lumenal side at the apical portions of the epithelium. This results in very little or no CEA entering into the circulatory system (<5 ng/mL). However, in colorectal adenocarcinoma CEA is overexpressed

7

and is not shed in the lumen of the colon. This often leads to elevated serum CEA levels that serve as a marker for colonic cancer. Over 90% of colorectal carcinomas express high levels of CEA, with over 95% of all cells positive by immunohistochemistry in well-differentiated colon cancer (*60*). In addition, high percentages of cells overexpress CEA in medium and poorly differentiated colorectal tumors.

CEA is also expressed in high levels in other tumors of epithelial origin, including over 50% of breast and lung cancers (*61*). The complete absence of CEA in normal breast tissue was established by immunohistochemistry with CEA-specific monoclonal antibodies (*62*). On the other hand, CEA is expressed in 56% of breast tumors, with greater than 15% of the cells positive by immunohistochemistry. CEA-positive breast cancer cells appear to regulate expression of the antigen differentially, with most cells expressing CEA at some point during the cell cycle, especially when terminally differentiated. In the case of breast carcinomas, CEA is found at elevated levels in the plasma of 60% of patients (*63*); however, these levels are not high enough to interfere with antibody-directed radioimaging. CEA is, therefore, an excellent candidate for tumor targeting in the course of diagnostic imaging and radiotherapy with mAbs. A human/murine chimeric monoclonal antibody, cT84.66, that displays high specificity and high affinity (10^{10} M^{-1}) for CEA (*64*) has been produced at City of Hope and is currently being used in clinical imaging and Phase I therapy trials.

Tumor Imaging and Therapy with Radiometal-Labeled cT84.66

The human/murine chimeric anti-CEA mAb cT84.66 has been conjugated with a benzylisothiocyanate derivative of DTPA, labeled with ^{111}In and ^{90}Y, and evaluated in athymic nude mice bearing CEA-expressing LS174T human colorectal carcinoma xenografts (*65*). In this system, tumor accumulation of the ^{111}In-labeled mAb was approximately 70% ID/g at 48 h, and the corresponding value for ^{90}Y was 50% ID/g. For both radiometals, liver uptake of the radiolabeled conjugate was approximately 7% ID/g, and bone uptake was limited to 2.5% ID/g, after 48 h.

Comparison of ^{111}In-labeled cT84.66-DTPA to ^{131}I-labeled ZCE025, a murine anti-CEA mAb, revealed that the higher photon emission of ^{111}In rendered cT84.66 a superior imaging agent. It has also been shown that the ^{111}In-labeled cT84.66-DTPA conjugate provides good tumor localization in a nude mouse model bearing MCF-7 breast tumor xenografts (66). In that study, tumor uptake was 15.0% ID/g at 48 h, compared to 6.3% ID/g in the liver, and at 144 h the tumor to blood ratio was 2.74. These experiments provided excellent tumor images as early as 24 h.

Clinical imaging trials of ^{111}In-labeled cT84.66-DTPA (67) demonstrated that the positive predictive value of this agent was 81.4%, despite the fact that all hepatic lesions were observed as photopenic and thus were counted as negative results. With the exception of one patient who developed an anti-cT84.66 response, no side effects were seen. Dose escalation of unlabeled antibody prior to administration of the ^{111}In dose did not produce any significant differences in sensitivity of imaging. While most anti-CEA antibody imaging trials have focused on colorectal cancer, several trials have been directed at breast or lung cancer. Riva *et al.* (68) found 74-79% sensitivity for detection of breast cancer lesions with [131]I- or ^{111}In-labeled anti-CEA F(ab')$_2$ fragments. Lind *et al.* (69) showed 83% sensitivity for detection of primary breast tumors or axillary metastases with a ^{99m}Tc-labeled anti-CEA Fab' fragment.

At City of Hope, therapy studies on nude mice with subcutaneous LS174T human colorectal carcinoma xenografts (70) showed that a single dose of 120 μCi of ^{90}Y-labeled cT84.66-DTPA caused a 95% decrease in tumor size over a period of 2 to 3 weeks, with a 300% increase in survival. A lag in tumor growth corresponding to a three-log cell kill (71) was obtained in mice receiving 120 μCi of ^{90}Y-labeled mAb. Complete cures were obtained in this model when the dose was increased to 200-300 μCi, but the animals required bone marrow transplant support to offset myelosuppression (72). Studies performed with the nude mouse MCF-7 breast tumor xenograft model, again using 120 μCi of ^{90}Y-labeled cT84.66-DTPA, showed a 12-fold inhibition of tumor growth compared to untreated control animals (66).

Our group has evaluated ^{90}Y-labeled cT84.66-DTPA in patients with metastatic CEA-producing malignancies in a dose-escalation Phase I trial. Initial results of this trial (73) indicated

that the radioimmunoconjugate localized effectively to CEA-producing tumors and nonhepatic metastases without side effects. However, a significant variation among patients in the clearance rate of antibody and CEA-antibody complexes from blood to liver was seen. This resulted in a reciprocal relationship between estimated liver and red marrow doses. In addition, 2 of 3 patients receiving multiple administrations of radiolabeled mAb developed a human anti-chimeric antibody response. Because the cT84.66-DTPA conjugate had exhibited some loss of ^{90}Y and bone uptake in the animal model (65), all patients required a prophylactic infusion of calcium DTPA to prevent skeletal accumulation of ^{90}Y.

Further improvements in RIT of solid tumors will likely occur in an adjuvant setting or in the treatment of microscopic or occult disease. Such improvements will probably require the use of radiolabeled antibodies with lower immunogenicity, higher tumor uptake, faster blood clearance, better tumor to blood ratios, and less dose to the bone marrow, the dose-limiting organ. In this respect, support with autologous bone marrow transplantation and/or stem cell growth factors is encouraging, as is the development of antibody conjugates carrying radiometal chelates with greater *in vivo* stability and significantly reduced deposition of the radionuclide in bone and bone marrow.

This Report

This report describes the investigation of all four of the strategies described above for improving radiometal labeling by antibody-DOTA conjugates: 1) the use of chelate-antibody linker systems, 2) the optimization of radiometal labeling conditions, 3) the introduction of functional groups to augment the formation of type I complexes, and 4) the site-specific conjugation of the chelator to hydrophilic and/or solvent-exposed domains of mAbs. The new bifunctional DOTA derivatives described here have been prepared by simplified synthetic routes that take advantage of water-soluble chemistry and circumvent the need for lengthy sequences of protection and

deprotection reactions. The methods of synthesis and conjugation presented here could be applied to any of the polyazamacrocyclic polycarboxylate chelating agents.

The synthesis and evaluation of DOTA derivatives for site-specific conjugation to oxidized antibody carbohydrate residues and reduced hinge region disulfide bonds, respectively, is described. The reagents for site-specific conjugation also incorporate additional structural features such as "pendant-type" carboxyl groups and variable chelator-antibody linker lengths. In addition, as part of an NIH-funded research program at City of Hope, personnel in the Department of Radioimmunotherapy have obtained the biodistributions of two new mAb-DOTA conjugates in an animal model of human cancer.

The *in vitro* and *in vivo* evaluation of mAb conjugates prepared with maleimidocysteineamido-DOTA derivatives are described in this report. The studies revealed that selection of linker systems with inherent chemical lability in the bloodstream and other normal tissues may have distinct biodistribution advantages. These advantages can be realized provided that the blood clearance kinetics are sufficiently slow as to allow high tumor uptake and an increase in the tumor to blood ratio. While these two objectives may seem to be mutually exclusive, they can both be realized if the majority of tumor uptake occurs relatively early, in the first 24-48 h, and the linker system displays differential stability between tumor and normal tissue. Furthermore, chemically labile linker systems, such as those employed by the maleimidocysteineamido-DOTA derivatives, may have important implications for the biodistribution of radiometal-labeled mAb fragments and bioengineered antibody constructs.

EXPERIMENTAL PROCEDURES

General. The mAb cT84.66 was prepared as described previously (*64*), and the mAb ZCE025 was obtained from Hybritech. DOTA internal salt and trisodium salt were purchased from Parish Chemical Co. (Orem, UT). Sulfo-NHS, EDC, triethylamine (Sequanal Grade), and BMH were purchased from Pierce. EMCH was purchased from Molecular BioSciences, Inc.

11

(Huntsville, AL). Purified human serum albumin (99%, fatty acid and globulin free) and L-cysteine were purchased from Sigma. DTPA was purchased from Fluka. EDTA, isobutyl chloroformate, hydrazine monohydrochloride, anhydrous hydrazine, carbohydrazide, *tert*-butyl carbazate, sodium periodate, 1,3-diaminopropan-2-ol, cobalt powder (99.995%), yttrium chloride hexahydrate (99.999%), and Oxone® (potassium hydrogen persulfate) were purchased from Aldrich. Ethylene glycol was obtained from Baker. Human serum albumin (25% (w/v), USP) was obtained from Armour Pharmaceutical Co. Normal saline (0.9% sodium chloride, injection, USP) was purchased from American Regent Laboratories, Inc. and Baxter Healthcare Corp. Sodium bicarbonate, dibasic potassium phosphate, sodium citrate, and citric acid were purchased from Mallinckrodt. Chelex® 100 (Biotechnology Grade, 100-200 mesh, sodium form) was obtained from Bio-Rad. Glacial acetic acid (Optima) was purchased from Fisher. All buffers used for radiolabeling reactions were passed over a Chelex® 100 column (1 × 15 cm). Ultrapure water (18 MΩ-cm) was used for all procedures, and all other reagents were of the highest purity available. ^{111}InCl$_3$ was obtained from Amersham, and ^{90}YCl$_3$ was obtained from Nordion and Hanford. ^{57}CoCl$_2$ and Na^{131}I were obtained from ICN. All laboratory glassware was washed with a mixed acid solution (*74*) and thoroughly rinsed with ultrapure water.

HPLC was performed at room temperature on a Beckman System Gold chromatograph or a Spectra-Physics system (SP8800 pump, SP4400 ChromJet integrator, *WIN*ner/386™ data acquisition system). The columns, solvent systems, and gradients used are described below. UV detection was accomplished at 214 nm or 280 nm using a Shimadzu SPD-6A or Spectra-Physics Spectra 100 detector. Radioactivity detection was accomplished using a Technical Associates PRS-5 analyzing miniscaler/ratemeter. TLC was performed on EM Science plastic-backed silica gel plates (Kieselgel 60 F$_{254}$, 0.2 mm layer thickness), using 10% (w/v) aqueous ammonium acetate (Fisher HPLC Grade):methanol (1:1) as the mobile phase. Radiation counting of TLC plates was performed with a Packard Cobra™ Auto-Gamma® Model 5003 counting system or with a Beckman LS 6000IC liquid scintillation counter.

Laser desorption mass spectra were recorded on a Kratos Kompact MALDI III spectrometer, using α-cyano-4-hydroxycinnamic acid as the matrix. Low mass MALDITOF mass spectra were recorded in reflectron mode and calibrated using a synthetic peptide (TQLPNEVDA, m/z = 1009.04 $(M+Na)^+$) as an external standard. Electrospray mass spectra were recorded on a Finnigan LCQ ion trap mass spectrometer equipped with a custom nanospray interface built at City of Hope. The mass spectrometer was operated under manual control with the automatic gain control active. In a few cases, manual control of the ion injection time was utilized to improve the quality of weaker product ion spectra. NMR spectra were recorded at pH 2.6 (not corrected for the deuterium isotope effect) on a Varian Unity spectrometer, operating at 300 MHz for ^{1}H and 75 MHz for ^{13}C, or a Varian Unity Plus spectrometer, operating at 500 MHz for ^{1}H and 125 MHz for ^{13}C. ^{1}H chemical shifts are reported relative to the monoprotonated solvents (HOD, 4.80 ppm, $CD_3(SO)CD_2H$, 2.50 ppm), and ^{13}C chemical shifts are reported relative to 1,4-dioxane (66.66 ppm) as an internal reference. Concentrations of antibody were determined by UV spectrophotometry, measuring the absorbance at 280 nm (A_{280} at 1 mg/mL = 1.42, within 5% of the concentration determined by amino acid analysis). UV measurements were obtained on a Pharmacia LKB Ultrospec III spectrophotometer, using a 1-cm sample cell.

Cysteineamido-DOTA (1). To a solution of 100 mg (213 µmol) of trisodium DOTA and 92.3 mg (425 µmol) of sulfo-NHS in 1 mL of H_2O was added dropwise with continuous stirring a solution of 81.5 mg (425 µmol) of EDC in 151 µL of H_2O. The reaction mixture was stirred at room temperature for 1 h, after which a solution of 51.5 mg (425 µmol) of L-cysteine in 326 µL of H_2O was added dropwise with continuous stirring. The pH was adjusted to 7.0 with 50% NaOH, and the reaction mixture was stirred at room temperature for 22 h. The reaction mixture was then cooled to 4 °C, made 1 M in HCl with the addition of 155 µL of conc HCl, and stirred at 4 °C for 17 h. The acidified mixture was applied to a Dowex AG50W-X8 column (H^+ form, 1 × 6.5 cm), which was washed with 50 mL of H_2O and then eluted with a 40-mL step gradient from 0.5 M to 4 M NH$_4$OH. A mixture of the desired product, disubstituted cysteine adducts of DOTA, and unreacted DOTA eluted in 2 M NH$_4$OH and was lyophilized to a pale

13

yellow gum. The crude product was dissolved in 1 mL of H_2O and applied to a Dowex AG1-X4 column (HCO_2^- form, 1 × 11 cm), which was washed with 50 mL of H_2O and eluted with a 60-mL step gradient from 0.05 M to 2 M HCO_2H. Unreacted DOTA eluted in 0.2 M HCO_2H, and the desired product eluted in 0.5 M HCO_2H. These fractions were lyophilized to give white powders, which were dissolved in 1 mL of H_2O and concentrated to dryness by lyophilization. This process was repeated four times to remove residual HCO_2H. This procedure afforded 25.2 mg (29.3%) of DOTA, which was recrystallized from H_2O:CH_3OH (1:9) and used for other syntheses, and 23.3 mg (21.6%) of **1** as a white powder. ^1H NMR (D_2O) δ 2.93-3.06 (m, 2H), 3.16-3.24 (m, 8H), 3.42 (m, 8H), 3.56-3.71 (m, 2H), 3.84 (s, 6H), 4.56 (dd, 1H); ^{13}C NMR (D_2O) δ 25.42, 48.61, 50.97, 53.53, 54.41, 55.42, 56.16, 170.50, 173.71, 174.63; FAB MS m/z calcd for $C_{19}H_{34}N_5O_9S$ $(M + H)^+$ = 508.2077, found 508.2098.

Maleimidocysteineamido-DOTA (2). To a solution of 29.2 mg (106 μmol) of 1,6-*bis*-maleimidohexane in 1.0 mL of degassed *N,N*-dimethylformamide, under an argon atmosphere, was added dropwise with continuous stirring a solution of 5.4 mg (10.6 μmol) of **1** in 1.9 mL of degassed 50 mM K_2HPO_4, pH 7.5. The reaction mixture was stirred at room temperature for 2 h, after which it was extracted with 3 × 15 mL of ethyl acetate. The pH of the aqueous layer was adjusted to 1.5 with trifluoroacetic acid, and the desired product was purified by reversed phase HPLC using a 10 × 250 mm column (Vydac™ Protein & Peptide C_{18}, 5 μm, 300 Å), a flow rate of 4.0 mL/min, and a linear gradient from 0% to 60% solvent B (solvent A, 0.1% TFA; solvent B, 0.1% TFA/90% CH_3CN) in 60 min. The major peaks, eluting at retention times of 26.8 min and 27.2 min, were collected, pooled, and lyophilized to give 2.0 mg (24.5%) of **2** as a white powder. ^1H NMR (D_2O) δ 1.25 (m, 4H), 1.53 (m, 4H), 2.69 (dt, 2H), 3.01-3.49 (m, 23H), 3.66 (br s, 2H), 3.81 (br s, 6H), 4.08 (m, 1H), 6.81 (s, 2H); ^{13}C NMR (D_2O) δ 25.47, 26.58, 27.55, 30.00, 35.83, 36.27, 37.55, 39.09, 39.87, 48.27, 48.86, 50.77, 51.56, 52.58, 134.34, 173.50, 174.23, 178.69, 179.82, 180.88; FAB MS m/z calcd for $C_{33}H_{50}N_7O_{13}S$ $(M + H)^+$ = 784.3187, found 784.3205. A 5-μg aliquot of the product was reinjected onto the HPLC, using a 4.6 × 250 mm column (Vydac™ Protein & Peptide C_{18}, 5 μm, 300 Å), a flow rate of 1.0

mL/min, and a linear gradient from 0% to 60% solvent B (solvent A, 0.1% TFA; solvent B, 0.1% TFA/90% CH_3CN) in 60 min. Two peaks were observed at retention times of 26.5 min (peak area 49.5%) and 26.8 min (peak area 50.5%). The two peaks gave identical mass spectra and presumably represent diastereomers of the product.

Maleimidosulfonylcysteineamido-DOTA (3). A solution of 2.0 mg (2.6 µmol) of **2** in 0.4 mL of H_2O was cooled to 0 °C, and 10.2 µL (2.4 mg, 3.8 µmol) of a 23% (w/w) solution of Oxone® in H_2O was added with continuous stirring. The reaction mixture was then stirred at room temperature for 4 h, after which 1.0 mg (5.1 µmol) of sodium metabisulfite in 15.2 µL of H_2O was added. The reaction mixture was stirred for 30 min at room temperature, and the desired product was purified by reversed phase HPLC using a 10 × 250 mm column (Vydac™ Protein & Peptide C_{18}, 5 µm, 300 Å), a flow rate of 4.0 mL/min, and a linear gradient from 0% to 60% solvent B (solvent A, 0.1% TFA; solvent B, 0.1% TFA/90% CH_3CN) in 60 min. The major peak, eluting at a retention time of 25.8 min, was collected and lyophilized to afford 1.0 mg (48.1%) of **3** as a white powder. ^1H NMR (D_2O) δ 1.26 (m, 4H), 1.55 (m, 4H), 3.12-3.84 (m, 13H), 3.27 (s, 5H), 3.49 (t, 6H), 3.55 (t, 6H), 4.07-4.11 (m, 2H), 4.24-4.30 (m, 2H), 6.82 (s, 2H); ^{13}C NMR (D_2O) δ 25.33, 26.40, 27.58, 30.34, 35.69, 36.54, 37.56, 38.78, 39.43, 47.88, 48.65, 51.52, 52.38, 53.09, 134.35, 170.15, 171.02, 172.47, 173.48, 176.51; FAB MS m/z calcd for $C_{33}H_{50}N_7O_{15}S$ $(M + H)^+ = 816.3086$, found 816.3051. A 5-µg aliquot of the product was reinjected onto the HPLC, using a 4.6 × 250 mm column (Vydac™ Protein & Peptide C_{18}, 5 µm, 300 Å), a flow rate of 1.0 mL/min, and a linear gradient from 0% to 60% solvent B (solvent A, 0.1% TFA; solvent B, 0.1% TFA/90% CH_3CN) in 60 min. A single peak was observed at a retention time of 25.7 min.

Preparation of cT84.66-MCDOTA and cT84.66-MSCDOTA Conjugates. An aliquot of 21.5 mg of cT84.66 in 2 mL of PBS, pH 7.4, was dialyzed against 1 L of PBS/20 mM DTPA, pH 7.4, for 24 h at 4 °C and then against 1 L of PBS, pH 7.4, over Chelex® 100, for 43.5 h at 4 °C, with one buffer change. To 17.2 mg (115 nmol) of cT84.66 in 2.05 mL of PBS, pH 7.4, was added 230 µL (2.30 µmol) of freshly prepared 10 mM DTT in degassed H_2O. The

reaction mixture was incubated at 37 °C for 3 h under an argon atmosphere, after which it was applied in equal volumes to 4 1-mL Sephadex G-25-50 spin columns. The mAb was eluted from the spin columns by centrifugation (*10*) at 1200 rpm for 2 min under argon. The eluents were pooled and the volume, concentration, and sulfhydryl titer of the reduced mAb solution were measured. Then to 4.68 mg (31.2 nmol) of reduced cT84.66 was added 245 µg (312 nmol) of **2** in 49.0 µL of degassed H_2O, and to 4.38 mg (29.2 nmol) of reduced cT84.66 was added 240 µg (294 nmol) of **3** in 48.0 µL of degassed H_2O. The reaction mixtures were incubated on a tube rotator under an argon atmosphere for 1.5 h at room temperature, after which they were dialyzed against 1 L of 0.25 M ammonium acetate/20 mM DTPA, pH 7.0, for 24 h at 4 °C. The conjugates were then dialyzed against 1 L of 0.25 M ammonium acetate, over Chelex® 100, for 138 h at 4 °C, with five buffer changes. Typical mAb recoveries ranged from 72% to 79% for the conjugation procedure.

Alternatively, preparations of cT84.66-MCDOTA and cT84.66-MSCDOTA were alkylated at unreacted cysteine residues with iodoacetic acid. After reaction with **2** or **3**, 100 µL (10 µmol) of freshly prepared 100 mM iodoacetic acid in degassed 0.2 M ammonium bicarbonate/1 mM EDTA, pH 8.4, was added. The reaction mixtures were incubated on a tube rotator in the dark under an argon atmosphere for 1 h at room temperature, and the carboxymethylated conjugates were then dialyzed as described above.

Radiolabeling of cT84.66-MCDOTA and cT84.66-MSCDOTA. The cT84.66-MCDOTA conjugate was labeled with the radiometals [111]In(III) and [90]Y(III), and the cT84.66-MSCDOTA conjugate was labeled with [111]In(III) only. In a typical [111]In(III) labeling reaction, 1.00 mCi of [111]InCl_3 in 68 µL of 0.04 *N* HCl was added to 110 µL of 0.25 M ammonium acetate, pH 5.7, followed by an aliquot of 0.2 mg of the mAb conjugate in 44 µL of 0.25 M ammonium acetate, pH 7.0. The reaction mixture was incubated at 43 °C for 45 min, after which the solution was made 1 mM in EDTA with the addition of 24 µL of 10 mM EDTA, pH 6.5. The reaction mixture was incubated at 37 °C for 15 min, and then the ^{111}In-labeled antibody was purified by size exclusion HPLC using a TosoHaas TSKgel® G2000 SW column (10 µm, 7.5 × 300 mm) and an

isocratic mobile phase of normal saline at a flow rate of 0.5 mL/min. The mAb peak, eluting at a retention time of 8.3 min, was collected in 0.5-mL fractions containing 1 drop of 25% (w/v) HSA each.

In a typical ^{90}Y labeling reaction, 1.90 mCi of ^{90}YCl$_3$ in 24 μL of 0.05 N HCl was added to 48 μL of 0.25 M ammonium acetate, pH 5.7. Then 0.2 mg of cT84.66-MCDOTA in 44 μL of 0.25 M ammonium acetate, pH 7.0, was added, and the reaction mixture was incubated at 43 °C for 1 h. The solution was made 1 mM in DTPA with the addition of 13 μL of 10 mM DTPA, pH 6.0, and incubated at 37 °C for 15 min. The ^{90}Y-labeled conjugate was purified by size exclusion HPLC in the same manner as the ^{111}In-labeled antibody.

The cT84.66-MCDOTA conjugate was labeled with ^{131}I using the Iodogen method (75). An aliquot of 0.4 mg of cT84.66-MCDOTA in 100 μL of 0.25 M ammonium acetate, pH 7.0, was placed in a polypropylene tube that had been coated with 100 μg of Iodogen. Then 0.4 mCi of Na^{131}I in 7.3 μL of PBS, pH 7.4, was added, and the reaction mixture was incubated at room temperature for 2 min. The ^{131}I-labeled conjugate was purified by gel filtration HPLC on two Pharmacia Superose® 12 HR 10/30 columns (1 × 30 cm) in series, using an isocratic mobile phase of normal saline and a flow rate of 0.5 mL/min. The mAb peak, eluting at a retention time of 42 min, was collected in 0.5-mL fractions containing 1 drop of 25% (w/v) HSA each.

Immunoreactivity Determination. A dilution of the purified ^{111}In- or ^{90}Y-labeled cT84.66-MCDOTA conjugate, containing approximately 200,000 cpm of radioactivity, was mixed with a 20-fold molar excess of purified CEA (76, 77) in 150 μL of 1% HSA/PBS, pH 7.4. A control sample was prepared in an identical manner, except that CEA was not added. The reaction mixtures were incubated at 37 °C for 15 min with continuous end-over-end mixing, after which aliquots of 100 μL were analyzed by gel filtration HPLC, using two Pharmacia Superose® 6 HR 10/30 columns (1 × 30 cm) in series and an isocratic mobile phase of 0.05 M Na$_2$SO$_4$/0.02 M NaH$_2$PO$_4$/0.05% NaN$_3$, pH 6.8, at a flow rate of 0.5 mL/min. Immunoreactivity was calculated as the percentage of the total radioactivity shifted to complexes with apparent molecular weights higher than that of the mAb.

17

Serum Stability Studies. An aliquot of radiolabeled cT84.66-MCDOTA or cT84.66-MSCDOTA containing approximately 1.6×10^7 cpm of ^{111}In radioactivity or 4.0×10^7 cpm of ^{90}Y radioactivity was added to 1.1 mL of fresh human serum containing 10 μL of 10 % NaN_3. The mixture was incubated at 37 °C throughout the study, during which 100-μL samples were analyzed by gel filtration HPLC on two Pharmacia Superose® 12 HR 10/30 columns (1 × 30 cm) in series, using an isocratic mobile phase of 0.05 M Na_2SO_4/0.02 M NaH_2PO_4/0.05% NaN_3, pH 6.8, and a flow rate of 0.5 mL/min. Serum samples were analyzed at intervals ranging from 6 to 72 h for 7 to 8 days to determine conjugate stability.

Stability Studies in Aqueous Solutions. The carboxymethylated cT84.66-MCDOTA conjugate was labeled with ^{111}In and purified by size exclusion HPLC as described above, except that the mAb peak was collected in 0.5-mL fractions without HSA. Aliquots of ^{111}In-labeled carboxymethylated cT84.66-MCDOTA containing 1.6×10^7 cpm of radioactivity were added to 1.1 mL of PBS/0.1% NaN_3, pH 7.4, 1.1 mL of 1 mM DTPA/PBS/0.1% NaN_3, pH 7.2, and 1.1 mL of 1 mM DTT/ PBS/0.1% NaN_3, pH 7.4, respectively. The three mixtures were incubated at 37 °C over the course of the study, during which 100-μL samples were analyzed by gel filtration HPLC as described for the serum stability studies. Samples of the aqueous solutions were analyzed at intervals ranging from 12 to 48 h for 7 days to determine conjugate stability.

Bifunctional Chelate Stability Studies. To 100 μg (128 nmol) of **2** in 20.0 μL of H_2O was added 388 μg (1.28 μmol) of freshly prepared $YCl_3 \cdot 6H_2O$ in 77.6 μL of 0.25 M ammonium acetate, pH 5.7. The reaction mixture was incubated at 43 °C for 1 h, after which the Y(III) complex of **2** was purified by reversed phase HPLC, using a 4.6 × 250 mm column (Vydac™ Protein & Peptide C_{18}, 5 μm, 300 Å), a flow rate of 1.0 mL/min, and a linear gradient from 0% to 60% solvent B (solvent A, 0.1% TFA; solvent B, 0.1% TFA/90% CH_3CN) in 60 min. The major peak, eluting at a retention time of 24.7 min, was collected, and the correct structure of the Y(III) chelate of **2** was confirmed by ESI MS and MS^2. This fraction was lyophilized to a white powder, redissolved in 20.0 μL of H_2O, and two 10.0-μL aliquots of the resulting solution were added to 0.5 mL of PBS, pH 7.4, and 0.5 mL of PBS, pH 5.4, respectively. Two control

18

reactions were set up in which **2** was dissolved in PBS, pH 7.4, and PBS, pH 5.4, respectively. The four reaction mixtures were incubated at 37 °C throughout the study, during which 50-μL samples were analyzed by reversed phase HPLC, using a 2 × 250 mm column (Column Engineering Reliasil C_{18}, 5 μm, 300 Å), a flow rate of 0.2 mL/min, and a linear gradient from 0% to 60% solvent B (solvent A, 0.1% TFA; solvent B, 0.1% TFA/90% CH_3CN) in 60 min. Samples were analyzed at intervals ranging from 3 h to 287 h over a period of 23 days to determine the stability of the bifunctional chelate. The peaks corresponding to the major decomposition products were collected and stored at -80 °C prior to analysis by ESI MS, MS^2, and MS^3.

To 100 μg (123 nmol) of **3** in 20.0 μL of H_2O was added 373 μg (1.23 μmol) of freshly prepared $YCl_3 \cdot 6H_2O$ in 74.6 μL of 0.25 M ammonium acetate, pH 5.7. The reaction mixture was incubated at 43 °C for 1 h, after which the Y(III) complex of **3** was purified by reversed phase HPLC in the same manner as the Y(III) complex of **2**. The major peak, eluting at a retention time of 24.3 min, was collected, and the correct structure of the Y(III) chelate of **3** was confirmed by ESI MS and MS^2. This fraction was lyophilized, redissolved in H_2O, and added to PBS, pH 7.4, and PBS, pH 5.4, in the same manner as the Y(III) complex of **2**. Two control reactions were also set up in which **3** was dissolved in PBS, pH 7.4, and in PBS, pH 5.4. The four reaction mixtures were incubated at 37 °C throughout the study, and for 5 days samples were analyzed by reversed phase HPLC at intervals ranging from 3 h to 72 h, using the method employed for **2** and its Y(III) chelate. The peaks corresponding to the major decomposition products were collected and stored at -80 °C prior to analysis by ESI MS, MS^2, and MS^3.

Hydrazido-DOTA (16) (Scheme 3 (top)). To a solution of 100 mg (213 μmol) of trisodium DOTA and 92.3 mg (425 μmol) of sulfo-NHS in 1 mL of H_2O was added dropwise with continuous stirring a solution of 81.5 mg (425 μmol) of EDC in 151 μL of H_2O. The reaction mixture was stirred at room temperature for 1 h, after which a solution of 29.1 mg (425 μmol) of hydrazine monohydrochloride in 46.5 μL of H_2O was added dropwise with continuous stirring. The pH was adjusted to 4.0 with 50% NaOH, and the reaction mixture was stirred at room temperature for 22 h. The reaction mixture was then cooled to 4 °C, made 1 M in HCl with the

19

addition of 118 μL of conc HCl, and stirred at 4 °C for 20 h. The acidified mixture was applied to

a Dowex AG50W-X8 column (H$^+$ form, 1 × 6.5 cm), which was washed with 50 mL of H$_2$O and

then eluted with a 40-mL step gradient from 0.5 to 4 M NH$_4$OH. A mixture of the desired

product, dihydrazide adducts of DOTA, several multisubstituted DOTA hydrazide dimer species,

and unreacted DOTA eluted in 2 M NH$_4$OH and was lyophilized to a pale yellow gum. The crude

product was dissolved in 1 mL of H$_2$O and applied to a Dowex AG1-X4 column (HCO$_2^-$ form, 1 ×

7.5 cm), which was washed with 50 mL of H$_2$O and then eluted with a 40-mL step gradient from

0.05 to 0.5 M HCO$_2$H. The desired product eluted in 0.05-0.1 M HCO$_2$H, and unreacted DOTA

eluted in 0.2 M HCO$_2$H. These fractions were lyophilized to give white powders, which were

dissolved in 1 mL of H$_2$O and concentrated to dryness by lyophilization. This process was

repeated four times to remove residual HCO$_2$H. This procedure afforded 17.5 mg (20.4%) of

DOTA, which was recrystallized from H$_2$O:CH$_3$OH (1:9) and used for other syntheses, and 12.4

mg (13.9%) of **16** as a white powder. MALDITOF MS *m/z* 419.54 (M + H)$^+$.

Hydrazido-DOTA (16) (Scheme 3 (middle)). DOTA internal salt (38.0 mg, 94.0

μmol) was dissolved in 3.8 mL of *N,N*-dimethylformamide and 0.9 mL of triethylamine, under an

argon atmosphere, over a period of 4 h at room temperature. The solution was cooled to 0 °C, and

12.2 μL (12.8 mg, 93.7 μmol) of isobutyl chloroformate was added dropwise with continuous

stirring over a 1 to 2 min period. The reaction mixture was stirred at 0 °C for 15 min, after which 3

μL (3.1 mg, 95.5 μmol) of anhydrous hydrazine was added with continuous stirring. The reaction

mixture was allowed to warm up to room temperature and was stirred at room temperature for 12

h. Then to the reaction mixture was added dropwise 5 mL of H$_2$O with continuous stirring. This

mixture was applied to a Dowex AG1-X4 column (HCO$_2^-$ form, 1 × 6.5 cm), which was washed

with 50 mL of H$_2$O and then eluted with a 40-mL step gradient from 0.05 to 0.5 M HCO$_2$H. The

desired product eluted in 0.1 M HCO$_2$H, and unreacted DOTA eluted in 0.2 M HCO$_2$H. These

fractions were lyophilized to give white powders, which were dissolved in 1 mL of H$_2$O and

concentrated to dryness by lyophilization. This process was repeated four times to remove residual

HCO$_2$H. This procedure afforded 15.1 mg (39.8%) of DOTA, which was recrystallized from

$H_2O:CH_3OH$ (1:9) and used for other syntheses, and 6.8 mg (17.3%) of **16** as a white powder.

^1H NMR (DMSO-d_6) δ 2.70 (m, 4H), 3.00-3.07 (m, 12H), 3.43 (s, 6H), 3.48 (s, 2H); ^{13}C NMR

(DMSO-d_6) δ 49.96, 50.15, 50.66, 51.38, 55.58, 55.81, 56.16, 168.61, 169.60, 170.71; FAB

MS m/z calcd for $C_{16}H_{31}N_6O_7$ $(M + H)^+ = 419.2254$, found 419.2275.

Hydrazido-DOTA (16) (Scheme 3 (bottom)). DOTA internal salt (94.2 mg, 233

μmol) was dissolved in 9.3 mL of N,N-dimethylformamide and 2.3 mL of triethylamine, under an

argon atmosphere, over a period of 2 h at room temperature. The solution was cooled to 0 °C, and

30.2 μL (31.8 mg, 233 μmol) of isobutyl chloroformate was added dropwise with continuous

stirring. The reaction mixture was stirred at 0 °C for 20 min, after which 30.8 mg (233 μmol) of

tert-butyl carbazate in 0.2 mL of N,N-dimethylformamide was added dropwise with continuous

stirring. The reaction mixture was allowed to warm up to room temperature and was stirred at

room temperature for 17 h. Then to the reaction mixture was added dropwise 12.4 mL of H_2O

with continuous stirring, and the mixture was concentrated to dryness in vacuo to give an off-white

semisolid. The crude product was dissolved in 5 mL of trifluoroacetic acid, and the resulting

mixture was stirred at room temperature for 1 h. The solvent was removed by rotary evaporation

to give a pale yellow oil, which was dried in vacuo overnight. This oil was dissolved in 5 mL of

5% triethylamine and applied to a Dowex AG1-X4 column (HCO_2^- form, 1.5 × 6.2 cm), which

was washed with 55 mL of H_2O and then eluted with a 44-mL step gradient from 0.05 to 0.5 M

HCO_2H. The desired product eluted in 0.2 M HCO_2H, and unreacted DOTA eluted in 0.5 M

HCO_2H. These fractions were lyophilized to give white powders, which were dissolved in 1 mL

of H_2O and concentrated to dryness by lyophilization. This process was repeated four times to

remove residual HCO_2H. This procedure afforded 37.7 mg (40.0%) of DOTA, which was

recrystallized from $H_2O:CH_3OH$ (1:9) and used for other syntheses, and 11.5 mg (11.8%) of **16**

as a white powder. MALDITOF MS m/z 419.82 $(M + H)^+$.

Carbohydrazido-DOTA (17). To a solution of 500 mg (1.06 mmol) of trisodium

DOTA and 463 mg (2.13 mmol) of sulfo-NHS in 5 mL of H_2O was added dropwise with

continuous stirring a solution of 408 mg (2.13 mmol) of EDC in 408 μL of H_2O. The reaction

21

mixture was stirred at room temperature for 1 h, after which a solution of 192 mg (2.13 mmol) of carbohydrazide in 1 mL of H_2O was added dropwise with continuous stirring. The pH was adjusted to 5.0 with 50% NaOH, and the reaction mixture was stirred at room temperature for 20 h. The reaction mixture was then cooled to 4 °C, made 1 M in HCl with the addition of 636 μL of conc HCl, and stirred at 4 °C for 20 h. The acidified mixture was applied to a Dowex AG50W-X8 column (H^+ form, 2.5 × 5.1 cm), which was washed with 250 mL of H_2O and then eluted with a 200-mL step gradient from 0.5 to 4 M NH_4OH. A mixture of the desired product, dicarbohydrazide adducts of DOTA, and unreacted DOTA eluted in 1-2 M NH_4OH and was lyophilized to a yellow foam. The crude product was dissolved in 5 mL of H_2O and applied to a Dowex AG1-X4 column (HCO_2^- form, 2.5 × 8.9 cm), which was washed with 250 mL of H_2O and then eluted with a 200-mL step gradient from 0.05 to 0.5 M HCO_2H. The desired product eluted in 0.1 M HCO_2H, and unreacted DOTA eluted in 0.2-0.5 M HCO_2H. These fractions were lyophilized to give white powders, which were dissolved in 5 mL of H_2O and concentrated to dryness by lyophilization. This process was repeated four times to remove residual HCO_2H. This procedure afforded 251 mg (58.6%) of DOTA, which was recrystallized from H_2O:CH_3OH (1:9) and used for other syntheses, and 63.6 mg (12.6%) of **17** as a white powder. ^1H NMR (D_2O) δ 3.01 (m, 2H), 3.08 (m, 6H), 3.31-3.52 (m, 6H), 3.44 (s, 4H), 3.48 (s, 2H), 3.56 (m, 2H), 3.83 (dd, 2H); ^{13}C NMR (D_2O) δ 48.33, 48.66, 51.03, 51.85, 53.51, 53.93, 56.86, 170.06, 172.18, 175.48, 177.46; FAB MS m/z calcd for $C_{17}H_{33}N_8O_8$ $(M + H)^+ = 477.2421$, found 477.2406.

Hydrazidocysteineamido-DOTA (18). To a solution of 15.4 mg (30.3 μmol) of **1** in 5.8 mL of degassed 50 mM K_2HPO_4, pH 7.5, under an argon atmosphere, was added dropwise with continuous stirring a solution of 7.3 mg (28.8 μmol) of ε-maleimidocaproic acid hydrazide in 0.4 mL of degassed N,N-dimethylformamide. The reaction mixture was stirred at room temperature for 2 h, after which the pH was adjusted to 1.6 with the addition of 85 μL of trifluoroacetic acid. The desired product was purified by reversed phase HPLC using a 10 × 250 mm column (Vydac™ Protein & Peptide C_{18}, 5 μm, 300 Å), a flow rate of 4.0 mL/min, and a linear gradient from 0% to 60% solvent B (solvent A, 0.1% TFA; solvent B, 0.1% TFA/90% CH_3CN)

in 60 min, beginning 25 min after injection. The major peaks, eluting at retention times of 37.0 min and 37.7 min, were collected, pooled, and lyophilized to give 12.2 mg (54.9%) of **18** as a white solid. ^{1}H NMR (D_2O) δ 1.31 (dt, 2H), 1.60 (dt, 2H), 1.66 (dt, 2H), 2.36 (t, 2H), 2.74 (dt, 1H), 3.09 (m, 1H), 3.21-3.45 (m, 18H), 3.54 (t, 2H), 3.77 (br s, 2H), 3.85 (br s, 6H), 4.12 (m, 1H), 4.74 (m, 1H); ^{13}C NMR (D_2O) δ 24.14, 25.44, 26.45, 32.85, 35.84, 36.26, 38.99, 39.71, 40.71, 48.22, 51.53, 52.55, 54.22, 55.86, 173.97, 174.52, 178.61, 179.55, 179.77; FAB MS *m/z* calcd for $C_{29}H_{49}N_8O_{12}S$ $(M + H)^+$ = 733.3191, found 733.3204.

Prelabeling of cT84.66 with Hydrazido-DOTA[^{90}Y(III)]. To 4.01 mCi (81.7 pmol) of ^{90}YCl$_3$ in 100 μL of 0.05 *N* HCl was added 100 μL of 0.25 M ammonium acetate, pH 7.0, followed by 34.2 μg (81.7 nmol) of **16** in 1.71 μL of H_2O. The reaction mixture was incubated at 43 °C for 30 min, after which the solution was made 1 mM in DTPA with the addition of 22.4 μL of 10 mM DTPA, pH 6.0. The reaction mixture was incubated at 37 °C for 15 min, and a 1:100 dilution of the mixture was analyzed by TLC to determine the percentage of ^{90}Y incorporation. The reaction mixture was applied to a DE52 spin column (CH$_3$CO$_2^-$ form, 0.5 mL). The spin column was centrifuged at 2500 rpm for 2 min, and the eluent was collected. Then 125 μL of H_2O was applied to the column, which was centrifuged again at 2500 rpm for 2 min, and a second fraction was collected. This process was repeated three times to collect a total of five fractions. The five fractions and the spin column were counted in a dose calibrator, and it was determined that fractions 1-4 contained the purified hydrazido-DOTA[^{90}Y] complex. The hydrazido-DOTA[^{90}Y] solution was concentrated *in vacuo* to a volume of approximately 10 μL. Then to 1.0 mg (6.67 nmol) of cT84.66 in 92.9 μL of PBS, pH 7.4, was added 10.3 μL of 2.5 M sodium acetate, pH 5.0, followed by 20 μL of 29.3 mM NaIO$_4$. This mixture was allowed to stand at 4 °C for 1 h in the dark, and then 20 μL of 49.3 mM Na$_2$S$_2$O$_5$ was added. The resulting mixture was allowed to stand at room temperature for 20 min in the dark, after which it was immediately added to the concentrated solution of hydrazido-DOTA[^{90}Y]. The reaction mixture was incubated on a tube rotator at 43 °C for 30 min in the dark. Then 20 μL of 15 mM NaBH$_3$CN was added, and the reaction mixture was allowed to stand at room temperature for 30 min in the

dark. The ^{90}Y-labeled antibody was purified by size exclusion HPLC using a TosoHaas TSKgel®

G2000 SW column (10 µm, 7.5 × 300 mm) and an isocratic mobile phase of normal saline at a

flow rate of 0.5 mL/min. The mAb peak, eluting at 8.3 min retention time, was collected in 0.5-

mL fractions containing 1 drop of 25% (w/v) HSA each.

Conjugation of cT84.66 with Hydrazido-DOTA. An aliquot of 15 mg of

cT84.66, 4.39 mg/mL in PBS/0.02% NaN$_3$, pH 7.4, was dialyzed against 1 L of 0.25 M sodium

acetate/20 mM DTPA, pH 5.0, for 24 h at 4 °C and then against 1 L of 0.25 M sodium acetate, pH

5.0, over Chelex® 100, for 44 h at 4 °C, with one buffer change. To 13.1 mg (87.3 nmol) of

cT84.66 in 2.90 mL of 0.25 M sodium acetate, pH 5.0, was added 262 µL (7.69 µmol) of 29.3

mM NaIO$_4$, and the reaction mixture was incubated at 4 °C for 1 h in the dark. Then 769 µL (154

µmol) of 200 mM ethylene glycol was added, and the resulting mixture was allowed to stand at

room temperature for 20 min in the dark. The reaction mixture was applied in equal volumes to 4

1-mL Sephadex G-25-50 spin columns, and the oxidized mAb was eluted by centrifugation (*10*) at

1200 rpm for 2 min. The eluents from the spin columns were pooled, and 3.65 mg (8.73 µmol) of

16 in 183 µL of H$_2$O was added. The reaction mixture was incubated on a tube rotator at room

temperature for 1 h in the dark and then divided into two equal aliquots. To one aliquot was added

131 µL (1.97 µmol) of 15 mM NaBH$_3$CN, and this mixture was allowed to stand at room

temperature for 30 min in the dark. The conjugates were dialyzed against 1 L of 0.25 M

ammonium acetate/20 mM DTPA, pH 7.0, for 24 h at 4 °C and then against 1 L of 0.25 M

ammonium acetate, over Chelex® 100, for 138 h at 4 °C, with five buffer changes.

Radiolabeling of cT84.66-DOTA Hydrazone. To 55 µL of 0.25 M ammonium

acetate, pH 6.0, was added 1.00 mCi of ^{111}InCl$_3$ in 87.6 µL of 0.04 *N* HCl. Then 0.2 mg of the

mAb conjugate in 76 µL of 0.25 M ammonium acetate, pH 7.0, was added, and the resulting

mixture was incubated at 43 °C for 45 min. The reaction mixture was challenged with the addition

of 24.3 µL of 10 mM EDTA, pH 6.5. After this mixture was incubated at 37 °C for 15 min, it was

injected onto two Pharmacia Superose® 12 HR 10/30 columns (1 × 30 cm) in series and eluted

24

using an isocratic mobile phase of normal saline and a flow rate of 0.5 mL/min. Fractions of 0.5 mL, containing 1 drop of 25% (w/v) HSA each, were collected.

Conjugation of ZCE025 with Hydrazido-DOTA, Carbohydrazido-DOTA, and HC-DOTA. An aliquot of 36.8 mg of ZCE025 in 6 mL of PBS, pH 7.4, was dialyzed against 1 L of 50 mM NaH_2PO_4/100 mM NaCl/20 mM DTPA, pH 6.0, for 21 h at 4 °C and then against 1 L of 50 mM NaH_2PO_4/100 mM NaCl, pH 6.0, over Chelex® 100, for 47 h at 4 °C, with one buffer change. To 34.2 mg (228 nmol) of ZCE025 in 12.4 mL of 50 mM NaH_2PO_4/100 mM NaCl, pH 6.0, was added 568 μL (284 μmol) of 0.5 M $NaIO_4$. The reaction mixture was incubated on ice for 75 min in the dark, after which 400 μL (400 μmol) of 1 M 1,3-diaminopropan-2-ol was added, and the pH was adjusted to 6.0 with 22 μL of cold acetic acid. This mixture was incubated on ice for 40 min in the dark and then applied in equal volumes to 6 1-mL Sephadex G-25-50 spin columns. The oxidized mAb was collected by centrifugation (*10*) at 1200 rpm for 2 min. The eluents were pooled and then divided into three equal aliquots. To the three aliquots of 11.4 mg (76 nmol) of oxidized ZCE025 were added, respectively, 3.18 mg (7.60 μmol) of **16** in 159 μL of H_2O, 3.62 mg (7.60 μmol) of **17** in 181 μL of H_2O, and 5.57 mg (7.60 μmol) of **18** in 278 μL of H_2O. The three reaction mixtures were incubated on a tube rotator at room temperature for 2 h, after which they were each divided into two equal aliquots. To one aliquot of each conjugate was added 132 μL (33 μmol) of 0.25 M $NaBH_3CN$, and these mixtures were incubated on the tube rotator at room temperature for 4 h. The conjugates were dialyzed against 1 L of 0.25 M ammonium acetate/20 mM DTPA, pH 7.0, for 25 h at 4 °C and then against 1 L of 0.25 M ammonium acetate, over Chelex® 100, for 137 h at 4 °C, with five buffer changes.

RESULTS AND DISCUSSION

MALEIMIDOCYSTEINEAMIDO-DOTA DERIVATIVES: NEW REAGENTS FOR SITE-SPECIFIC CONJUGATION OF RADIOMETAL CHELATES TO ANTIBODY HINGE REGION SULFHYDRYL GROUPS

It has been shown that the chelation of metals by the macrocyclic ligand DOTA is often a two-step process in which a reversibly formed initial adduct (a type I complex) slowly transforms to the final chelate (a type II complex) (46, 47). Given this mechanism, it is possible that low radiochemical yields observed for labeling antibody-macrocycle conjugates, compared to free ligand, may be a result of competition between nonspecific metal-binding sites on the protein surface and formation of the type I complex. Macrocyclic BCAs bearing "pendant-type" carboxyl groups have been synthesized by Takenouchi et al. (78, 79), and the addition of a side chain carboxylate was shown to accelerate the formation of Y(III) complexes. These authors reasoned that the Y(III) ion was captured quickly but loosely by the pendant donor group, forming a more stable type I complex and raising the local metal concentration in the vicinity of the macrocyclic backbone, thus increasing the ultimate rate of complexation.

The serum stabilities of the pendant-type bifunctional chelates were found to be identical to those of the corresponding nonpendant-type chelates, indicating that the pendant donor has no effect on type II complex stability. However, the Y(III)-binding properties of only the free chelating agents were investigated, and it was not determined whether the same effects would be borne out at the antibody conjugate level. Structural modifications leading to better kinetics of type I complex formation might lead to improved radiometal labeling efficiency for antibody-macrocycle conjugates.

A simplified synthetic strategy was developed for introducing a similar pendant-type carboxylate donor via peptide bond formation between one carboxyl group of DOTA and the α-amino group of an amino acid. Previous work in our group (36) demonstrated that amide bond

formation between DOTA and endogenous antibody amino groups allowed for the formation of extremely stable ^{111}In(III) and ^{90}Y(III) chelates on the mAb conjugates; that is, the conversion of one carboxyl group of DOTA to an amide did not affect type II complex stability to an appreciable degree. Therefore, a monocysteineamide derivative of DOTA was synthesized to introduce not only the pendant carboxylate donor group, but also an orthogonal functionality for attachment to mAbs. The DOTA monocysteineamide compound was subsequently derivatized for antibody conjugation by reaction with 1,6-*bis*-maleimidohexane. Maleimidocysteineamido-DOTA derivatives containing both sulfide and sulfone linkers were prepared and conjugated in a site-specific manner to lightly reduced interchain disulfide bonds of the human/murine chimeric anti-CEA mAb cT84.66 (*64*). The interchain cysteine residues of an antibody reside the relatively solvent-exposed hinge region of the protein, and site-specific conjugation of the macrocycle to this domain might make the chelator more accessible to the radiometal in solution during the labeling reaction.

The results reported here show that the cT84.66 conjugate prepared with maleimidocysteineamido-DOTA (MC-DOTA, **2**) exhibited significantly improved rates of radiometal complexation under carrier-free conditions, leading to substantial increases in radiolabeling yields with ^{111}In and ^{90}Y. Furthermore, *in vitro* studies of the radiometal-labeled antibody conjugates and free chelate complexes of the sulfide compound MC-DOTA and its sulfone derivative (MSC-DOTA, **3**) revealed that these molecules underwent pH-dependent cleavage reactions in aqueous media. The results indicated that both of these BCAs are chemically labile at physiological temperature and pH but significantly more stable under moderately acidic conditions. This attachment of kinetically stable radiometal chelates to monoclonal antibodies using pH-dependent chemically labile linkers offers the possibility of creating radioimmunoconjugates with favorable biodistribution properties.
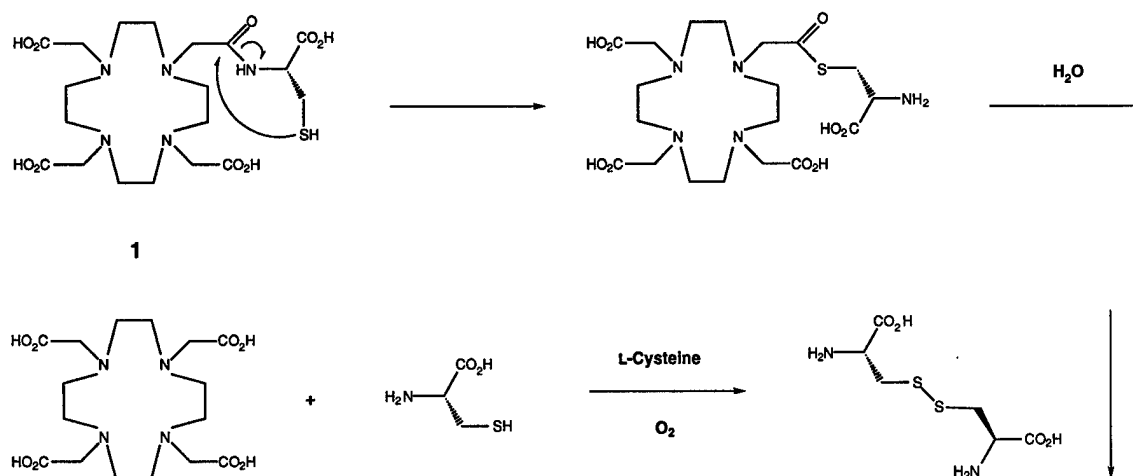
Synthesis

The synthesis of the maleimidocysteineamido-DOTA derivatives MC-DOTA (**2**) and MSC-DOTA (**3**) is shown in Scheme 1. These compounds were prepared by a simple, straightforward synthetic route, taking advantage of water-soluble chemistry to circumvent the need for lengthy sequences of protection and deprotection reactions. Thus, the syntheses and purifications can be completed in a relatively short period of time, on the order of 2 weeks. DOTA *N*-hydroxysulfosuccinimide ester was prepared by a modification of the procedure for direct conjugation to proteins (*36*). Reaction of the active ester with L-cysteine at pH 7.0 produced the key intermediate, the monocysteineamide derivative of DOTA (**1**). This reaction was once commonly employed in peptide synthesis (*80*) and used more recently to synthesize entire proteins by native chemical ligation (*81*). The mechanism of coupling active esters to cysteine involves nucleophilic attack of the ionized thiolate to form an intermediate thioester, which in aqueous solution rearranges via a pentacyclic transition state to the more stable amide (*80*).

Unfortunately, this reaction is readily reversed, and in aqueous media compound **1** decomposes over a period of hours to DOTA and L-cysteine, which oxidizes to the insoluble disulfide dimer (Figure 1). This decomposition pathway appears to be independent of pH. Fortunately, conversion of the free thiol of **1** to a thioether alleviates this problem. The synthesis of a monohistidine amide derivative of DOTA (**19**), from the reaction of DOTA *N*-hydroxysulfosuccinimide ester with L-histidine methyl ester (Scheme 2), was also proposed. However, the imidazole group of compound **19** is likely to catalyze hydrolysis of the amide bond between DOTA and amino acid in a manner similar to that observed for the cysteineamide adduct. Because the imidazole functionality of **19** was intended to participate in metal ion coordination, derivatization of this group to improve hydrolytic stability was not considered feasible, and compound **19** was not synthesized. The syntheses of tetracysteineamide and tetrahistidineamide derivatives of DOTA, also proposed, were not carried out for the same reasons. Therefore, efforts

Scheme 1
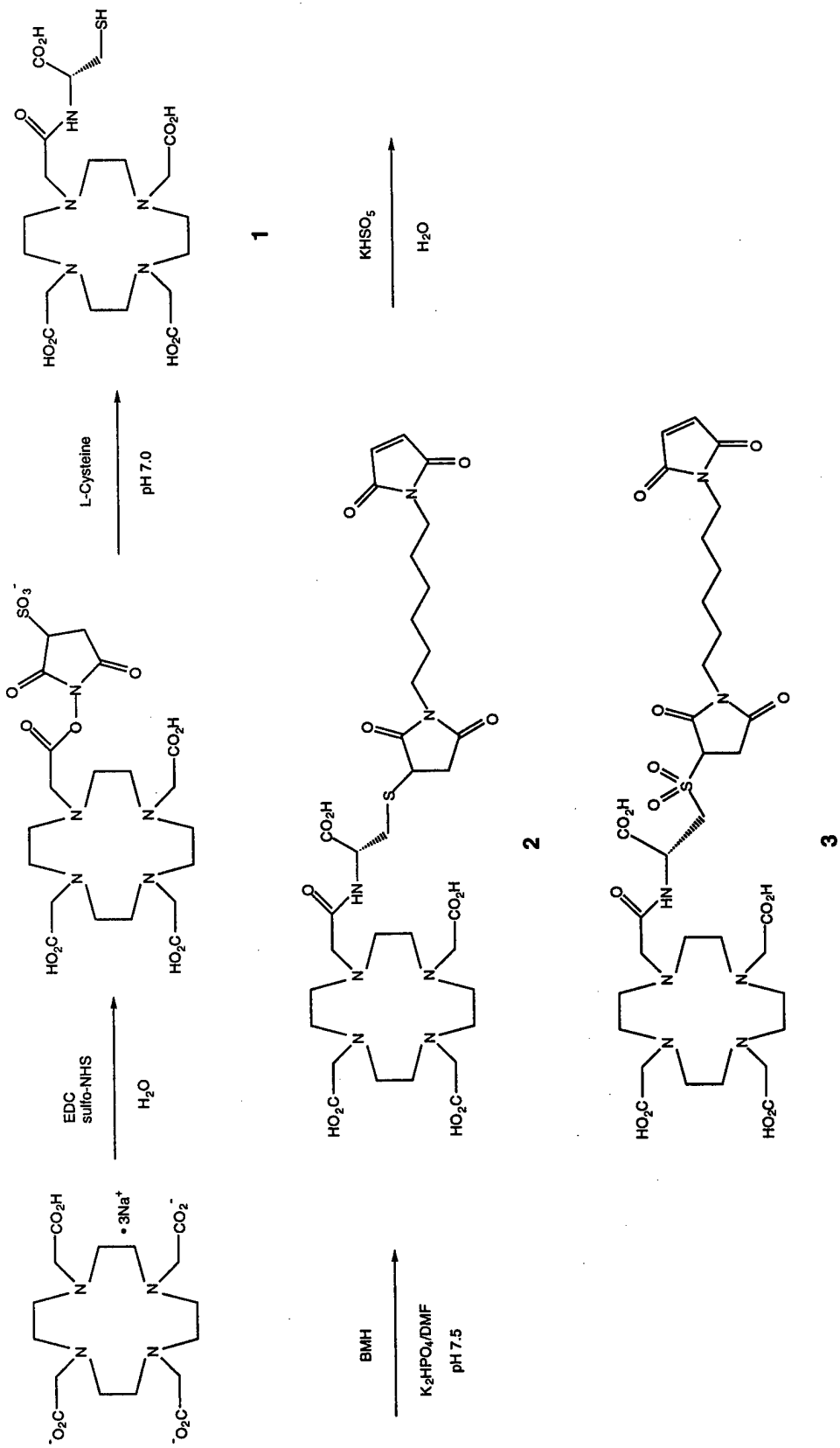
Figure 1. Proposed mechanism for the decomposition of cysteineamido-DOTA in aqueous solution.

to synthesize amino acid derivatives of DOTA focused on the preparation of **1** and conversion of the thiol to a sulfide or sulfone linker for attachment to antibodies.

The thiol group of **1** was exploited as an orthogonal functionality for antibody conjugation. After purification by sequential cation- and anion-exchange chromatography, the DOTA cysteineamide adduct **1** was reacted with an excess of the sulfhydryl-specific homobifunctional reagent 1,6-*bis*-maleimidohexane. The major product, **2**, could be purified easily by reversed phase HPLC by virtue of its long, hydrophobic side chain. Two by-products from the preparation of **2** were also collected and identified by mass spectrometry. The side product eluting at a retention time of 22.1 min was determined to be the adduct of BMH and two molecules of DOTA cysteineamide, and the compound eluting at 24.2 min was identified as a product resulting from the addition of one molecule of water to **2**. MC-DOTA (**2**) was oxidized with potassium hydrogen persulfate (Oxone®), a reagent which is highly chemoselective for conversion of sulfides to sulfones (*82*), to give MSC-DOTA (**3**). During the purification of **3** by reversed phase HPLC, a trace by-product eluting at a retention time of 24.4 min was collected and identified by mass spectrometry as the sulfoxide.

30

Scheme 2
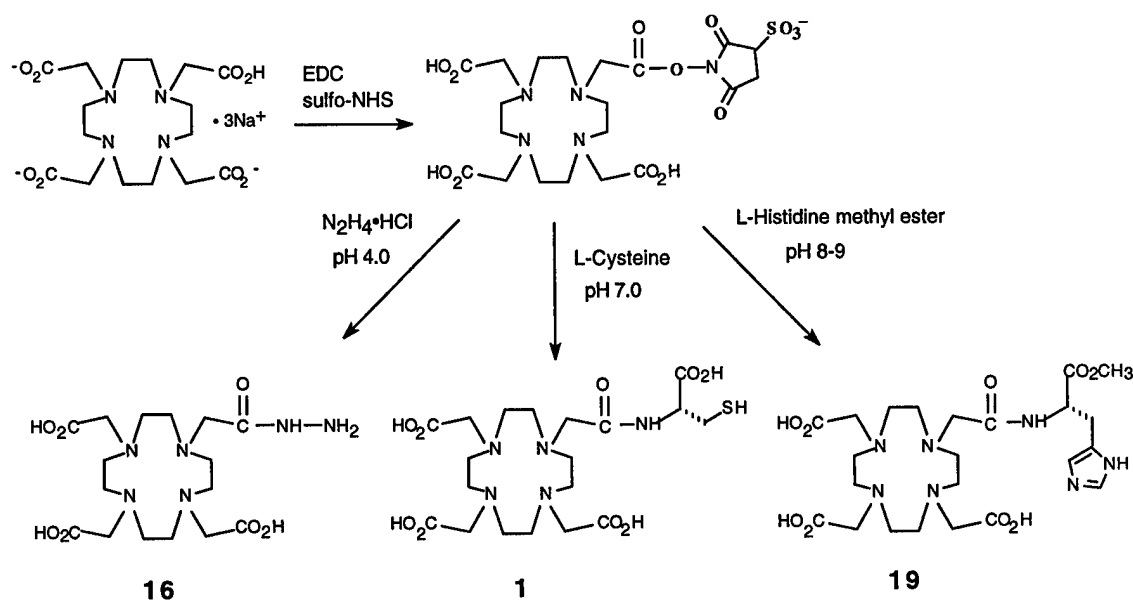
Antibody Conjugation

MC-DOTA and MSC-DOTA were conjugated to the human/murine chimeric anti-CEA mAb cT84.66, isotype IgG$_1$, κ, using a modification of the method of Willner *et al.* (*83*). Antibody reduction was monitored using Ellman's reagent (*84, 85*). Treatment of cT84.66 with 20 molar equiv of DTT (1 mM) resulted in the generation of 10.3 ± 0.7 reactive sulfhydryl groups per antibody molecule, and further addition of DTT did not increase the SH titer (data not shown). This titer was slightly higher than that anticipated for a human IgG$_1$ mAb, which contains four interchain disulfide bonds. However, these results were similar to those obtained by Willner and coworkers, who generated a titer of 9.6 sulfhydryl groups per molecule of the isotype-matched mAb BR64 at a DTT:mAb molar ratio of 20:1. The mAb was fully reduced in a reproducible

manner under these conditions, allowing the extent of conjugation to be controlled by the amount of maleimide reagent added.

As shown in Table 1, conjugation of lightly reduced cT84.66 with MC-DOTA at six BCA:mAb molar ratios, ranging from 1:1 to 40:1, resulted in average incorporations of 0.5 to 6.3 chelates per antibody molecule, as determined by a modification of a ^{57}Co(II) binding assay (10, 36). The reduced antibody was maximally modified with 6.3 chelates/mAb after reaction with 20 molar equiv of MC-DOTA. The conjugation results suggested that at least two of the reduced interchain cysteine residues of cT84.66 remained unreactive to modification.

Table 1. Conjugation and ^{90}Y Radiolabeling Yields for cT84.66-MCDOTA Conjugates[a]

MC-DOTA:mAb	chelates/mAb	labeling efficiency (%)	specific activity (mCi/mg)
1:1	0.542	0.982	0.0982
2:1	0.655	3.64	0.364
4:1	1.32	25.8	2.58
10:1	3.80	81.2	8.12
20:1	6.28	95.8	9.58
40:1	6.34	97.1	9.71

[a]Radiolabeling was performed for 1 h at 43 °C, using 2.00 mCi of ^{90}Y and 0.200 mg of mAb conjugate. Immunoreactivity of all ^{90}Y-labeled conjugates was 100%.

SDS polyacrylamide gel electrophoresis of the six cT84.66-MCDOTA conjugates under non-reducing conditions (Figure 2) showed that the conjugation reaction is highly specific for reduced interchain disulfide residues. The addition of increasing amounts of MC-DOTA to reduced cT84.66 resulted in progressive conversion of the intact mAb to species which, in the presence of SDS, dissociated into various combinations of the heavy and light polypeptide chains: H_2L, H_2, HL, and modified and unmodified H and L chains. The maximally modified conjugate

clearly showed 100% modification of the light chain. Therefore, the heavy chain likely contained the unreactive interchain cysteine residues. Steric hindrance may have played a role in preventing all of the heavy chain cysteines from being modified.
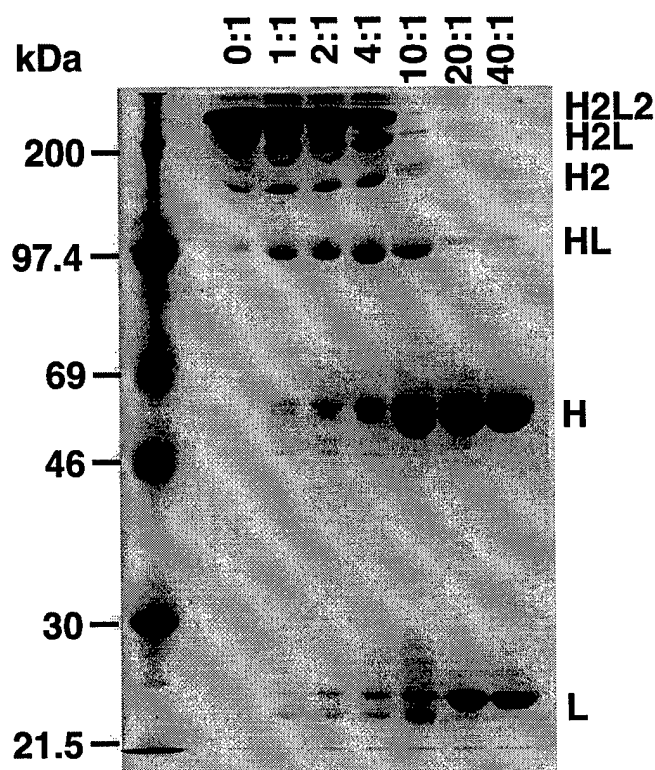
Figure 2. Non-reducing SDS polyacrylamide gel electrophoresis of unconjugated cT84.66 and cT84.66-MCDOTA conjugates prepared with 1 to 40 molar equiv of MC-DOTA. The MC-DOTA:mAb conjugation ratio is shown above each lane. Molecular weight markers are shown to the left. Aliquots of 8 to 12 μg of the conjugates were loaded onto a 10% polyacrylamide gel (8 × 8 cm) with a 3% stacking layer (2 × 8 cm).

The same six preparations were also analyzed by gel filtration chromatography (Figure 3), which revealed that, under non-denaturing conditions, all of the conjugates exist as species with an apparent molecular size of 150 kDa.
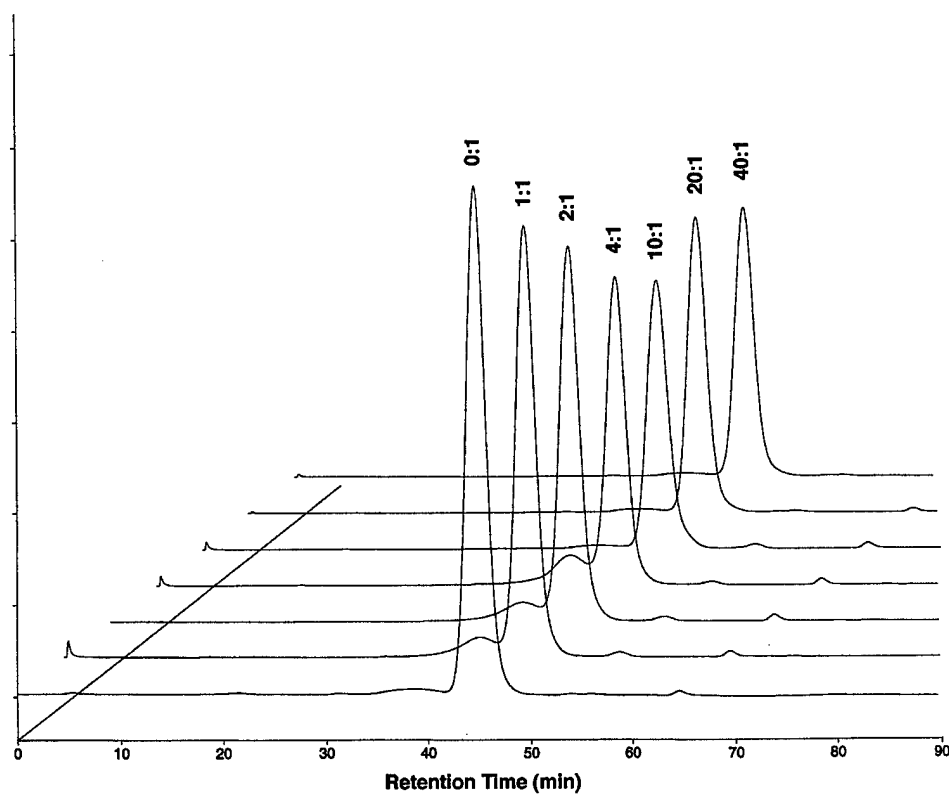
Figure 3. Gel filtration chromatography of unconjugated cT84.66 and cT84.66-MCDOTA conjugates prepared with 1 to 40 molar equiv of MC-DOTA. The MC-DOTA:mAb conjugation ratio is shown above each chromatogram. Aliquots of 80 to 120 µg of the conjugates were injected onto two Pharmacia Superose 12 HR 10/30 columns (1 × 30 cm) in series and eluted with an isocratic mobile phase of 0.05 M Na$_2$SO$_4$/0.02 M NaH$_2$PO$_4$/0.05% NaN$_3$, pH 6.8, at a flow rate of 0.5 mL/min. Absorbance was monitored at 280 nm. The peak eluting at 45 min retention time corresponds to an apparent molecular size of 150 kDa.

Antibody Radiolabeling

Also shown in Table 1 are radiochemical yields and radioimmunoconjugate specific activities for ^{90}Y labeling of the six cT84.66-MCDOTA conjugates. The conjugate prepared at an MC-DOTA:mAb molar ratio of 10:1, modified with an average of 3.8 chelates per antibody molecule, was the least modified product to give high specific activity labeling with ^{90}Y. Using the standard labeling conditions at 43 °C, the average yield for ^{90}Y incorporation into this cT84.66-MCDOTA conjugate was 78.6% after 60 min, and the average ^{111}In incorporation was 96.6% after 45 min (Table 2). In contrast, average labeling yields for the cT84.66 conjugate prepared with DOTA N-hydroxysulfosuccinimide ester, also modified with 3.8 chelates per mAb, were 56.4% for ^{90}Y and 73.5% for ^{111}In. The efficiency of ^{111}In incorporation into the cT84.66-MSCDOTA conjugate was 72.9% for a single experiment, affording a radioimmunoconjugate with a specific activity of 3.65 mCi/mg.

Table 2. Radiolabeling Yields for cT84.66 DOTA-OSSu and MC-DOTA Conjugates^a

radiometal	T (°C)	time (min)	cT84.66-DOTA labeling efficiency (%)	cT84.66-MCDOTA labeling efficiency (%)
^{111}In	43	45	73.5 ± 12.2	96.6 ± 2.5
^{90}Y	43	60	56.4 ± 3.4	78.6 ± 3.7

^{a}Average number of chelates per mAb was 3.8 for both conjugates. Immunoreactivity of all radiolabeled conjugates was 100%. Radiochemical yields represent the average of 3 experiments.

For both MC-DOTA and DOTA-OSSu, conjugates modified with an average of 1-2 chelates per antibody displayed an approximate 4-fold reduction in radiometal labeling yield. The "threshold" modification value of 3-4 chelates per mAb, required for the conjugate to carry high

radiometal activity, was in good agreement with the findings of other groups (*86, 87*). However, a direct comparison of the cT84.66 conjugates prepared with MC-DOTA and DOTA-OSSu showed that the MC-DOTA conjugate afforded an average 22-23% increase in radiolabeling yields for both ^{111}In and ^{90}Y. At present, it cannot be concluded unequivocally whether this improvement in radiometal labeling is attributable to the "pendant-type" carboxyl group of MC-DOTA, the change in conjugation site to the hinge region of the mAb, or the addition of a longer linker to the macrocycle. Using modifications of the water-soluble route for the synthesis of MC-DOTA, each of these parameters can now be tested independently for their respective contributions to radiolabeling yields.

Immunoreactivity of Radiolabeled cT84.66-MCDOTA

The immunoreactivity of ^{111}In- and ^{90}Y-labeled cT84.66-MCDOTA was determined by a solution-phase assay using purified CEA. Gel filtration chromatography on tandem Superose 6 columns routinely allowed separation of the 2:1 CEA:mAb complex, the 1:1 CEA:mAb complex, and free antibody. The binding percentages for a 1:190 dilution of the ^{111}In-labeled and a 1:50 dilution of the ^{90}Y-labeled mAb were both 100% after a 15-min incubation with 20 molar equiv of CEA at 37 °C. In each case, only the 2:1 CEA:mAb complex was observed by gel filtration chromatography, indicating that both antigen-combining sites remained fully immunoreactive.

Serum Stability of cT84.66-MCDOTA and cT84.66-MSCDOTA

The kinetic stabilities of ^{111}In- and ^{90}Y-labeled cT84.66-MCDOTA and ^{111}In-labeled cT84.66-MSCDOTA were studied in fresh human serum at 37 °C. The serum samples were analyzed by gel filtration chromatography with radioactivity detection, and the area of each radioactive peak was divided by the total area of all radioactive peaks in the chromatogram to determine the percentage of radiometal associated with that fraction.

The serum stability results for ^{111}In-labeled cT84.66-MCDOTA are shown in Figure 4. Fifty percent of the radiolabel was lost from the antibody fraction of the mixture after approximately 27 h, resulting in the transfer of ^{111}In to a fraction with an apparent molecular weight of 70 kDa and to a low molecular weight fraction (<1350 Da). After 7 days, 24.7% of the ^{111}In label remained bound to the mAb, 61.3% was associated with the 70 kDa fraction, and 14.0% of the activity was obtained as a low molecular weight species. Addition of CEA to the serum and reanalysis by gel filtration chromatography revealed that only the 150 kDa fraction was immunoreactive. Similar results were obtained for ^{90}Y-labeled cT84.66-MCDOTA (data not shown). Carboxymethylation of unconjugated cysteine residues in cT84.66-MCDOTA with iodoacetic acid resulted in a moderate improvement in serum stability. In that case, 50% of the ^{111}In label was lost from the mAb in about 47 h, but after 8 days 21.1% of the ^{111}In activity was bound to the mAb fraction, 59.3% eluted in the 70 kDa fraction, and 19.6% eluted as a low molecular weight species (data not shown). In contrast, the ^{131}I-labeled cT84.66-MCDOTA conjugate was completely stable in human serum for a period of 7 days; 100% of the ^{131}I activity remained associated with the mAb fraction (data not shown).

The 70 kDa ^{111}In species was found to coelute with purified, ^{131}I-labeled human serum albumin by gel filtration chromatography. Also, the ^{90}Y activity associated with the 70 kDa peak was collected, analyzed by reducing and non-reducing SDS polyacrylamide gel electrophoresis with autoradiography detection, and found to migrate with an apparent molecular weight of 66.4 kDa (data not shown). No evidence that either radiometal associated with transferrin was obtained by gel filtration chromatography or gel electrophoresis. When the radiolabeled mAb was incubated with purified HSA at physiological temperature and pH, alkylation of Cys-34 of HSA with iodoacetic acid had no effect on the rate of transfer of ^{111}In to HSA.
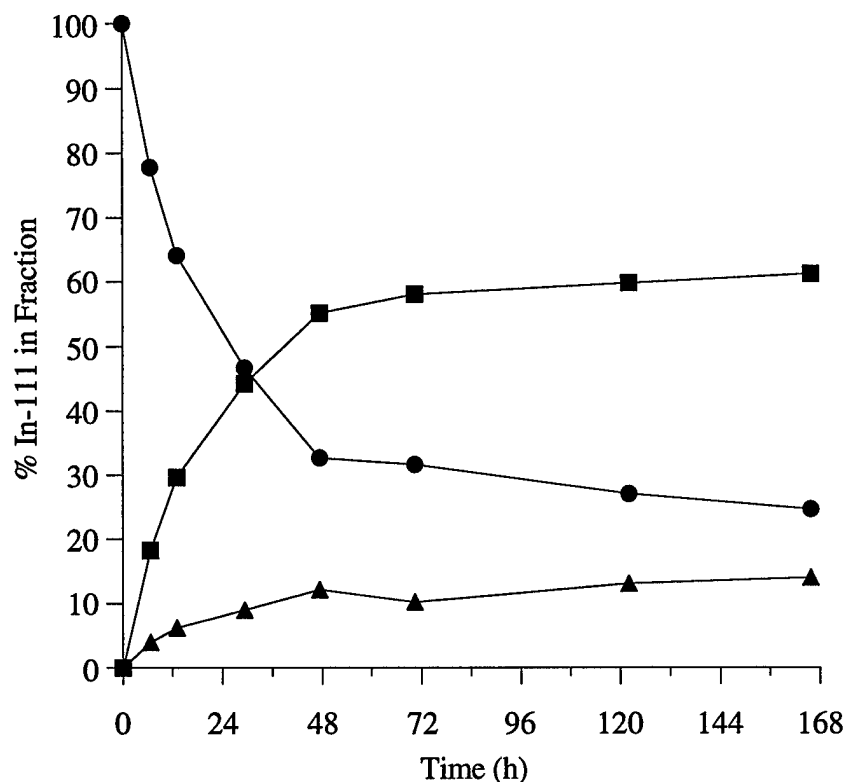
Figure 4. Percentage of ^{111}In associated with cT84.66-MCDOTA (●), serum albumin (■), and low molecular weight (▲) fractions as a function of time of incubation in human serum at 37 °C, determined by gel filtration HPLC.

The serum stability results for ^{111}In-labeled carboxymethylated cT84.66-MSCDOTA are shown in Figure 5. After 6 h at 37 °C, only 14.1% of the radiometal label remained with the mAb. However, unlike the cT84.66-MCDOTA conjugate, most of the ^{111}In activity remained in the low molecular weight fraction (83.1% at 6 h), with very little transfer to HSA (2.90% at 6 h). After 7 days, the amounts of the ^{111}In associated with cT84.66-MSCDOTA, HSA, and the low molecular weight species were 1.65%, 21.3%, and 77.1%, respectively.
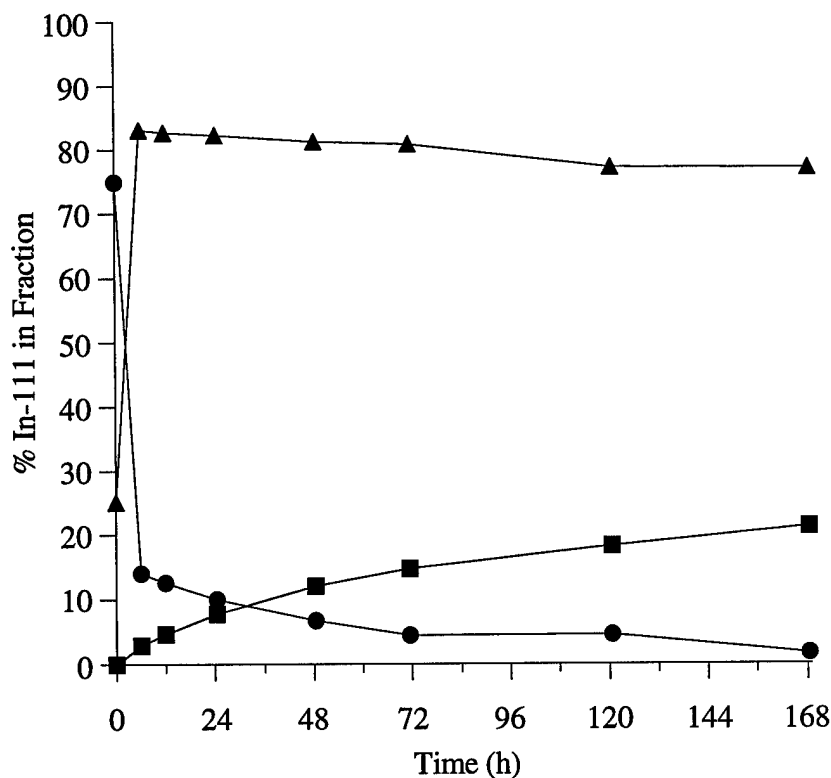
Figure 5. Percentage of ^{111}In associated with cT84.66-MSCDOTA (●), serum albumin (■), and low molecular weight (▲) fractions as a function of time of incubation in human serum at 37 °C, determined by gel filtration HPLC.

Both conjugates exhibited relatively rapid loss of radiometal in serum, and this process was approximately 10 times faster for the conjugate prepared with the sulfone compound. A dramatic difference in the fate of the radiometal was observed, depending on which type of chelate-antibody linker was used. Radiometal lost from the MC-DOTA conjugate was predominantly associated with serum albumin, while the vast majority of metal lost from the MSC-DOTA conjugate remained as a low molecular weight species.

Stability of cT84.66-MCDOTA in Aqueous Solutions

In the absence of other proteins, the kinetic stability of ^{111}In-labeled carboxymethylated cT84.66-MCDOTA was studied in aqueous media at physiological temperature and pH. At 37 °C in 1 mM DTPA, pH 7.2, 1 mM DTT, pH 7.4, and PBS, pH 7.4, the ^{111}In label was lost from the mAb component and converted to a low molecular weight species. Formation of the ^{111}In-labeled low molecular weight fraction was observed to follow slow, pseudo-first-order kinetics in all three mixtures. Therefore, the rates of formation of this species could be expressed in linear plots, where $\exp(-k_i t) \approx 1 - k_i t$ when $k_i t \ll 1$ (35). The observed rate constants for formation of the ^{111}In-labeled low molecular weight species were 0.336 to 0.361 h^{-1} ($r^2 = 0.985$-0.990) in 1 mM DTPA, 1 mM DTT, and PBS.

Large quantities of exogenous chelating agent or reducing agent had no effect on the observed rate of radiometal loss. These results, taken together with the results of the serum stability studies, were inconsistent with those expected for radiometal ion dissociation or a disulfide exchange reaction, suggesting that a solvent-mediated or intramolecular cleavage reaction involving the linker portion of the bifunctional chelates might be responsible for radiometal release. The cT84.66-MCDOTA conjugate, however, has afforded highly reproducible radiolabeling yields over a period of more than six months of storage under metal-free conditions at 4 °C and pH 7.0, indicating that the stability of the antibody conjugate is temperature-dependent.

Stability of MC-DOTA[Y(III)] and MSC-DOTA[Y(III)] in Aqueous Solution

The properties of the unconjugated Y(III) chelates of MC-DOTA and MSC-DOTA at physiological temperature were studied in order to elucidate the mechanisms of their decomposition reactions. The kinetic stabilities of the purified yttrium chelates of MC-DOTA and MSC-DOTA were evaluated in PBS at 37 °C and pH 7.4 or pH 5.4. Figure 6 shows the reversed phase

40

chromatograms of MC-DOTA[Y(III)] (4) before heating to 37 °C (A) and after incubation at 37 °C for 555 h at pH 7.4 (B) or at pH 5.4 (C). In the absence of chelated yttrium, MC-DOTA exhibited nearly identical reaction rates and produced identical proportions of the analogous decomposition products at the two pH values.

Figures 7 and 8 show the rates of formation of decomposition products from MC-DOTA[Y(III)] at pH 7.4 and pH 5.4, respectively. The kinetic profile at pH 7.4 (Figure 7) indicated that **4** was converted to compound **9** within 24 h, followed by the conversion of **9** to compounds **5, 6, 7,** and **8**. In addition, a second decomposition pathway produced compounds **10** and **11** in minor amounts (<15%, data not shown).
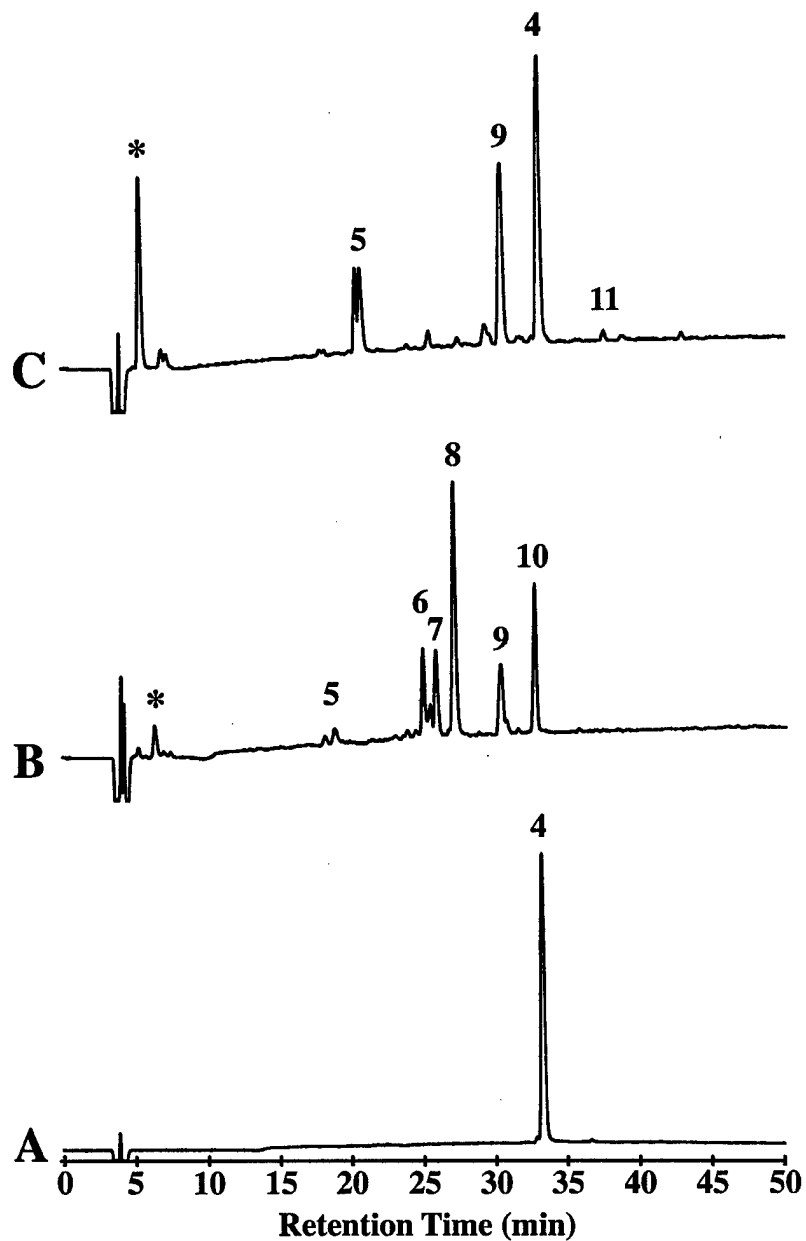
Figure 6. Reversed phase chromatograms of MC-DOTA[Y(III)] before incubation (A) and after incubation in PBS at 37 °C for 555 h at pH 7.4 (B) or for 555 h at pH 5.4 (C). Aliquots of 5 μg were injected onto a C_{18} column (2 × 250 mm, 5 μm, 300 Å) and eluted with a linear gradient from 0% to 60% solvent B (solvent A, 0.1% TFA; solvent B, 0.1% TFA/90% CH_3CN) in 60 min at a flow rate of 0.2 mL/min. Absorbance was monitored at 214 nm.
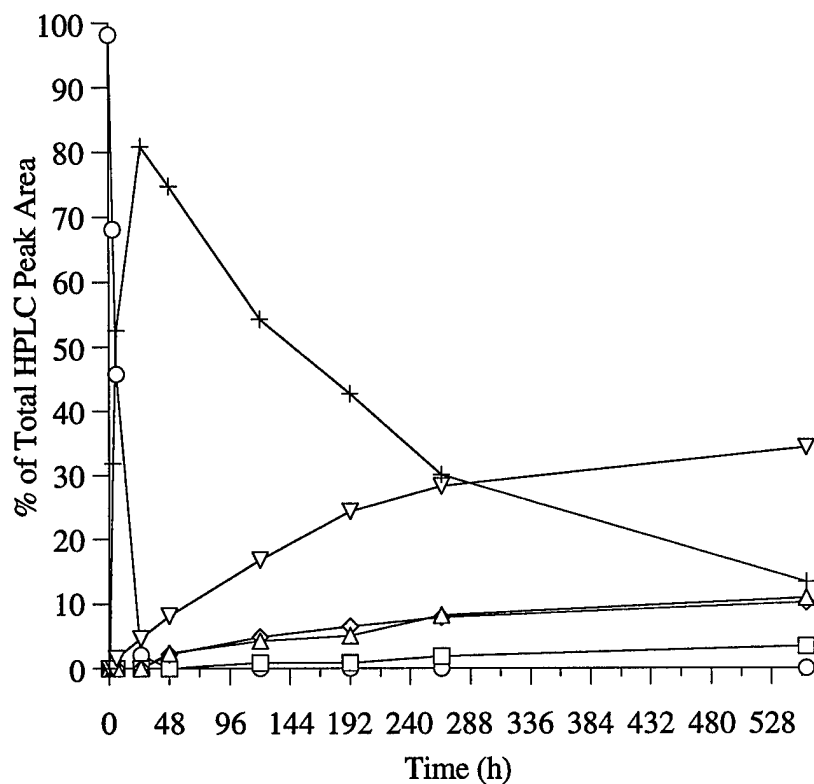
Figure 7. Peak areas, expressed as percentages of the total peak area, of MC-DOTA[Y(III)]

(O) and decomposition products **5** (□), **6** (◇), **7** (△), **8** (▽), and **9** (+) as a function of

time of incubation in PBS at 37 °C at pH 7.4.

At pH 5.4 (Figure 8), the reaction was considerably slower, and **4** was converted to compounds **9**

and **5**, with small quantities of **11** produced (<2%, data not shown) and negligible formation of

products **6, 7**, and **8**. The formation of compound **10** could not be confirmed at pH 5.4, because

the comparatively large quantity of unreacted MC-DOTA[Y(III)] eluted at a nearly identical

retention time.
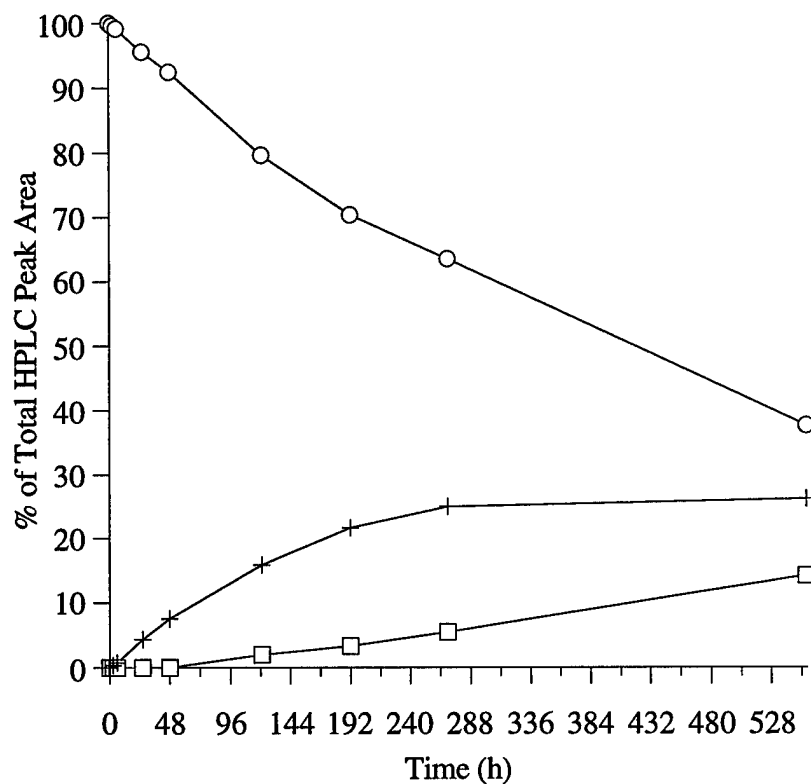
Figure 8. Peak areas, expressed as percentages of the total peak area, of MC-DOTA[Y(III)]

(◯) and decomposition products **5** (□), **6** (◇), **7** (△), **8** (▽), and **9** (+) as a function of

time of incubation in PBS at 37 °C at pH 5.4.

Shown in Figure 9 are the reversed phase chromatograms of purified MSC-DOTA[Y(III)]

(**12**) before heating to 37 °C (A), after incubation at 37 °C for 6 h at pH 7.4 (B), and after

incubation at 37 °C for 50 h at pH 5.4 (C).

44

Figure 9. Reversed phase chromatograms of MSC-DOTA[Y(III)] before incubation (A) and

after incubation in PBS at 37 °C for 6 h at pH 7.4 (B) or for 50 h at pH 5.4 (C). Aliquots of 5 µg

were injected onto a C_{18} column (2 × 250 mm, 5 µm, 300 Å) and eluted with a linear gradient from

0% to 60% solvent B (solvent A, 0.1% TFA; solvent B, 0.1% TFA/90% CH_3CN) in 60 min at a

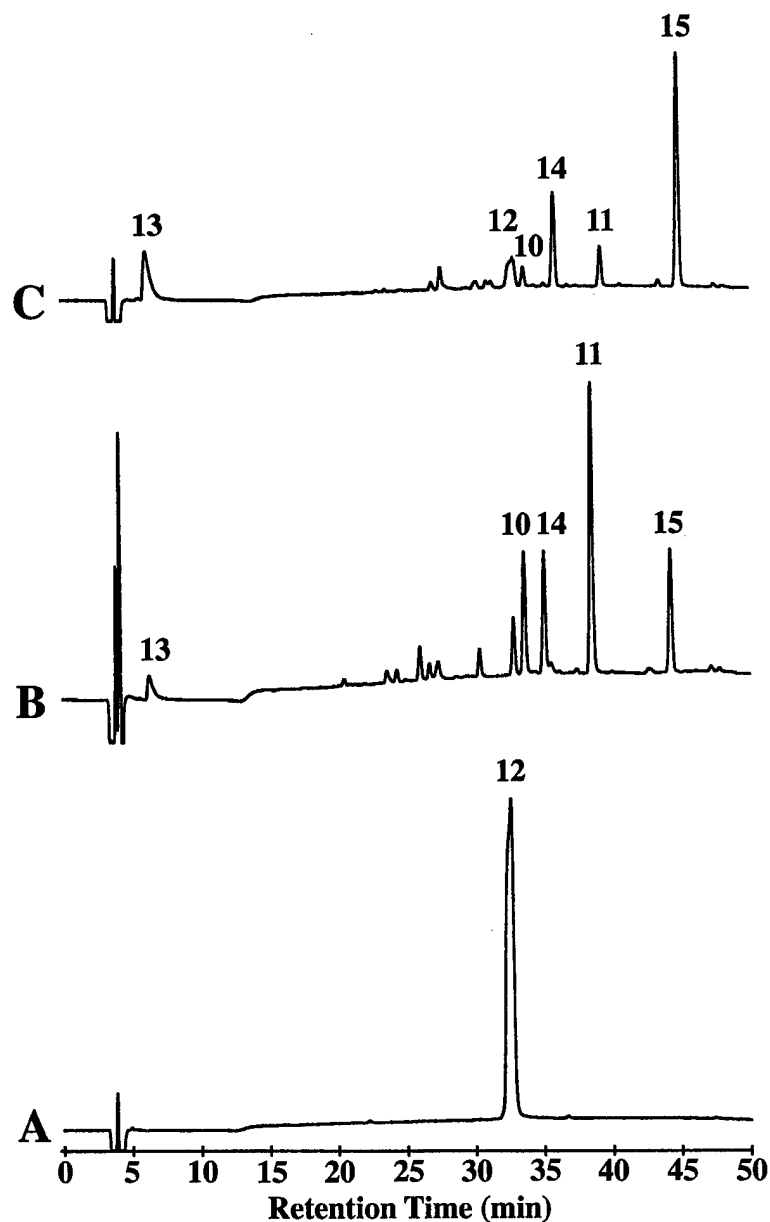flow rate of 0.2 mL/min. Absorbance was monitored at 214 nm.

Figures 10 and 11 show the rates of formation of decomposition products from MSC-

DOTA[Y(III)] at pH 7.4 and pH 5.4, respectively. The plot for the decomposition at pH 7.4

(Figure 10) indicated that **12** was rapidly converted to compounds **13** and **15**, after which **15** was

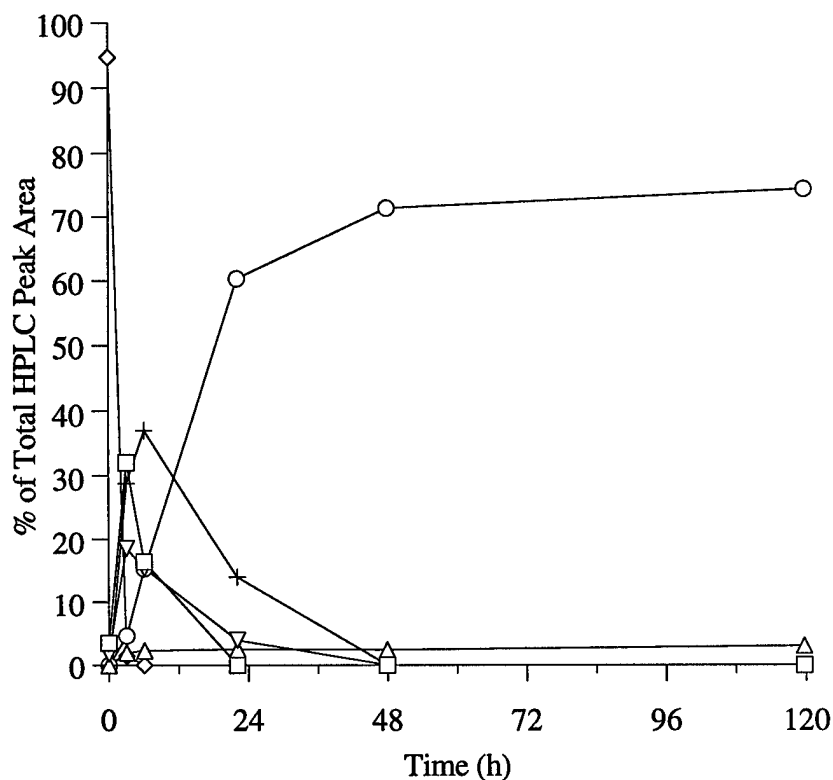converted to compound **11**, which in turn gave rise to product **10**.

Figure 10. Peak areas, expressed as percentages of the total peak area, of MSC-DOTA[Y(III)]

(◇) and decomposition products **10** (○), **11** (+), **13** (△), **14** (▽), and **15** (□) as a function

of time of incubation in PBS at 37 °C at pH 7.4.

The same decomposition products were obtained from MSC-DOTA[Y(III)] at pH 5.4, but at

significantly slower rates (Figure 11). Decomposition of MSC-DOTA produced identical

46

proportions of the analogous decomposition products at both pH values. However, the presence

of chelated yttrium resulted in an approximately 3-fold acceleration in the decomposition at pH 7.4

and an approximately 2-fold increase in the reaction rate at pH 5.4.
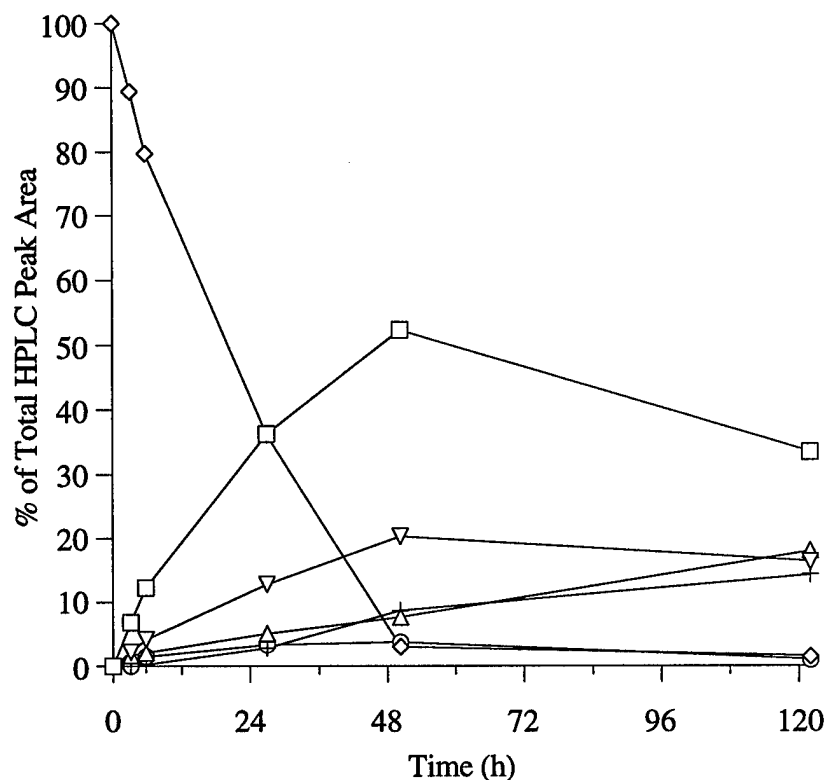
Figure 11. Peak areas, expressed as percentages of the total peak area, of MSC-DOTA[Y(III)]

(◇) and decomposition products **10** (○), **11** (+), **13** (△), **14** (▽), and **15** (□) as a function

of time of incubation in PBS at 37 °C at pH 5.4.

Mass Spectrometry Analysis of Decomposition Products from MC-DOTA[Y(III)] and MSC-DOTA[Y(III)]

After separation by reversed phase HPLC, fractions corresponding to MC-DOTA[Y(III)] (**4**) and its decomposition products **5-11** were collected and analyzed by ESI MS with collision-induced dissociation. Fractions were collected and analyzed from reaction mixtures incubated at pH 7.4 and pH 5.4, in the presence and absence of chelated yttrium, to determine the identities of products generated at both pH values and of the analogous products generated in the absence of yttrium. Table 3 summarizes the mass spectrometry results obtained for **4** and its decomposition products. Taken together, the results of mass spectrometry and kinetic analysis allowed a mechanism for the decomposition of MC-DOTA[Y(III)], which is depicted in Figure 12, to be proposed.

The mass spectrum of fraction **4** gave a singly charged molecular ion at $m/z = 870.54$, consistent with that expected for MC-DOTA[Y(III)] (calcd for $C_{33}H_{47}N_7O_{13}SY$, 870.20). MS^2 of the parent ion produced complete fragmentation of **4** to yield a number of characteristic product ions. The product ions at $m/z = 826.2, 782.3, 738.3,$ and 694.5 corresponded to loss of 1, 2, 3, and 4 molecules of CO_2, respectively, from the chelate carboxylate groups. The product ion at $m/z = 594.2$ corresponded to the yttrium chelate of DOTA cysteineamide, and the product ions at $m/z = 560.2$ and 516.1 were consistent with progressive loss of H_2S and CO_2 from DOTA cysteineamide[Y(III)]. The product ion at $m/z = 491.2$ was the smallest fragment obtained and corresponded to the yttrium chelate of DOTA monoamide.

Compound **9** afforded a singly charged molecular ion at $m/z = 888.04$, 18 mass units higher than **4** and consistent with the addition of H_2O to MC-DOTA[Y(III)]. MS^2 of the $m/z = 888.04$ ion yielded a major product ion at $m/z = 790.2$, which corresponded to the loss of maleic anhydride. MS^3 of the ion at $m/z = 790.2$ produced secondary product ions at $m/z = 594.1,$ 560.1, 516.0, and 491.1. Compared to **4**, decomposition product **9** appeared to arise from addition of H_2O, contain a maleic acid moiety, and otherwise possess fragmentation patterns

48

similar to the starting material. Thus, the structure of **9** was assigned to a hydrolysis product of **4** in which the maleimide ring had been opened.

Table 3. Mass Spectrometry Analysis of Decomposition Products from MC-DOTA[Y(III)]

| compound	MS m/z	MS^2 m/z	MS^3 m/z
4	870.54	826.2 (43)[a]	nd[b]
		782.3 (15)	
		764.2 (19)	
		746.3 (1)	
		738.3 (3)	
		720.3 (2)	
		711.2 (3)	
		694.5 (1)	
		594.2 (1)	
		560.2 (1)	
		516.1 (1)	
		491.2 (100)	
5	790.43	762.1 (50)	nd
		744.2 (20)	
		719.1 (20)	
		594.1 (1)	
		560.2 (1)	
		516.1 (3)	
		491.1 (100)	
6	906.57	888.1 (5)	
		808.2 (100)	790.1 (18), 763.0 (100), 692.0 (13), 607.0 (3), 594.1 (7), 560.1 (2), 516.2 (1), 491.0 (20)
7	906.30	888.1 (4)	
		808.1 (100)	790.1 (26), 763.0 (100), 692.0 (18), 607.1 (2), 594.1 (8), 560.1 (4), 516.1 (2), 491.1 (29)
8	906.38	888.1 (6)	
		808.2 (100)	790.1 (4), 763.1 (10), 737.0 (12), 710.1 (21), 692.1 (100), 676.0 (1), 648.1 (1), 607.2 (9), 594.1 (10), 560.1 (2), 515.9 (1), 491.1 (3)
9	888.04	870.1 (7)	762.1 (67), 744.1 (27), 702.2 (1), 607.2 (1),
		790.2 (100)	594.1 (2), 560.1 (2), 516.0 (3), 491.1 (100)

[a]Relative intensities are given in parentheses. [b]nd = not done.

Fractions **6, 7,** and **8** all gave singly charged molecular ions at a nominal m/z value of 906, an increase of 36 mass units compared to MC-DOTA[Y(III)], and major product ions at $m/z = 808$, corresponding to loss of maleic anhydride. In addition, all three of these decomposition products showed secondary product ions characteristic of the DOTA-cysteineamide[Y(III)] moiety, at $m/z =$ 594, 560, 516, and 491. The parent ion was consistent with the addition of 2 equiv of H_2O to **4**, and the only reasonable structure consistent with the mass spectral data was that of a hydrolysis product in which both the maleimide and succinimide rings of MC-DOTA[Y(III)] had been opened. This process would generate two regioisomeric products, each of which would exist as a pair of diastereomers. Compounds **6** and **7** gave nearly identical MS^3 spectra, with the major secondary product ions at $m/z = 790.1$ and 763.0. In contrast, compound **8** yielded major secondary product ions at $m/z = 710.1$ and 692.1. The fact that two HPLC peaks, **6** and **7**, gave identical mass spectra suggested that they represent one pair of diastereomers which chromatograph with different retention times on the reversed phase column. In the case of compound **8**, only one HPLC peak was obtained, which may represent the coelution of the other diastereomeric pair. A conclusive determination of which regioisomers correspond to fractions **6/7** and **8** could not be made on the basis of the MS data. However, opening of the succinimide ring should be favored at the site distal to the sulfide group for steric reasons. Since the peak area for fraction **8** was always greater than the combined peak areas for fractions **6** and **7**, their structures have been tentatively assigned as shown in Figure 12.

Compound **5** yielded a singly charged molecular ion at $m/z = 790.43$, consistent with the mass of a decomposition product arising from hydrolytic loss of maleic acid from **4**. MS^2 of **5** afforded product ions at $m/z = 594.1, 560.2, 561.1,$ and 491.1, indicative of the DOTA cysteineamide[Y(III)] moiety. Hydrolytic loss of maleic acid from MC-DOTA[Y(III)] generated the primary amine derivative of the bifunctional chelate, the only cleavage product observed in this experiment. The split peak obtained for fraction **5** suggested that this pair of diastereomers chromatographed with slightly different retention times. When collected separately, the two peaks from fraction **5** gave identical mass spectra.

The peak marked with an asterisk (*) in the chromatograms shown in Figure 6 was also analyzed by ESI MS. This fraction gave a singly charged molecular ion at m/z = 130.04. MS^2 of this parent ion generated product ions at m/z = 74.1 and 57.1. MS^3 of the product ion at m/z = 74.1 yielded the ion at m/z = 57.2 as the secondary product. Because these studies were performed in an ion trap instrument, the data were consistent with the structure of any isomer of dibutylamine. Dibutylamines are commonly used as stabilizers and vulcanization accelerants in the manufacture of rubber products (Lewis, R. G., personal communication.). The decomposition reactions were performed in screw-cap polypropylene vials containing rubber O-rings. It is likely that solvent evaporation and condensation was responsible for extraction of dibutylamine from the O-rings and introduction of this contaminant into the reaction mixtures. The observation that considerably more dibutylamine was obtained at pH 5.4 than at pH 7.4 supports this conclusion.
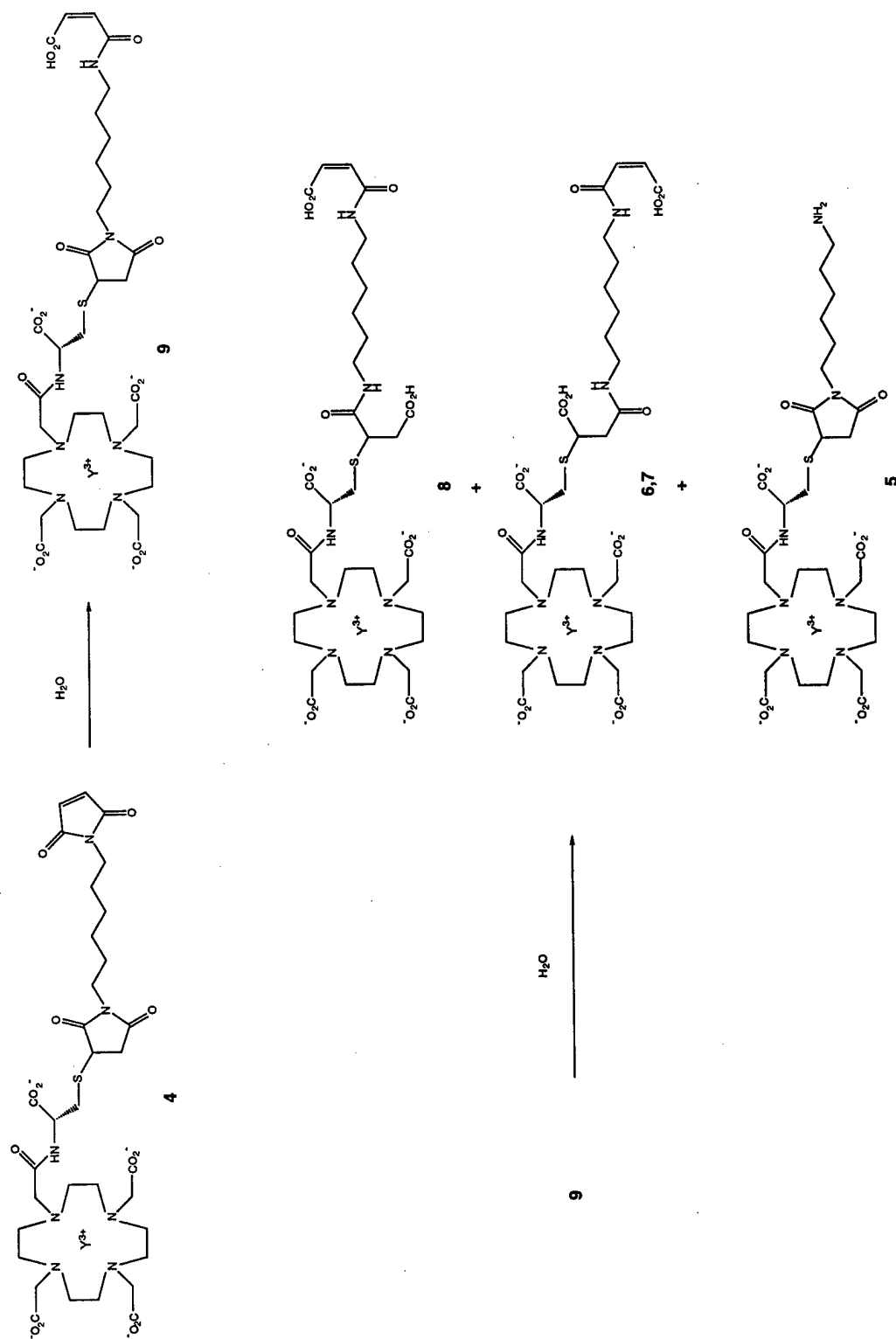
Figure 12. Proposed mechanism for the decomposition of MC-DOTA[Y(III)] in aqueous solution.

After separation by reversed phase HPLC, MSC-DOTA[Y(III)] (12) and its decomposition products, 10, 11, 13, 14, and 15, were collected and subjected to the same ESI MS analysis. Again, fractions were collected from reaction mixtures incubated at pH 7.4 and pH 5.4, with and without chelated yttrium, to verify that the same products were obtained at both pH values and that the analogous products were obtained in the absence of yttrium. Table 4 summarizes the ESI MS data for compounds 10-15, and the proposed reaction mechanism derived from the mass spectrometry and kinetic analysis is shown in Figure 13.

MSC-DOTA[Y(III)] (12) gave a singly charged molecular ion at m/z = 902.23 (calcd for $C_{33}H_{47}N_7O_{15}SY$, 902.19). MS^2 of this parent ion produced complete fragmentation of 12 to afford characteristic product ions at m/z = 858.2 and 814.3, corresponding to loss of 1 and 2 CO_2 molecules, respectively, as well as at m/z = 626.1, consistent with the structure of the yttrium chelate of DOTA cysteinesulfenic acid. The product ions at m/z = 560.2 and 516.1 resulted from loss of H_2SO_2 and CO_2 from DOTA cysteinesulfenic acid[Y(III)]. The product ion corresponding to DOTA monoamide[Y(III)] was also prominent at m/z = 491.2.

The initial products formed from the decomposition of MSC-DOTA[Y(III)] were compounds 13 and 15. Fraction 13 exhibited a singly charged molecular ion at m/z = 626.12, one product ion at m/z = 608.2, and secondary product ions at m/z = 560.2, 516.2, and 491.2. These data were consistent with the structure of the yttrium chelate of DOTA cysteinesulfenic acid. Fraction 15 generated a singly charged molecular ion of m/z = 277.09. MS^2 of 15 gave a product ion at m/z = 180.1, corresponding to loss of maleimide, and MS^3 afforded a major secondary product ion at m/z = 83.1, again consistent with loss of maleimide. On the basis of these product ions, along with the loss of several 14-mass unit fragments in the MS^3 spectrum, the structure of 15 was assigned as that of 1,6-*bis*-maleimidohexane. Thus, as depicted in Figure 13, the first step in the decomposition mechanism of MSC-DOTA[Y(III)] appeared to be a β-elimination reaction involving the sulfone and succinimide groups, generating 13 and 15 as cleavage products.

**Table 4. Mass Spectrometry Analysis of Decomposition Products from MSC-DOTA[Y(III)]**

compound	MS m/z	MS^2 m/z	MS^3 m/z
10	312.99	295.0 (100)^a	
		277.1 (23)	
		215.1 (36)	197.1 (2), 117.1 (100)
		197.1 (61)	
		117.1 (27)	
11	295.01	277.1 (100)	180.0 (100), 162.1 (3), 138.0 (7), 124.0 (17), 110.1 (15)
		197.1 (12)	
12	902.23	858.2 (17)	nd^b
		814.3 (1)	
		776.3 (1)	
		732.2 (2)	
		706.4 (1)	
		626.1 (9)	
		608.1 (19)	
		560.2 (65)	
		516.1 (29)	
		491.2 (100)	
13	626.12	608.2 (100)	590.1 (5), 560.2 (15), 542.2 (100), 516.2 (55), 491.2 (13)
14	277.08	259.1 (13)	nd
		249.1 (100)	
		224.9 (17)	
		195.0 (91)	
		178.0 (23)	
		124.1 (5)	
15	277.09	180.1 (100)	162.1 (15), 152.3 (8), 138.0 (32), 124.1 (95), 122.1 (21), 110.1 (100), 98.1 (18), 96.2 (8), 83.1 (74)
		162.1 (3)	
		138.1 (5)	
		124.1 (17)	
		110.1 (13)	

^{a}Relative intensities are given in parentheses. ^{b}nd = not done.

Compounds **10** and **11** gave mass spectra which were consistent with the structures of hydrolysis products derived from 1,6-*bis*-maleimidohexane. Fraction **11** had a singly charged molecular ion at m/z = 295.01, 18 mass units higher than **15**. MS^2 of **11** yielded a peak at m/z =

277.1, corresponding to loss of H_2O in the gas phase to generate BMH as a product ion, and MS^3 produced a fragmentation pattern similar to that observed for **15**. The structure of compound **11** was assigned as the BMH hydrolysis product in which one of the maleimide rings had been opened. Fraction **10** gave a singly charged molecular ion at $m/z = 312.99$, 36 mass units higher than **15**, and upon MS^2 analysis afforded product ions at $m/z = 295.0$, representing loss of H_2O, and $m/z = 215.1$, representing loss of maleic anhydride. MS^3 of the ion at $m/z = 215.1$ produced loss of a second molecule of maleic anhydride to give a secondary product ion at $m/z = 117.1$, corresponding to the ion expected for 1,6-hexanediamine. Thus, the structure of **10** was assigned as a BMH hydrolysis product in which both maleimide rings had been opened.

MS of fraction **14**, like that of **15**, showed a singly charged molecular ion at $m/z = 277.08$. However, the MS^2 fragmentation pattern of **14** was dramatically different from that obtained for compound **15** and was not consistent with any reasonable structure that could be derived for a possible MSC-DOTA[Y(III)] decomposition product. At this point, it is not possible to assign an unequivocal structure to compound **14**.
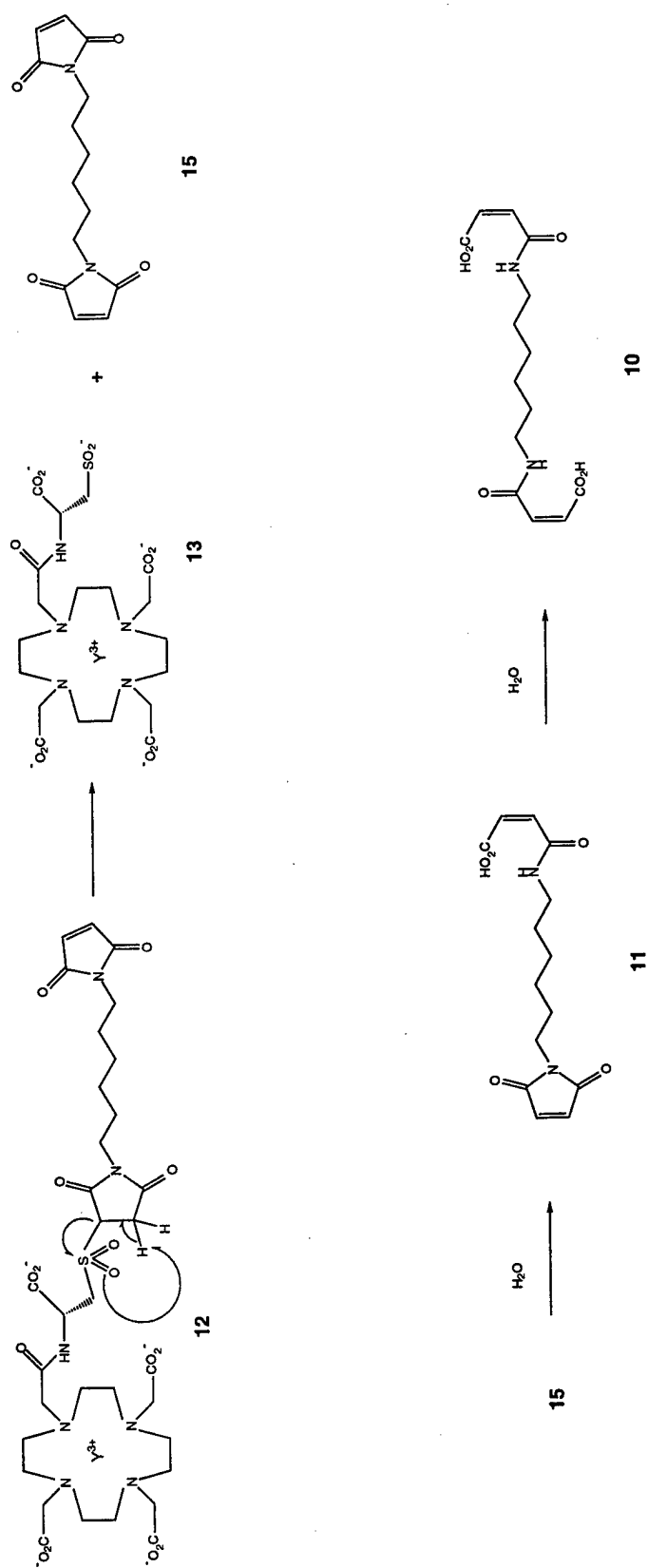
Figure 13. Proposed mechanism for the decomposition of MSC-DOTA[Y(III)] in aqueous solution.

HYDRAZIDO-DOTA DERIVATIVES: NEW REAGENTS FOR SITE-SPECIFIC CONJUGATION OF RADIOMETAL CHELATES TO ANTIBODY CARBOHYDRATE RESIDUES

The hydrazido-DOTA derivatives described in this report were originally designed as antibody prelabeling reagents. The three steps involved in prelabeling are chelation of the radiometal by the unconjugated BCA, purification of the radiometal chelate complex, and conjugation of the bifunctional chelate to the mAb. Meares and coworkers employed this method for ^{111}In and ^{90}Y labeling of a bifunctional peptide derivative of DOTA, which was then conjugated to the chimeric anti-adenocarcinoma mAb L6 (37). Because the antibody is present in large excess to the radiometal chelate during the conjugation reaction, the prelabeling approach has several potential advantages. Faster rates of radiometal binding are attainable by use of a large excess of unconjugated BCA. Each radiolabeled antibody molecule is singly modified, limiting potential immunogenicity and undesirable normal organ uptake while increasing immunoreactivity. One-step chemical modification and radiolabeling minimizes manipulation of the mAb.

The rationale for antibody prelabeling with the hydrazido-DOTA derivatives was that the protein-reactive hydrazide group should be more stable to hydrolysis than anhydride, active ester, and isothiocyanate functionalities. Reaction of hydrazide BCAs with the aldehyde groups generated by carbohydrate oxidation allows the formation of either hydrazone- or hydrazide-linked radiometal chelates, depending on whether the conjugate is treated subsequently with a reducing agent. Acid-labile hydrazone-linked immunoconjugates have been shown to effect tumor cell killing by the pH-sensitive intracellular release of chemotherapeutic agents (88, 89). In the case of transition metal radioimmunoconjugates, comparison of the biodistributions of mAbs modified with hydrazone- and hydrazide-linked DOTA might reveal important differences in the metabolism of the radiometal chelate.

In many situations conventional "cold kit" postlabeling of a mAb-chelator conjugate is desirable. Using the human/murine chimeric anti-CEA mAb cT84.66 (64) and the murine anti-CEA mAb ZCE025 (90), both prelabeling and postlabeling methods of radiometal chelate

57

conjugation were evaluated for hydrazido-DOTA derivatives. In the case of postlabeling, the length of the linker between chelating agent and antibody may be important, because the carbohydrate moiety resides on the interior surface of the C_H2 domain. To examine this potential effect, three new hydrazide derivatives of DOTA were synthesized: hydrazido-DOTA (**16**, linker length ~3.75 Å), carbohydrazido-DOTA (**17**, linker length ~7.5 Å), and hydrazidocysteineamido-DOTA (HC-DOTA, **18**, linker length ~20 Å).

Synthesis

Three synthetic routes to hydrazido-DOTA (**16**) are shown in Scheme 3. Reaction of isobutyl formoyl DOTA with 1 equiv of anhydrous hydrazine (Scheme 3 (middle)) in *N,N*-dimethylformamide:triethylamine (4:1), followed by purification of the desired product by anion-exchange chromatography, afforded the highest yield (17.3%) of the monohydrazide derivative of DOTA. Three by-products from the preparation of **16** were collected and identified by mass spectrometry. The side product eluting immediately before hydrazido-DOTA was determined to be the dihydrazide derivative of DOTA, while the tetrahydrazide and cyclic hydrazide derivatives of DOTA eluted at progressively higher concentrations of formic acid than the desired product. The aqueous-phase reaction of the sulfo-NHS ester of DOTA with 2 equiv of hydrazine monohydrochloride at pH 4.0 (Scheme 3 (top)) provided a 13.9% yield of hydrazido-DOTA.
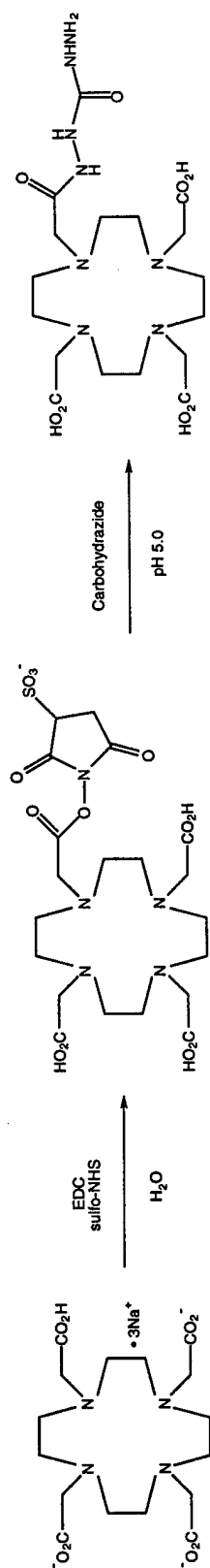
Scheme 3
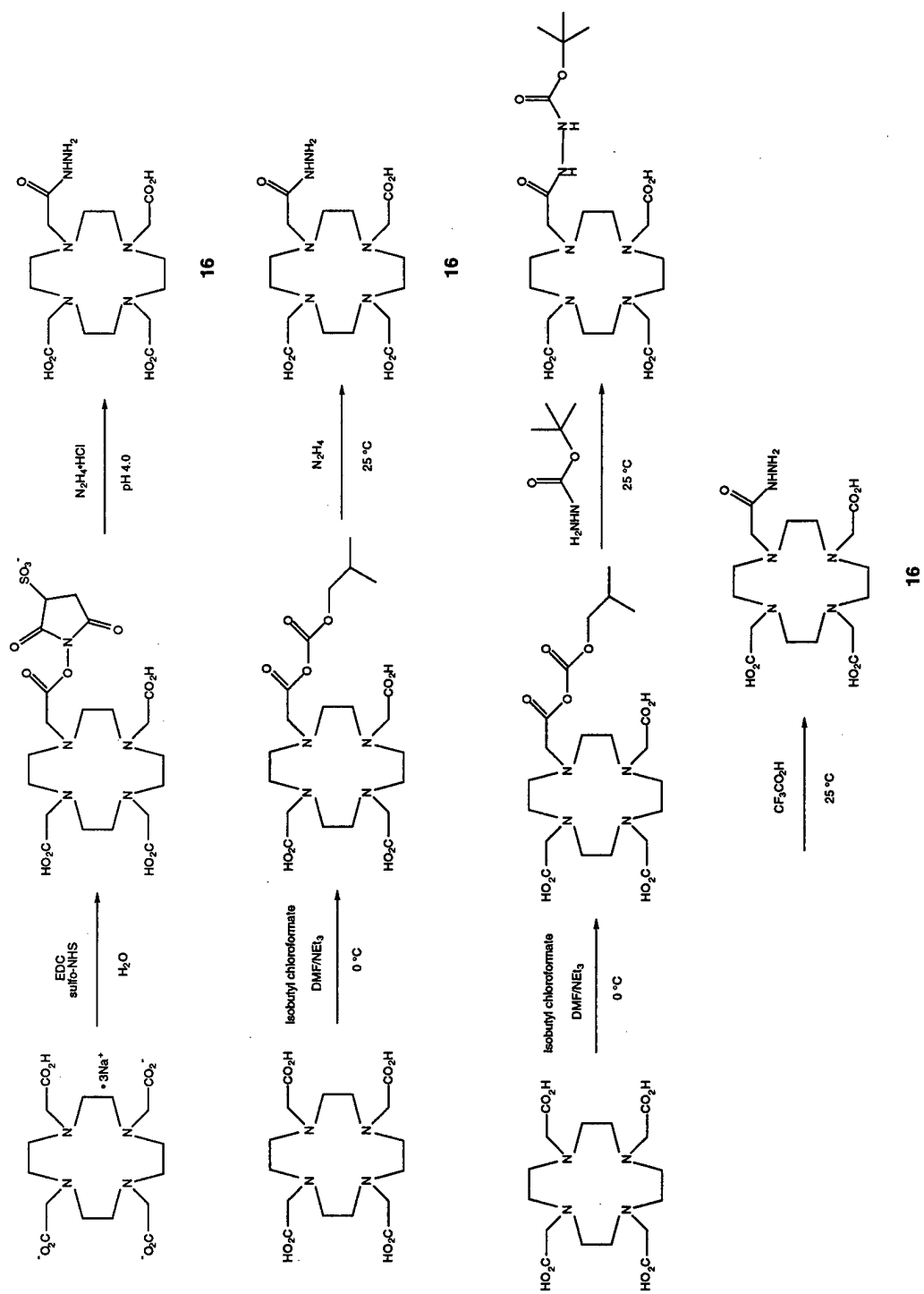
However, this method required sequential cation- and anion-exchange steps to purify the product, and, compared to the organic-phase reaction, larger quantities of the di- and trihydrazide derivatives of DOTA were obtained as by-products. An attempt was made to improve the synthesis by reacting the DOTA mixed anhydride with *tert*-butyl carbazate (Scheme 3 (bottom)), followed by deprotection with trifluoroacetic acid and purification by anion-exchange chromatography. Unfortunately, this route necessitated the time- and labor-intensive removal of DMF and TFA prior to deprotection and purification, respectively, and di-, tri-, and tetrahydrazide derivatives of DOTA were obtained as side products. The overall yield of hydrazido-DOTA synthesized from *tert*-butyl carbazate was 11.8%.

The synthesis of carbohydrazido-DOTA (**17**) is shown in Scheme 4. Because carbohydrazide is only sparingly soluble in organic solvents, carbohydrazido-DOTA had to be synthesized in aqueous solution from the sulfo-NHS ester of DOTA. After activation of DOTA with 2 equiv each of EDC and sulfo-NHS, the resulting active ester was reacted with 2 equiv of carbohydrazide at pH 5.0. The desired product was purified by sequential cation- and anion-exchange chromatography to give the monocarbohydrazide derivative of DOTA in 12.6% yield. Three side products from this reaction were identified by mass spectrometry. The dicarbohydrazide derivative of DOTA eluted immediately before the desired product, while DOTA monohydrazide and DO3A (1,4,7,10-tetraazacyclododecane N,N',N''-triacetic acid) eluted at higher concentrations of formic acid than carbohydrazido-DOTA. In the preparation of hydrazido-DOTA and carbohydrazido-DOTA, unreacted DOTA was recovered in 20-60% yield, recrystallized from $H_2O:CH_3OH$ (1:9), and recycled for other syntheses.

Scheme 4

EDC
sulfo-NHS

H₂O

Carbohydrazide

pH 5.0

17

As shown in Scheme 5, hydrazidocysteineamido-DOTA (HC-DOTA, **18**) was prepared by Michael addition of cysteineamido-DOTA (**1**) to ε-maleimidocaproic acid hydrazide (EMCH). Compound **1** was synthesized from the reaction of DOTA-OSSu with L-cysteine, a reaction similar to those employed for peptide synthesis (*80*) and synthesis of proteins by native chemical ligation (*81*). After reaction of **1** with EMCH, HC-DOTA (**18**) could be purified by reversed phase HPLC. Unfortunately, the starting material EMCH coeluted from the reversed phase column with the desired product. However, pure HC-DOTA was obtained in 54.9% yield when cysteineamido-DOTA was reacted with 0.95 equiv of EMCH, all of which was consumed by the essentially quantitative Michael addition. Under the conditions used for reversed phase HPLC, compound **18** eluted in two major peaks with retention times of 37.0 min and 37.7 min. When collected separately, these two peaks gave identical mass spectra consistent with the structure of the desired product. Therefore, the two product peaks probably represent a pair of diastereomers.

Antibody Prelabeling

The structure of the *N*-linked oligosaccharide of the human/murine chimeric anti-carcinoembryonic antigen mAb cT84.66, determined by mass spectrometry (*91*), is shown in Figure 14. Reaction of carbohydrate residues with periodate results in the preferential oxidation of *cis vic*-diols to pairs of aldehydes, with concomitant scission of the carbon-carbon bonds. Because of stereoelectronic and steric effects, oxidation of *trans vic*-diols by periodate is much slower than the reaction at *cis* diols. Thus, the primary site for carbohydrate-specific attachment of bifunctional chelates is the dialdehyde generated at the fucose (Fuc) residue. It should be noted that terminal galactose (Gal) residues are also easily oxidized by periodate. However, the mass spectra of the glycopeptide derived from cT84.66 suggest that terminal galactosylation is heterogeneous; therefore, Gal residues probably do not represent a major component of the carbohydrate sequence.

Scheme 5

L-Cysteine

pH 7.0

1

EDC
sulfo-NHS

H₂O

EMCH

K₂HPO₄/DMF
pH 7.5

18

63
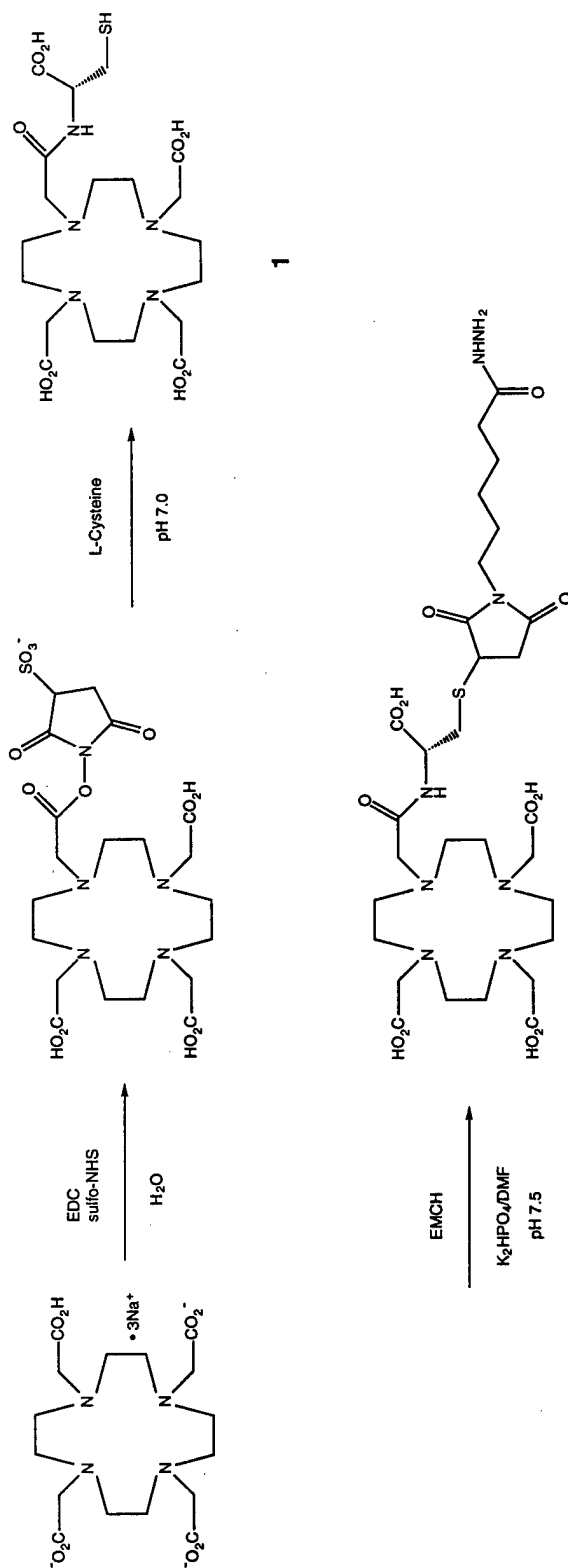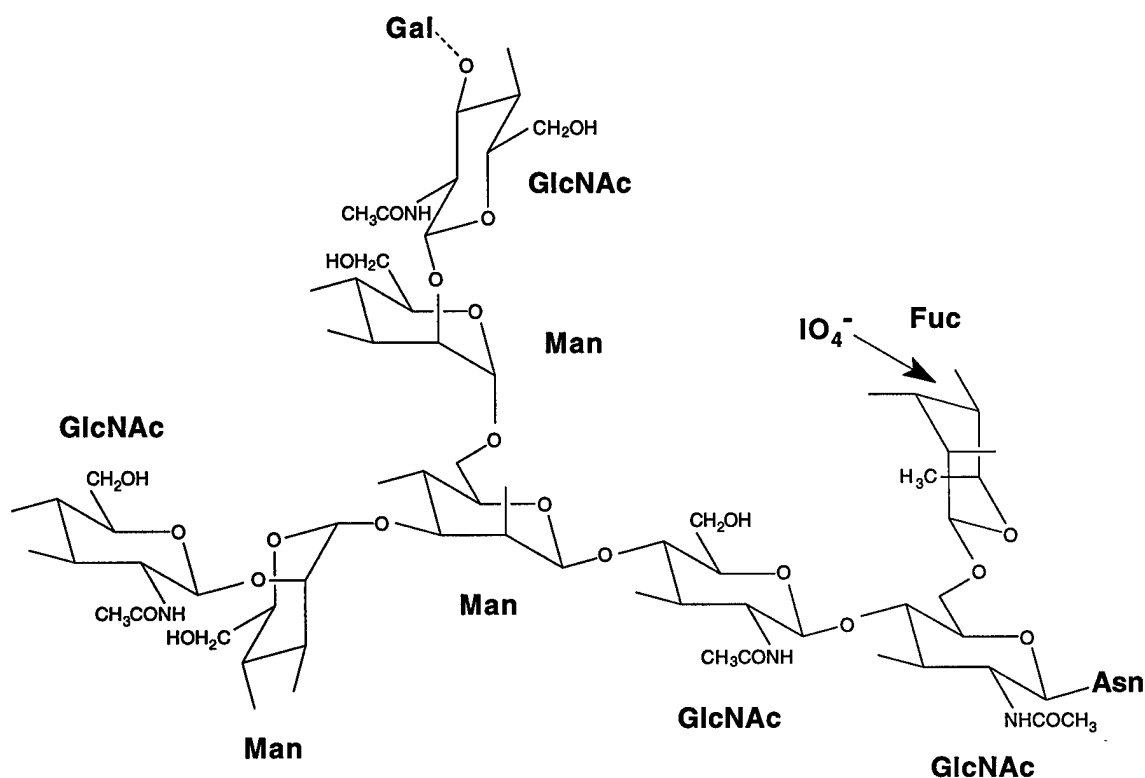
Figure 14. Structure of the carbohydrate moiety of cT84.66.

Hydrazido-DOTA was prelabeled with ^{90}Y(III) and conjugated to cT84.66. Radiochemical yields for each step of the prelabeling procedure are given in Table 5. Carrier-free ^{90}YCl$_3$ was chelated by a 1000-fold molar excess of hydrazido-DOTA in ammonium acetate, pH 7.0. After 30 min at 43 °C, the reaction mixture was challenged with 1 mM DTPA, pH 6.0, for 15 min at 37 °C, and TLC analysis indicated that 95.6% of the radiometal had been converted to the hydrazido-DOTA chelate. The hydrazido-DOTA[^{90}Y] complex was purified in 60.7% yield by spin column anion-exchange chromatography and concentrated *in vacuo* to a volume of approximately 10 μL.

The purified radiometal chelate was then conjugated to the mAb. Prior to conjugation, cT84.66 was oxidized with 4.75 mM NaIO$_4$, and the reaction was quenched with the addition of 7 mM sodium metabisulfite. The oxidized mAb was added immediately to the concentrated solution

64

of hydrazido-DOTA[^{90}Y], and the conjugation reaction was allowed to proceed for 30 min at 43 °C. The conjugate was reduced with 2 mM sodium cyanoborohydride and purified by size exclusion HPLC. HPLC analysis showed that only 2.2% of the hydrazido-DOTA[^{90}Y] complex was conjugated to cT84.66 and that approximately 90% of the mAb had been converted to soluble aggregates.

Table 5. Radiochemical Yields for Prelabeling of Periodate-Oxidized cT84.66 with Hydrazido-DOTA[^{90}Y(III)]

Step	Yield (%)
Chelation	95.6
Purification	60.7
Conjugation	2.2

Previous experience with cT84.66 has shown that antibody aggregates react with BCAs and can be labeled with radiometals with the same efficiency as the intact mAb. Therefore, the low yield for conjugation of cT84.66 with hydrazido-DOTA[^{90}Y(III)] might be attributable to a loss of reactivity of the BCA upon complexation of the radiometal. Unlike anhydride, active ester, or isothiocyanate reagents, hydrazido-DOTA is a nucleophilic BCA designed to react with electrophiles generated on the mAb. It is conceivable that chelation of a large radiometal ion with relatively high positive charge density resulted in an inductive effect that reduced the electron density around the hydrazide nucleophile, rendering it less reactive to aldehyde groups on oxidized antibody carbohydrate residues.

The prelabeling procedure resulted in extensive aggregation of cT84.66. It was subsequently determined that quenching of the periodate oxidation with metabisulfite was not sufficient to prevent antibody aggregation. When cT84.66 was treated with 2 mM NaIO$_4$ and the

reaction was quenched with 4 mM and 40 mM $Na_2S_2O_5$, the amount of mAb aggregation was 73.9% and 67.7%, respectively, after an additional 4 to 5 h at room temperature (data not shown). Ethylene glycol proved to be a superior reagent for reducing the extent of aggregation of cT84.66. Oxidation of the mAb with 2 mM $NaIO_4$, followed by the addition of 40 mM ethylene glycol, resulted in the formation of only 26.3% mAb aggregates after an additional 4 h at room temperature (data not shown). On the basis of these results, it was decided to oxidize cT84.66 with periodate, quench the oxidation with ethylene glycol, and conjugate the oxidized mAb with hydrazido-DOTA. This approach was amenable to postlabeling with radiometals.

Conjugation of cT84.66 with Hydrazido-DOTA

Hydrazido-DOTA was conjugated to cT84.66 after oxidation of the mAb with 2.4 mM $NaIO_4$ and quenching of the excess periodate with 39 mM ethylene glycol. The oxidized cT84.66 was purified by spin column gel filtration chromatography and conjugated with hydrazido-DOTA at a BCA:mAb molar ratio of 100:1. Alternatively, the resulting DOTA hydrazone conjugate was converted to a hydrazide conjugate by reduction with 1 mM $NaBH_3CN$. The number of chelates conjugated per antibody molecule was determined by a modification of a [57]Co(II) binding assay (10, 36). TLC analysis revealed that the DOTA hydrazone conjugate was modified with an average of 3.4 chelates per mAb and the DOTA hydrazide conjugate was modified with an average of 2.4 chelates per mAb.

Gel filtration HPLC (Figure 15) and SDS polyacrylamide gel electrophoresis (Figure 16) analysis of the cT84.66-DOTA hydrazone and hydrazide conjugates showed that in both cases approximately 76% of the mAb had been converted to dimers and higher molecular weight species. Performing all steps of the conjugation procedure at 4 °C and reacting unconjugated aldehydes with sodium borohydride or hydroxylamine had no effect on the extent of mAb aggregation (data not shown). The aggregate species remained intact in the absence of cyanoborohydride reduction and even under the strongly denaturing conditions of SDS gel electrophoresis. This result suggested

that stable covalent bonds had been formed between antibody molecules during the oxidation and conjugation process. The reaction of cT84.66 with periodate may have resulted in the formation of unusually stable Schiff bases between aldehyde groups on the oxidized carbohydrate of one mAb molecule and lysine residues of other mAb molecules, leading to aggregation.

Radiolabeling of cT84.66-DOTA Hydrazone

An attempt was made to label the cT84.66-DOTA hydrazone conjugate with [111]In(III) at a ratio of 5.00 mCi/mg. [111]InCl$_3$ in 0.04 N HCl and cT84.66-DOTA hydrazone in 0.25 M ammonium acetate were added sequentially to 0.25 M ammonium acetate, pH 6.0, and the reaction mixture was incubated at 43 °C for 45 min. The reaction mixture was challenged with 1 mM EDTA, pH 6.5, for 15 min at 37 °C, injected onto two Pharmacia Superose 12 HR 10/30 columns (1 × 30 cm) in series, and eluted with an isocratic mobile phase of normal saline. Gel filtration HPLC indicated that only 0.1% of the ^{111}In label was incorporated into the mAb fraction. This small amount of radioactivity was associated with the highest molecular weight fraction (void peak) of the cT84.66-DOTA hydrazone conjugate.
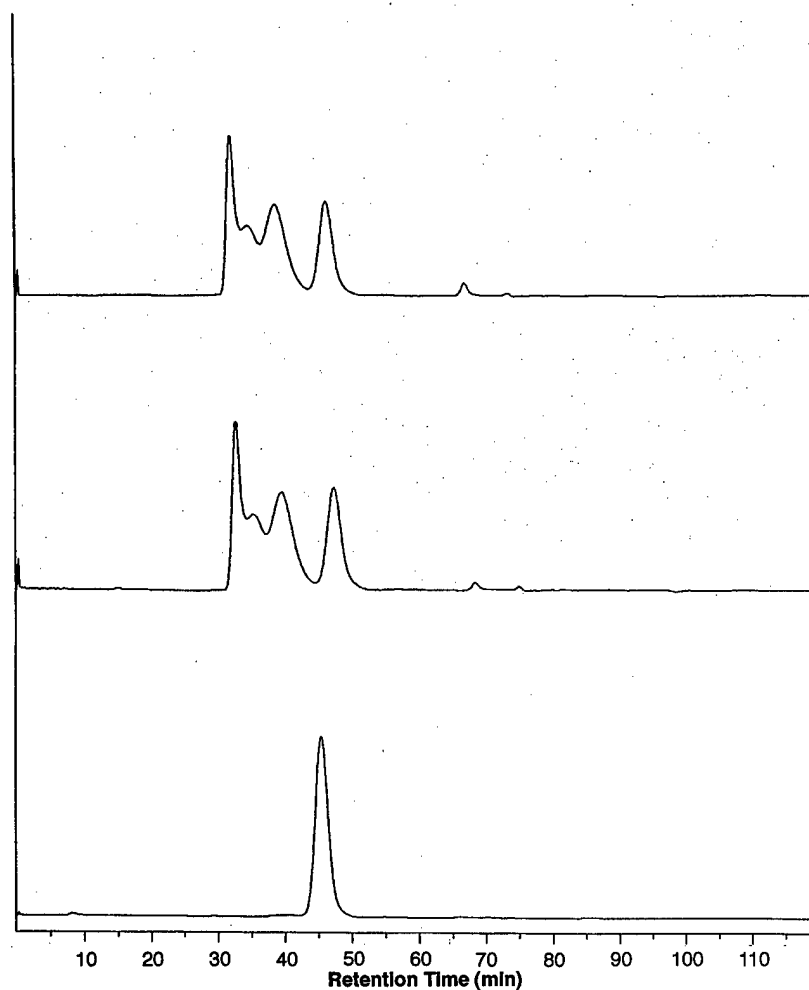
Figure 15. Gel filtration chromatography of unoxidized and unconjugated cT84.66 (bottom), cT84.66-DOTA hydrazone (middle), and cT84.66-DOTA hydrazide (top). Aliquots of 50 µg of the conjugates were injected onto two Pharmacia Superose 12 HR 10/30 columns (1 × 30 cm) in series and eluted with an isocratic mobile phase of 0.05 M Na_2SO_4/0.02 M NaH_2PO_4/0.05% NaN_3, pH 6.8, at a flow rate of 0.5 mL/min. Absorbance was monitored at 280 nm. The peak eluting at 45 min retention time corresponds to an apparent molecular size of 150 kDa.
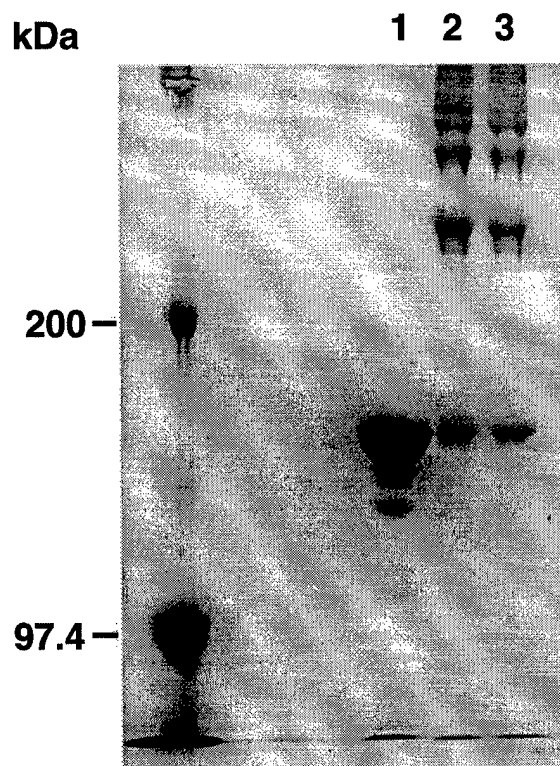
Figure 16. Non-reducing SDS polyacrylamide gel electrophoresis of unoxidized and unconjugated cT84.66 (lane 1) and cT84.66-DOTA hydrazone (lane 2) and hydrazide (lane 3) conjugates. Molecular weight markers are shown to the left. An aliquot of 5 µg of each conjugate was loaded onto a 5% polyacrylamide gel (8 × 8 cm) with a 3% stacking layer (2 × 8 cm).

A plausible explanation for this low radiometal labeling yield is that the antibody carbohydrate moiety resides on the interior surface of the C_H2 domain, and the BCA is inaccessible to the radiometal when a relatively short linker is employed. It should be noted that the fucose residue in particular is located proximal to the peptide backbone of the protein. In order to achieve rapid and efficient radiometal labeling, it may be necessary to space the bifunctional chelating agent away from the interior of the C_H2 domain with a longer linker.

Conjugation of ZCE025 with Hydrazido-DOTA, Carbohydrazido-DOTA, and HC-DOTA

Oxidation of cT84.66 with periodate and conjugation with hydrazido-DOTA resulted in extensive aggregation of the mAb, and the ^{111}In labeling efficiency of the cT84.66-DOTA hydrazone conjugate was extremely low. Because of these difficulties, the murine anti-CEA mAb ZCE025, which has successfully undergone carbohydrate oxidation and site-specific BCA conjugation (92), was selected for reaction with a series of hydrazido-DOTA derivatives with progressively longer chelator-antibody linkers. The three DOTA derivatives hydrazido-DOTA (16, linker length ~3.75 Å), carbohydrazido-DOTA (17, linker length ~7.5 Å), and hydrazidocysteineamido-DOTA (HC-DOTA, 18, linker length ~20 Å) were used for these experiments.

ZCE025 was oxidized according to the literature procedure with 22 mM $NaIO_4$, and the excess periodate was quenched with the addition of 1,3-diaminopropan-2-ol to a final concentration of 30 mM. The oxidized antibody was purified by spin column gel filtration chromatography and then conjugated with compounds 16, 17, and 18 at a BCA:mAb molar ratio of 100:1. Aliquots of the resulting hydrazone conjugates were converted to hydrazide conjugates by reduction with 10 mM $NaBH_3CN$. Gel filtration HPLC analysis of the ZCE025 conjugates (Figure 17) showed that aggregation of the mAb was minimal and that all of the conjugates exist as species with an apparent molecular size of 150 kDa. The ZCE025 conjugates were analyzed by [57]Co(II) binding (10, 36) to determine the number of chelates per mAb. All of the conjugates exhibited the same amount of nonspecific [57]Co binding (<1%) as the unconjugated antibody control, indicating that in each case no BCA conjugation had taken place.
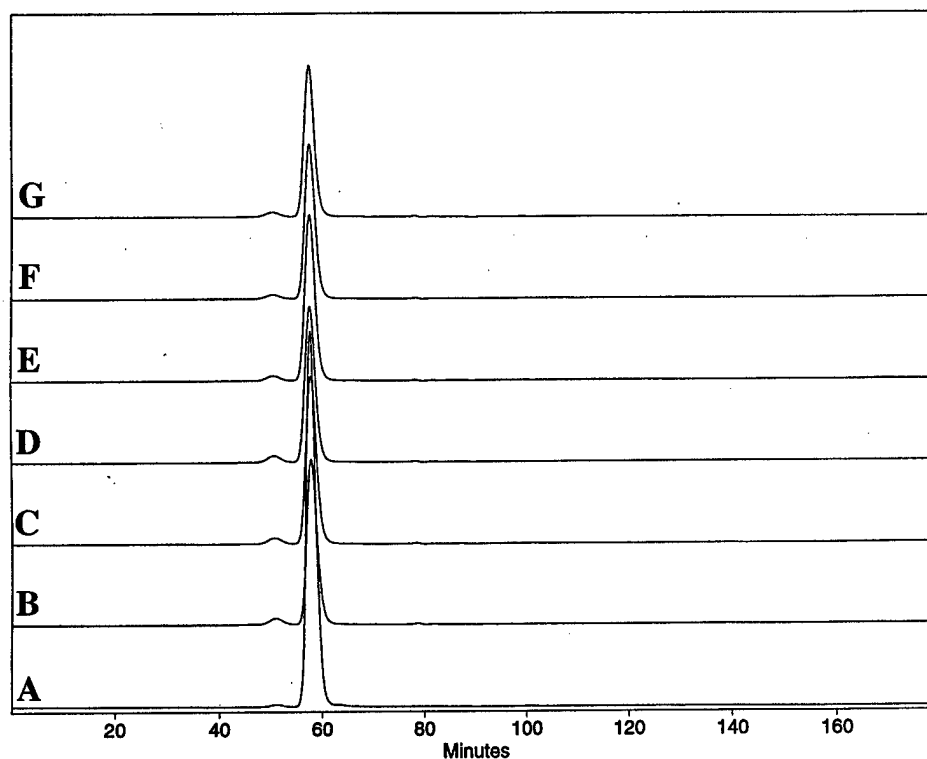
Figure 17. Gel filtration chromatography of unoxidized and unconjugated ZCE025 (A),

ZCE025-DOTA hydrazone (B), ZCE025-DOTA carbohydrazone (C), ZCE025-HCDOTA

hydrazone (D), ZCE025-DOTA hydrazide (E), ZCE025-DOTA carbohydrazide (F), and ZCE025-

HCDOTA hydrazide (G). Aliquots of 20 to 30 µg of the conjugates were injected onto two

Pharmacia Superose 6 HR 10/30 columns (1 × 30 cm) in series and eluted with an isocratic mobile

phase of 0.05 M Na_2SO_4/0.02 M NaH_2PO_4/0.05% NaN_3, pH 6.8, at a flow rate of 0.5 mL/min.

Absorbance was monitored at 280 nm. The peak eluting at 60 min retention time corresponds to an

apparent molecular size of 150 kDa.

The carbohydrate conjugation procedure developed by Pochon *et al.* (*92*) was applied to the

modification of ZCE025 with an aminooxy derivative of the chelating agent desferrioxamine.

These authors stated that when an alkyl or aryl amine is reacted with oxidized carbohydrate

residues, formation of undesirable Schiff bases between aldehydes and side chain or terminal amines of the antibody can interfere with conjugation and result in unwanted cross-links. Pochon and coworkers exploited the low pK_a of the aminooxyacetyl group to form aldehyde oximes readily at pH 3 to 5. Under these conditions, the aliphatic amino groups of the mAb would be mostly protonated and much less likely to form Schiff bases. Alkyl and acyl hydrazides, on the other hand, have pK_a values in the range of 4 to 5. Because of these higher acid dissociation constants, conjugation of ZCE025 to the hydrazido-DOTA derivatives was performed at pH 6.0. At this pH, it is possible that formation of kinetically unstable but thermodynamically stable Schiff bases between mAb aldehydes and amino groups impeded the reaction of oxidized ZCE025 with the hydrazido-DOTA compounds. However, it is more likely that extensive Schiff base formation occurred when the antibody was treated with the quench reagent 1,3-diaminopropan-2-ol, despite purification of the oxidized mAb from the low molecular weight reactants by gel filtration chromatography. Reaction with 1,3-diaminopropan-2-ol could also have prevented conjugation of the bifunctional chelating agents.

BIODISTRIBUTION OF [111]IN- AND ^{90}Y-LABELED DOTA AND MALEIMIDOCYSTEINEAMIDO-DOTA CONJUGATED TO CHIMERIC ANTI-CARCINOEMBRYONIC ANTIGEN ANTIBODY IN XENOGRAFT-BEARING NUDE MICE

Macrocyclic ligands have been advocated as one possible methodology to reduce yttrium loss *in vivo* (*25, 27, 93, 94*). Meares and coworkers (*25, 27, 93*) have demonstrated bone uptakes on the order of 2% ID/g in nude mice receiving 1,4,7,10-tetraazacyclododecane N,N',N'',N'''-tetraacetic acid (DOTA) derivatives labeled with ^{90}Y and conjugated to Lym-1 (*25*) and chimeric L6 (*93*) antibodies. In these studies, the radiometal was incorporated into the BCA prior to mAb conjugation. Similar bone uptake values have been reported by Harrison *et al.* (*94*) using the anti-colon cancer antibody B72.3, which was covalently linked to DOTA before radiolabeling. In these earlier works, however, little numerical comparison was made between

indium and yttrium biodistributions in animals. Deshpande *et al.* (*25*) used the mAb Lym-1, which targets to B lymphocytes within the bone so as to confound analyses. Harrison and coworkers utilized only ^{90}Y in their B72.3 studies (*94*). One recent report (*93*) included both radiometals but did not analyze their differences statistically *in vivo*. The need to compare ^{111}In- and ^{90}Y-labeled antibody biodistributions for DOTA-based BCAs led to the evaluation of the cT84.66-DOTA and cT84.66-MCDOTA conjugates in a tumor-bearing mouse model. These studies were performed by personnel in the Department of Radioimmunotherapy at City of Hope, as part of an NIH-funded research program.

The human/murine chimeric anti-carcinoembryonic antigen mAb cT84.66 (*64*) has shown minimal crossreactivity with normal human or murine tissues, and biodistributions of ^{111}In- and ^{90}Y-labeled cT84.66 have been evaluated using a bifunctional DTPA derivative (*65*). Athymic nude mice implanted with CEA-expressing LS174T human colorectal tumor xenografts were used in that study. In the studies described here, the ^{111}In and ^{90}Y biodistributions of cT84.66 conjugated to two new DOTA derivatives were obtained in the LS174T-bearing nude mouse model. These studies were conducted by personnel in the Department of Radioimmunotherapy, as part of an NIH-funded research program at City of Hope. When endogenous primary amino groups of the mAb were reacted with the *N*-hydroxysulfosuccinimide ester of DOTA, the radiometal-labeled conjugate displayed extremely high kinetic stability *in vitro* (*36*). In contrast, radiometals conjugated to reduced interchain disulfide bonds in the mAb with maleimidocysteineamido-DOTA (MC-DOTA) were chemically labile at physiological temperature and pH. This BCA exhibited pH-dependent linker hydrolysis *in vitro*, which resulted in release of Y(III) in chelated form.

For both macrocycle-antibody conjugates, the biodistributions obtained with ^{111}In *versus* ^{90}Y were compared. Likelihood of bone uptake of yttrium was evaluated for each macrocycle. In addition, blood clearance curves were analyzed for all four combinations of label and BCA. The latter two studies provided information that can be used to select an optimal BCA for reducing bone marrow absorbed dose during clinical trials.

cT84.66-DOTA Biodistributions

The results of separate biodistribution studies for [111]In- and ^{90}Y-labeled cT84.66-DOTA are given in Figures 18 and 19, respectively, and Tables 8 and 9 (see Appendix), respectively. For both radiometals, blood was the dominant normal tissue out to 48 h. High uptakes were seen in the lung (18% ID/g) initially and in the liver as time exceeded 18 h. With the indium label, hepatic accumulation (11-14% ID/g) eventually exceeded that of yttrium (4-7% ID/g). Highest accumulation, however, was ultimately obtained in the tumor, where values approached 60% ID/g at time points as early as 18-24 h. This level of tumor uptake remained relatively constant out to 96 h for both radiometals.

Figure 18. (Top) Percent injected dose per gram (% ID/g) of blood (●), liver (■), bone

(○), and tumor (△) for ^{111}In-labeled cT84.66-DOTA in LS174T tumor-bearing nude mice.

(Bottom) Percent injected dose per gram (% ID/g) of spleen (▲), kidney (□), lung (◆), and

bowel (▽) for ^{111}In-labeled cT84.66-DOTA in LS174T tumor-bearing nude mice. Standard

errors of the mean (SE) are indicated; all data were corrected for radiodecay.
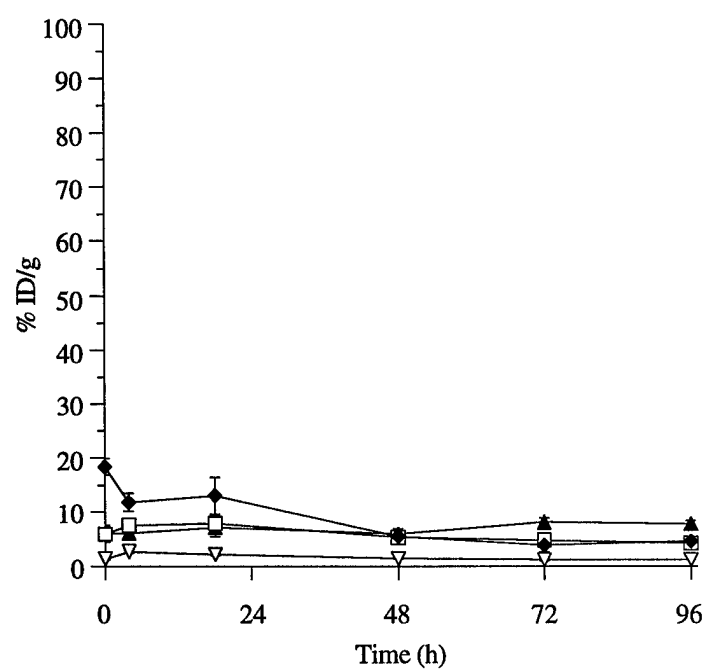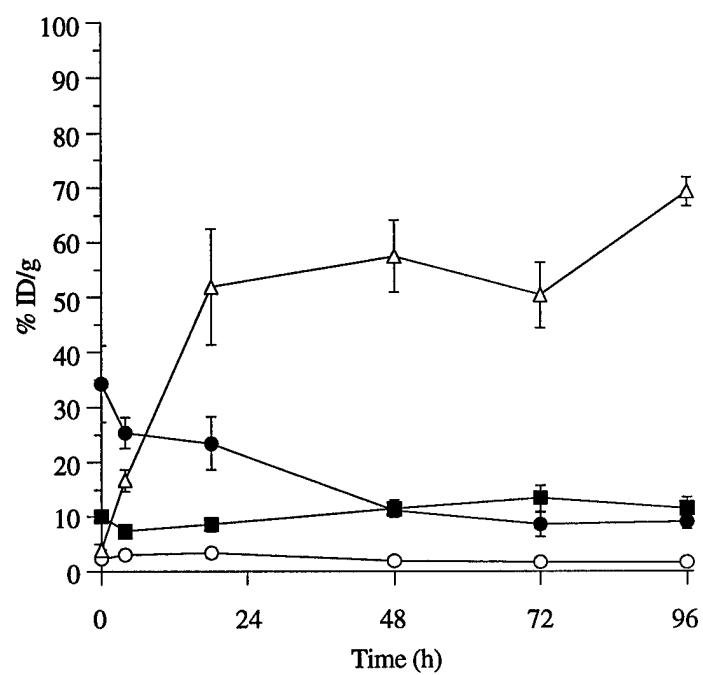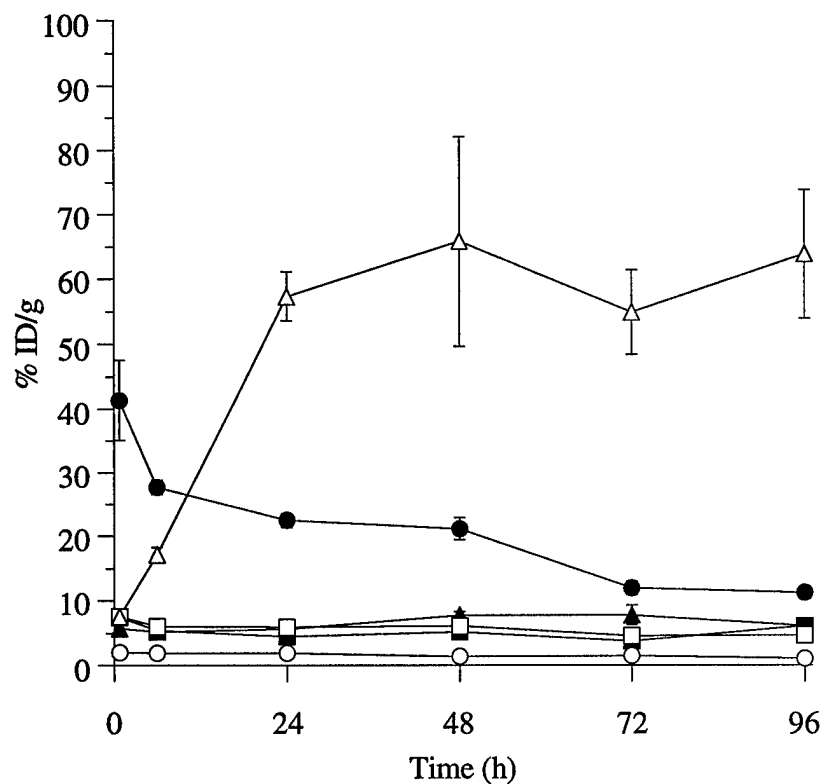
Figure 19. Percent injected dose per gram (% ID/g) of blood (●), liver (■), bone (○),

tumor (△), spleen (▲), and kidney (□) for ^{90}Y-labeled cT84.66-DOTA in LS174T tumor-

bearing nude mice. Standard errors of the mean (SE) are indicated; all data were corrected for

radiodecay.

cT84.66-MCDOTA Biodistributions

Organ and tissue uptakes for the simultaneous biodistribution of ^{111}In- and ^{90}Y-labeled

cT84.66-MCDOTA are shown in Figures 20 and 21, respectively, and Tables 10 and 11 (see

Appendix), respectively. As in the case of the DOTA conjugate, blood was the dominant normal

77

tissue out to 48 h. At early time points, lung accumulation was the second highest value with the indium label (9-17% ID/g). No lung data were obtained for yttrium. Hepatic uptakes for both labels approached 10% ID/g by the end of the experimental period. Tumor accumulation exceeded 60% ID/g for both radiometals at 48 h but began to decrease slowly at later time points.

Comparison of Radiometals

Comparison of the indium and yttrium uptakes resulting from the cT84.66-DOTA agent revealed that only the liver showed consistently different values at the three common time points (48, 72, and 96 h). At these intervals, hepatic uptake of ^{111}In was consistently higher (p < 0.05) than that of [90]Y. None of the other six tissues showed more than one point at which the uptakes differed significantly (p > 0.05).

Indium and yttrium uptakes from the cT84.66-MCDOTA biodistributions were evaluated using the Lin concordance coefficient (*95*). For blood, bone, tumor, and liver, pooled concordance coefficients were 0.9942, 0.8698, 0.9042, and 0.6460, respectively. Graphical representations of the blood and liver data are shown in Figures 22 and 23. Reference lines shown on each of the two graphs are the lines of identity. It was noteworthy that the reduced concordance of hepatic samples was a result of greater accumulation of ^{111}In from the MC-DOTA conjugate in liver tissues.

Figure 20. (Top) Percent injected dose per gram (% ID/g) of blood (●), liver (■), bone

(○), and tumor (△) for ^{111}In-labeled cT84.66-MCDOTA in LS174T tumor-bearing nude mice.

(Bottom) Percent injected dose per gram (% ID/g) of spleen (▲), kidney (□), lung (◆), and

bowel (▽) for ^{111}In-labeled cT84.66-MCDOTA in LS174T tumor-bearing nude mice. Standard

errors of the mean (SE) are indicated; all data were corrected for radiodecay.

80
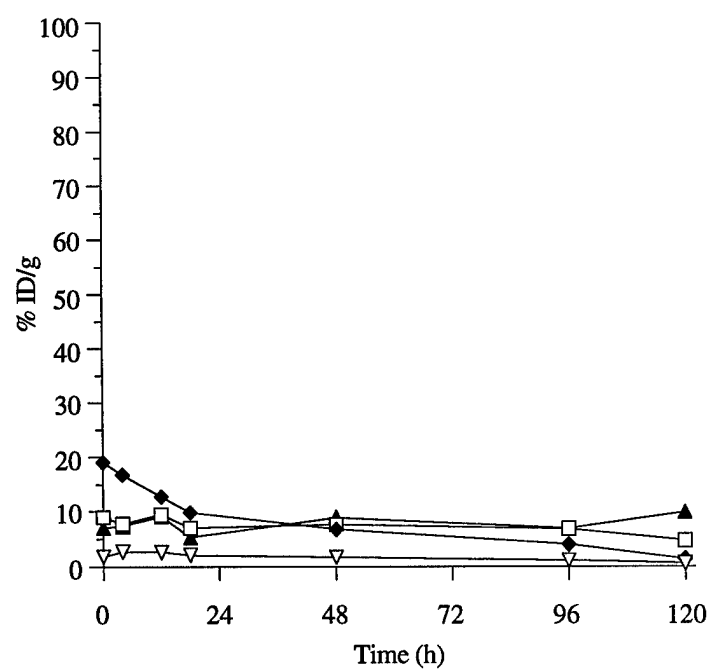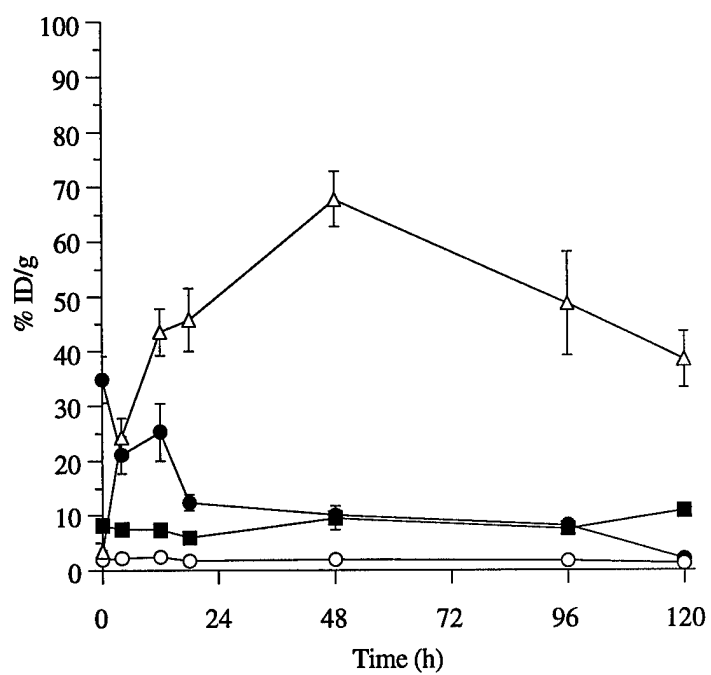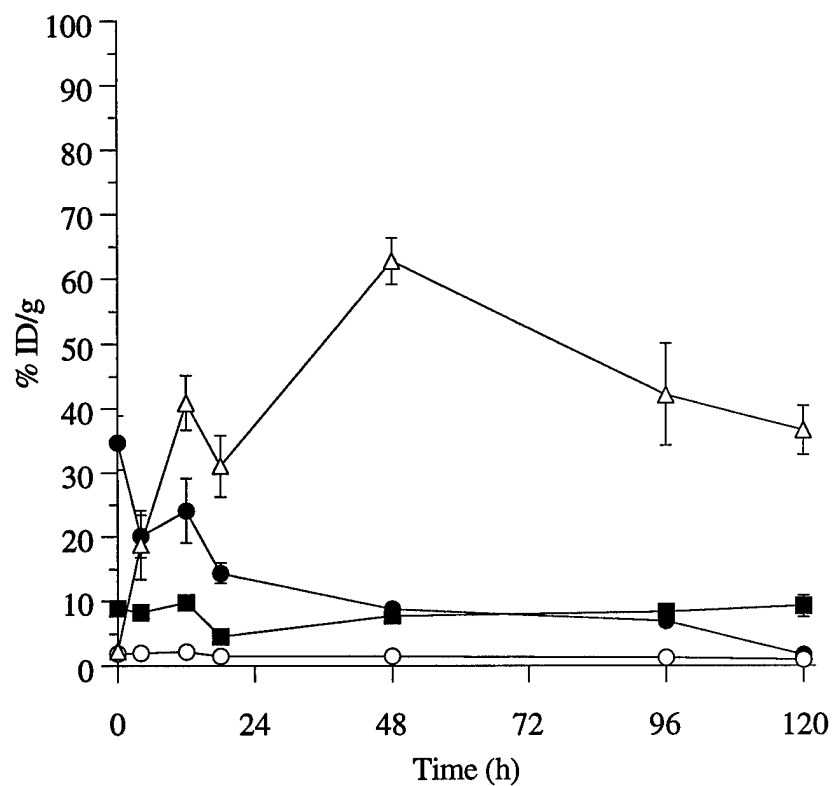
Figure 21. Percent injected dose per gram (% ID/g) of blood (●), liver (■), bone (○), and

tumor (△) for ^{90}Y-labeled cT84.66-MCDOTA in LS174T tumor-bearing nude mice. Standard

errors of the mean (SE) are indicated; all data were corrected for radiodecay.
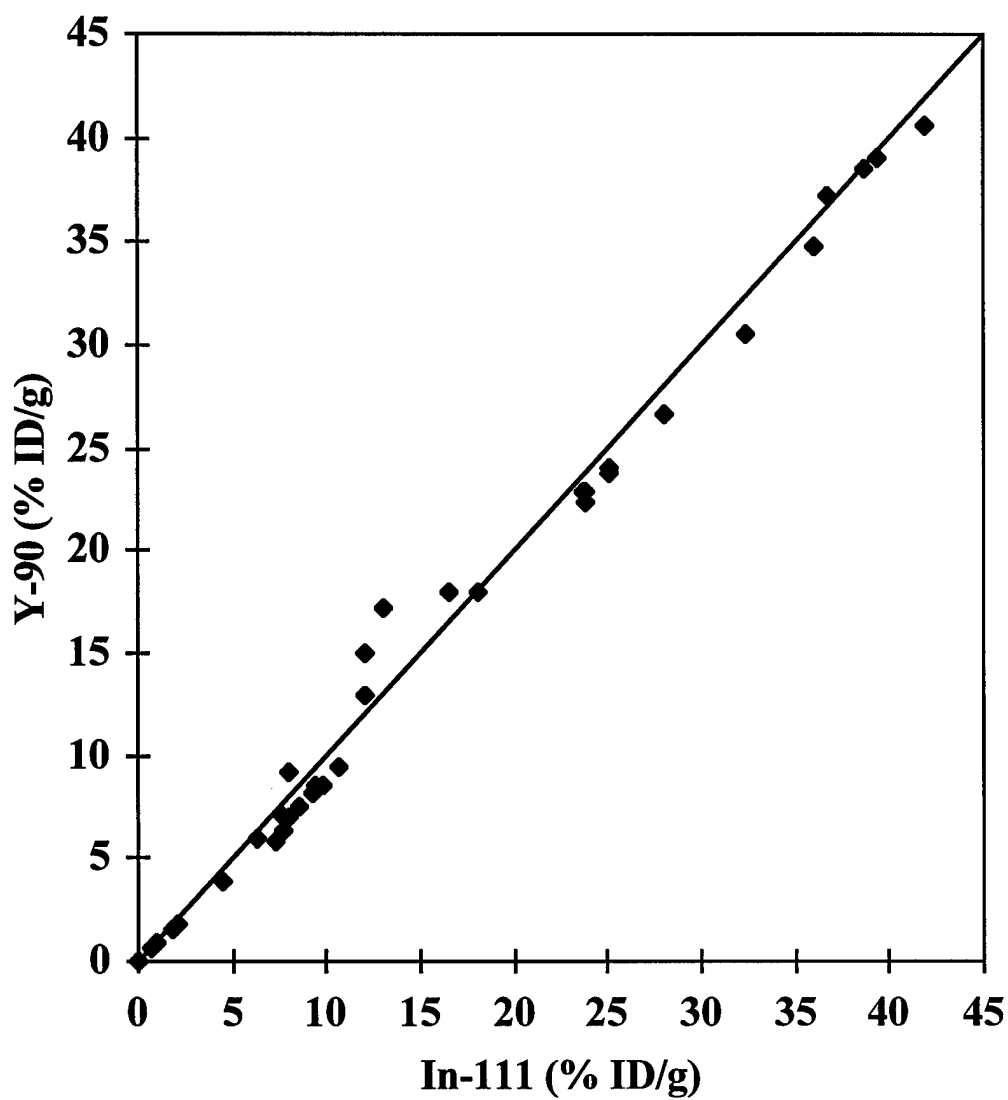
Figure 22. Concordance correlation analysis of blood data for cT84.66-MCDOTA. Uptakes are plotted along both axes, with the ^{111}In-labeled cT84.66-MCDOTA along the horizontal and the ^{90}Y-labeled cT84.66-MCDOTA along the vertical axis. All time points are considered. Reference line shown is the line of identity.
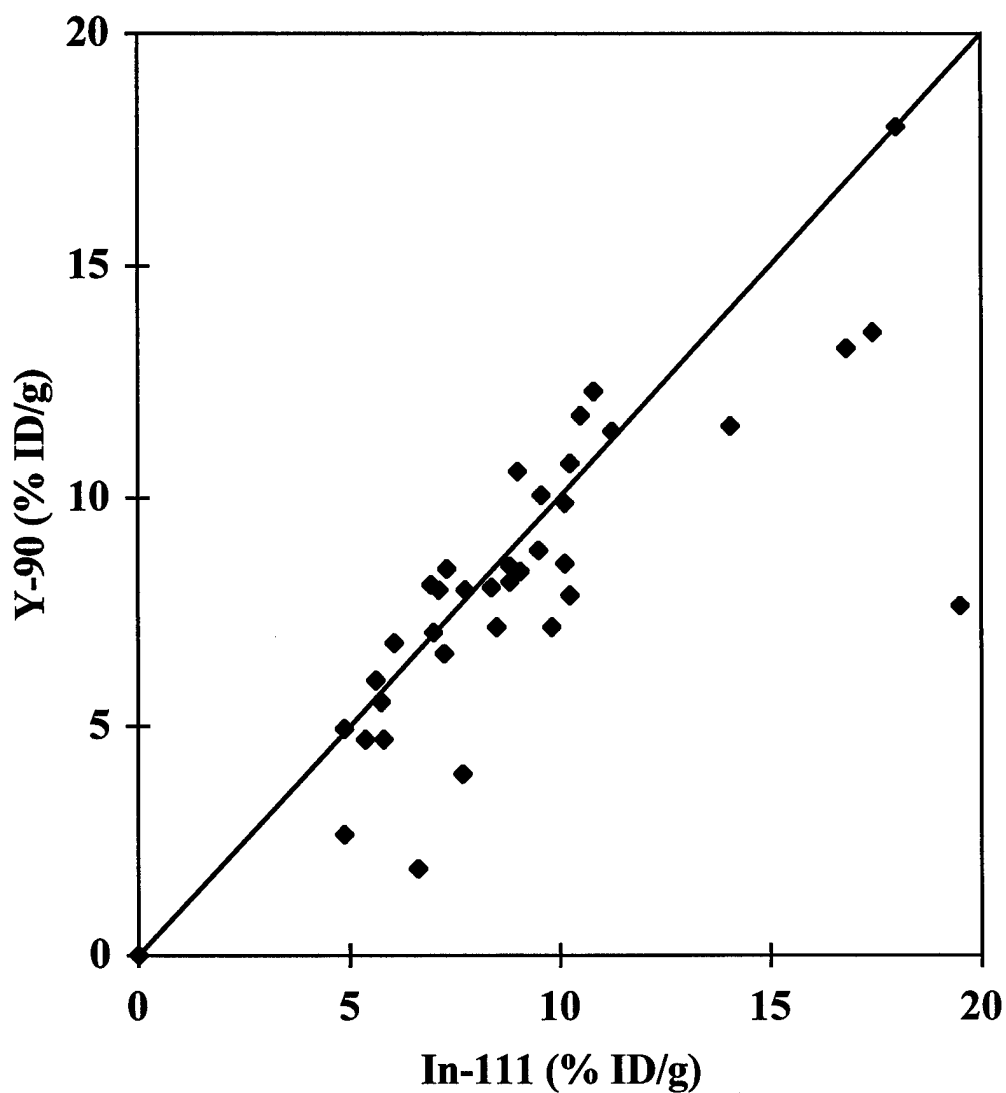
Figure 23. Concordance correlation analysis of liver uptake for cT84.66-MCDOTA. The ^{111}In-labeled cT84.66-MCDOTA is plotted along the horizontal and the ^{90}Y-labeled cT84.66-MCDOTA is plotted along the vertical axis. All time points are considered. Reference line shown is the line of identity.

Bifunctional Chelate Effects

The biodistribution properties of the cT84.66-DOTA and cT84.66-MCDOTA conjugates were compared for the ^{111}In label. Five time points were common to the two experiments: 0, 4, 18, 48, and 96 h. Blood values of ^{111}In were generally higher for cT84.66-DOTA than for cT84.66-MCDOTA throughout, but statistically significant differences were found only at 18 and 48 h. The cT84.66-MCDOTA conjugate showed significantly greater indium uptake in the kidneys at two of five times (48 and 96 h).

Corresponding tissue uptakes of ^{90}Y from cT84.66-DOTA and cT84.66-MCDOTA were also compared. Four tissues were available at two common time points. At both times, significantly lower yttrium blood levels were obtained with cT84.66-MCDOTA. No significant differences were observed for hepatic or bone uptakes.

[90]Y Loss from Macrocycle and Bone Uptake

Bone uptake of ^{90}Y was compared for the two macrocyclic BCAs using the t-statistic. Using data from Figures 19 and 21, no significant differences were seen in bone uptake at the 5% level of confidence. Initial values (t = 0) were on the order of 2% ID/g and decreased to 1.07% ID/g by the end of the experiment (t = 96 h) for ^{90}Y-labeled cT84.66-DOTA. In the case of cT84.66-MCDOTA, the experiments were carried out to 120 h, at which time the bone uptake had been further reduced to 0.95% ID/g.

Blood Curve Analyses

Results from the blood curve analyses are given in Table 6. Half-lives were determined from the rate constants by the relationship $T_{1/2} = \ln(2)/k$. The first exponential (k_1) could be estimated, but its error or that of its associated half-life was indeterminate for either macrocycle-

antibody conjugate. The primary reason for this difficulty appeared to be a slight inflection in the blood curves for cT84.66-DOTA and cT84.66-MCDOTA, making eqn 1 (see below) a more approximate representation for the early time points (96). For both radiometals, it was found that characteristic blood half-times were comparable for cT84.66-DOTA and cT84.66-MCDOTA. Initial biological half-times were generally on the order of 0.2 to 0.4 h, while the second biological half-time was much larger, on the order of 40 h or longer.

Table 6. Results of two-exponential fit of blood curves for cT84.66-DOTA and cT84.66-MCDOTA[a]

BCA-Label	A_1 (% ID/g)	A_2 (% ID/g)	k_1 (h^{-1})	k_2 (10^{-2} h^{-1})	$T_{1/2,1}$ (h)	$T_{1/2,2}$ (h)
DOTA-^{111}In	6.47 (6.1)	27.8 (5.3)	3.26 (--)	1.48 (0.44)	0.212 (--)	46.8 (14.0)
MCDOTA-^{111}In	11.4 (7.9)	23.5 (6.1)	3.31 (--)	1.60 (0.82)	0.209 (--)	43.3 (22.1)
DOTA-^{90}Y	42.4 (--)	29.7 (5.0)	1.69 (--)	1.02 (0.33)	0.410 (--)	68.0 (21.8)
MCDOTA-^{90}Y	11.2 (6.3)	23.5 (4.9)	3.49 (--)	1.72 (0.70)	0.199 (--)	40.3 (16.3)

[a]Standard deviations are shown in parentheses. The symbol (--) denotes that an error could not be estimated with the two-exponential fit of eqn (1).

Figure 24 shows the ^{90}Y blood clearance curves for cT84.66-DOTA and cT84.66-MCDOTA. The curve for the MC-DOTA conjugate was below that of the corresponding DOTA conjugate throughout the time range; significant differences were observed at both common time points (48 and 96 h). It should be noted that ^{111}In-labeled cT84.66-MCDOTA exhibited faster blood clearance throughout the experimental period, but this difference was only significant at two time points, as described above.
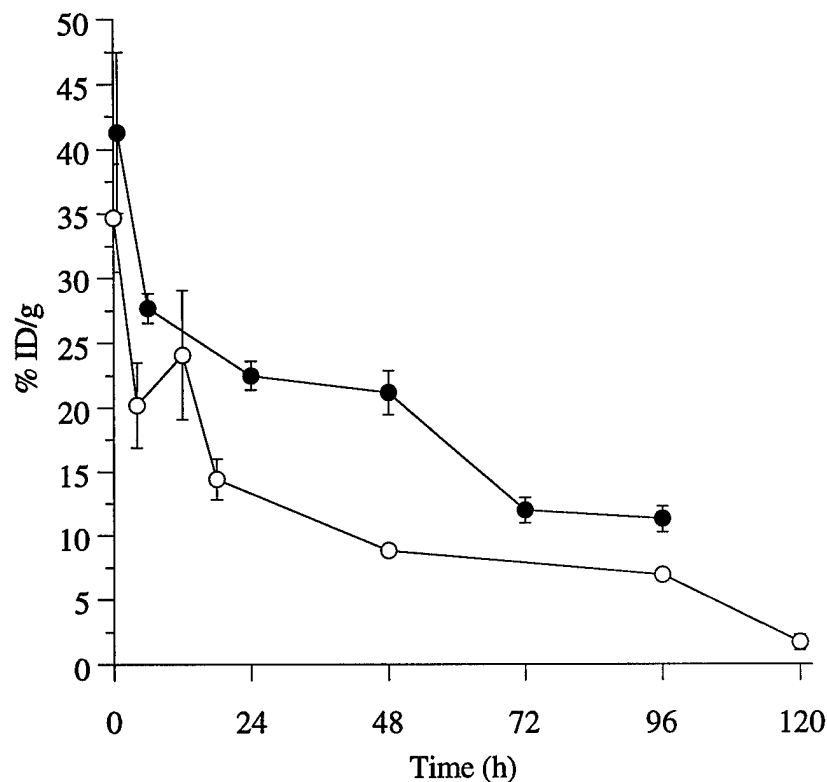
Figure 24. Blood clearance curves (% ID/g) for ^{90}Y-labeled cT84.66-DOTA (●) and cT84.66-MCDOTA (○). All data have been corrected for radiodecay. Measured standard errors of the mean (SE) are indicated.

RECOMMENDATIONS

Cyclen-Based Syntheses

The proposed Statement of Work outlined the synthesis, antibody conjugation, radiometal labeling, and *in vitro* evaluation of tris(3-sulfopropyl)-monoacetic acid, tetraethanethiol,

tetraacetohydroxamic acid, and triacetohydroxamic acid-monoacetohydrazide derivatives of cyclen, to be accomplished in Year 2 of the contract. However, the Principal Investigator was awarded a Ph.D. degree in Biological Sciences three and one half months into Year 2, and the contract was terminated. The results of preliminary investigations directed toward the synthesis of sulfopropyl, ethanethiol, and acetohydroxamate derivatives of cyclen are described below. This work is being continued by a graduate student in Dr. John E. Shively's laboratory at City of Hope.

Preparation of Cyclen Free Base

The free base of cyclen (1,4,7,10-tetraazacyclododecane) was prepared readily from a commercially available salt, providing a precursor for the synthesis of several novel derivatives with potential for faster complexation, high-stability chelation, and improved selectivity in metal ion binding. Cyclen free base was obtained from the inexpensive tetrahydrogensulfate salt (Parish) by treatment with a 60-fold excess of sodium hydroxide and continuous extraction into tetrahydrofuran (*97*). The ^{1}H NMR spectrum (200 MHz, CDCl$_3$) of this precursor was consistent with the correct structure, and the uncorrected melting point was 111.0-111.5 °C (lit. mp 110-113 °C).

Synthesis of 1,4,7,10-Tetraaza-*N,N',N''*-tris(3-sulfopropyl)-*N'''*-carboxymethylcyclododecane

As depicted in Scheme 6, the reaction of cyclen with 1,3-propanesultone afforded 1,4,7,10-tetraaza-*N,N',N''*-tris(3-sulfopropyl)cyclododecane (**20**). Cyclen free base was reacted for 44 h with 12 equiv of 1,3-propanesultone in refluxing dichloromethane containing 12 equiv of triethylamine. Compound **20** precipitated because of its insolubility in dichloromethane, preventing further reaction, and its identity was verified by MALDITOF MS. This intermediate

87

was then alkylated with bromoacetic acid in aqueous sodium hydroxide to form the desired

product, 1,4,7,10-tetraaza-N,N',N''-tris(3-sulfopropyl)-N'''-carboxymethylcyclododecane (**21**).

Scheme 6
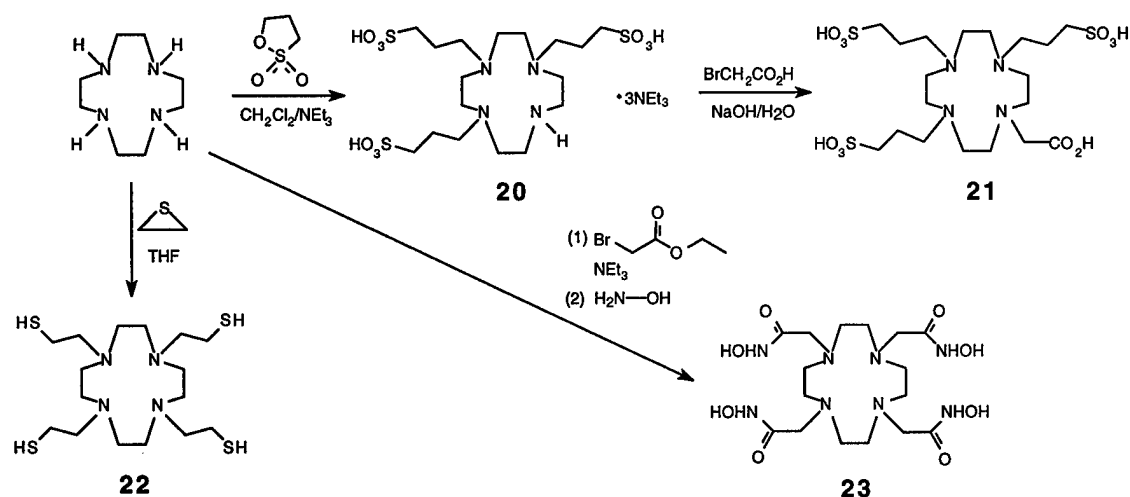
After evaporation of the solvent, the crude tris(3-sulfopropyl) derivative of cyclen was

triturated with benzene to remove excess 1,3-propanesultone, dissolved in aqueous sodium

hydroxide at pH 9.0, and reacted with excess sodium bromoacetate at 70-80 °C for 44 h,

maintaining the pH at 9.0 by periodic addition of sodium hydroxide. The MALDITOF mass

spectrum of the crude product confirmed the preparation of the desired compound, **21**.

The acetic acid group of compound **21** will allow water-soluble conjugation to mAbs via

the active ester reaction described above. Antibody conjugates of this novel chelator are expected

to undergo rapid and stable chelation of "hard," oxophilic radiometals on the basis of facile type I

complex formation. Unfortunately, compound **21** bound irreversibly to AG 1-X8 resin,

preventing its purification by strong anion-exchange chromatography. Present efforts to purify **21**

include crystallization and weak anion-exchange chromatography.

Synthesis of 1,4,7,10-Tetraazacyclododecane *N,N',N'',N'''*-tetraethanethiol

The tetraethanethiol derivative of 1,4,7,10-tetraazacyclododecane was synthesized in one step from cyclen and ethylene sulfide (Scheme 6). The reaction of cyclen free base with 5 equiv of ethylene sulfide was performed in refluxing tetrahydrofuran for 12 h. After removal of the solvent by rotary evaporation, analysis of the crude product by MALDITOF MS confirmed the preparation of 1,4,7,10-tetraazacyclododecane *N,N',N'',N'''*-tetraethanethiol (**22**), along with smaller amounts of thioether adducts. Work is in progress to optimize the conditions for this reaction and to purify the product by HPLC.

Compound **22** is expected to form extremely stable chelate complexes with all metal ions, including the oxo forms of Tc and Re. As a more hydrophobic chelating agent, this compound has good organic solubility, and it should be possible to purify it by reversed phase HPLC under ion pairing conditions. The tetraethanethiol compound will be conjugated to antibodies by reaction with 1 equiv of GMBS (*N*-γ-maleimidobutyryloxysuccinimide ester), followed by reversed phase HPLC purification and coupling to the ε-amino groups of mAb lysine residues.

Synthesis of 1,4,7,10-Tetraazacyclododecane *N,N',N'',N'''*-tetraacetohydroxamic acid

The planned synthesis of 1,4,7,10-tetraazacyclododecane *N,N',N'',N'''*-tetraacetohydroxamic acid (**23**), also depicted in Scheme 6, begins with the reaction of cyclen with an excess of ethyl bromoacetate and triethylamine in dichloromethane. The resulting tetraethyl ester of DOTA has been purified by flash chromatography on silica gel. This intermediate can be reacted with hydroxylamine to give the tetraacetohydroxamate product, **23**.

Compound **23** will be used as a model compound for metal ion binding studies, because antibody conjugation is not expected to be straightforward. Hydroxamic acid chelating agents have been used to prepare mAb conjugates radiolabeled with the oxo form of ^{99m}Tc (*98*). This chelation

chemistry could be improved and extended to include [186/188]Re radiolabeling as well, using macrocyclic acetohydroxamic acids derivatized for antibody conjugation.

Synthesis of 1,4,7,10-Tetraazacyclododecane *N*-(2-thioethyl)-*N'*,*N''*,*N'''*-tris(acetohydroxamic acid)

The synthesis of a triacetohydroxamic acid-monoacetohydrazide derivative of cyclen was originally proposed to allow orthogonal conjugation to periodate-oxidized carbohydrate on antibodies. However, because of the difficulties encountered in the carbohydrate conjugation of cT84.66 and ZCE025, a new strategy for synthesis of cyclen hydroxamate derivatives for conjugation to reduced interchain disulfide bonds of mAbs was devised (Scheme 7). Reaction of cyclen with 1 equiv of alkyl bromides in the absence of a base catalyst gives monosubstituted derivatives in high yields (*34*). Thus, reaction of cyclen free base with bromoethyl thiolacetate, prepared from ethylene dibromide and thiolacetic acid, should afford the hydrobromide salt of *N*-[2-(acetylthio)ethyl]-1,4,7,10-tetraazacyclododecane (**24**). Compound **24** is unreactive to further alkylation and can be purified by flash chromatography on silica gel. Reaction of **24** with excess ethyl bromoacetate and triethylamine will yield an acetylthioethyl-tris(ethyl acetate) intermediate. This intermediate can be reacted with hydroxylamine to introduce the hydroxamate groups, with concomitant deprotection of the thiol, to give product **25**. Compound **25** will then be conjugated to lightly reduced antibodies with a homobifunctional linker specific for thiols, such as 1,6-*bis*-maleimidohexane. In the case of MC-DOTA (**2**), this chelate-antibody linker system was shown to undergo hydrolysis at physiological temperature and pH, resulting in radiometal chelate release and improved tumor-to-blood ratios for [111]In- and ^{90}Y-labeled cT84.66.

Scheme 7

24   **25**
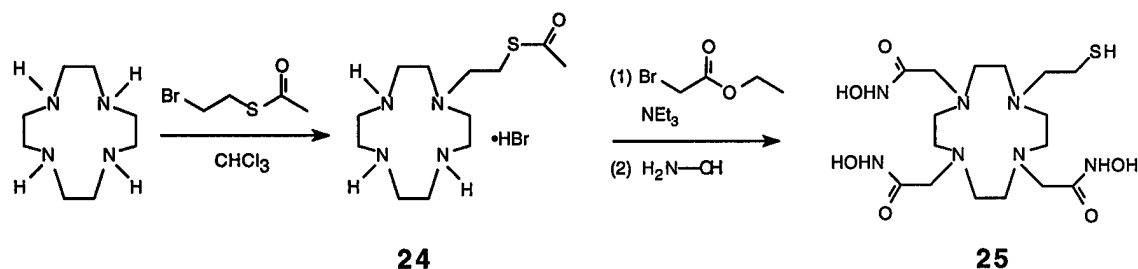
CONCLUSIONS

Maleimidocysteineamido-DOTA Derivatives

When MC-DOTA[Y(III)] (4) and MSC-DOTA[Y(III)] (12) were incubated in PBS at 37 °C, pH-dependent cleavage of the linker moiety occurred in both compounds. HPLC and ESI MS analysis of the reaction products revealed that MC-DOTA (2) and its yttrium chelate underwent imide bond hydrolysis, while MSC-DOTA (3) and its yttrium chelate decomposed by a β-elimination reaction involving the sulfone group. The decomposition of 2, 3, 4, and 12 occurred much faster at pH 7.4 than at pH 5.4, and neither yttrium compound showed any evidence of metal ion dissociation during the course of these reactions. Interestingly, MC-DOTA[Y(III)] showed a much slower rate of decomposition at pH 7.4 than the corresponding radiolabeled antibody conjugate, indicating that the protein also played a role in the decomposition reaction. Further evidence of the mAb's role in the decomposition of the MC-DOTA conjugate was provided by the modest, but significant, improvement in radiolabel stability upon alkylation of the unconjugated cysteines with iodoacetic acid.

In the case of MSC-DOTA and its Y(III) chelate, the same reaction products were generated in the same proportions at both pH values. The presence of chelated yttrium accelerated the elimination reaction 2- to 3-fold, indicating that the sulfone group is activated by the bound metal

ion. In contrast, imide bond hydrolysis of MC-DOTA was not significantly enhanced by chelated yttrium, but the profile of decomposition products depended on the pH of the reaction mixture. At pH 5.4, no products resulting from succinimide ring opening of MC-DOTA or its yttrium chelate were generated, although the cleavage product resulting from maleimide ring hydrolysis (5) was obtained in much greater yield than at pH 7.4. It could be argued that the maleimide ring of MC-DOTA is less stable to hydrolysis than the succinimide ring, causing it to open first to yield intermediate 9, which hydrolyzes further to generate compound 5 as the only observed cleavage product in this system. However, when MC-DOTA is conjugated to an antibody, the maleimide group is converted to a succinimide group. If the hydrolysis mechanism holds for the mAb conjugate, then loss of the radiolabel might occur by cleavage at one of the succinimide rings to release the radiometal chelate. Based on the HPLC results, this process would not be expected to occur to an appreciable degree at pH 5.4 but might occur at physiological pH. Maleimide ring opening (99) and succinimide ring opening on protein conjugates (100-106) have been observed or postulated to occur at pH > 7.5 in many other systems, but this is the first case in which succinimide ring cleavage may be responsible for release of a conjugated molecule from a protein.

Conjugation of kinetically stable radiometal chelates to monoclonal antibodies by means of a linker system that is chemically labile at physiological pH offers the possibility of imparting favorable biodistribution properties to the resulting radioimmunoconjugates. The serum studies of cT84.66-MSCDOTA suggested that this conjugate would probably exhibit an insufficient *in vivo* stability to be useful for tumor targeting with intact IgG. On the other hand, the *in vitro* serum half-life of cT84.66-MCDOTA was comparable to the biological half-life of radiolabeled IgGs in animal models and human subjects. Controlled hydrolysis of the linker between chelate and antibody might be expected to improve the clearance of radioactivity from normal organs and tissues, since the radiometal should be released in chelated form, and free chelates have been shown to clear by rapid urinary excretion (107-110).

In contrast, the increase in stability of the MC-DOTA linker and lack of succinimide hydrolysis at moderately acidic pH may have an important effect on the stability of the radiometal-

92

labeled antibody at the tumor site. The interstitial pH of solid tumors in both rodents and humans has been shown to be significantly lower than that of normal tissues (*111-119*); for reviews see (*120, 121*). The extracellular pH of malignant tissue has been measured in the range of 5.8-7.7, while normal tissues fall in the range of 7.0-8.1 (*120*). In general, tumors with a higher percentage of epithelial tissue are more acidic (*114*), and adenocarcinomas in particular fall in the lower ranges of extracellular pH, from 5.7 to 7.8 (*117*). Since the mAb cT84.66 recognizes the adenocarcinoma-associated antigen CEA and is not internalized upon binding, the increased stability of the MC-DOTA linker at moderately acidic pH may allow tumor uptake of the radiometal-labeled mAb to remain high. Biodistribution studies showed that [111]In- and ^{90}Y-labeled cT84.66-MCDOTA exhibited high tumor uptake, with improved blood clearance and low uptake in normal organs, in a nude mouse model of human colorectal adenocarcinoma.

The maleimidocysteineamido-DOTA derivatives described here allowed site-specific conjugation of macrocyclic radiometal chelates to reduced interchain disulfide bonds of antibodies. Compared to the conjugate prepared with an active ester of DOTA, cT84.66-MCDOTA showed increases in radiolabeling yields of 22-23% for ^{111}In and [90]Y. Using MC-DOTA, the goal of near-quantitative antibody labeling with both radiometals has been achieved. Immunoconjugates prepared with the two maleimidocysteineamido-DOTA derivatives exhibited linker-dependent loss of radiometal at physiological temperature and pH. This phenomenon has been attributed to imide bond hydrolysis for the sulfide compound MC-DOTA and to a β-elimination reaction in the case of the sulfone MSC-DOTA. It was found that the cleavage reactions were dramatically slower at moderately acidic pH. The use of such pH-dependent chemically labile linkers may be an important determinant of the *in vivo* distribution properties of antibody-radiometal chelate conjugates, based on the observed differences between the extracellular pH of solid tumors and that of normal tissues.

Hydrazido-DOTA Derivatives

It was unfortunate that all efforts to conjugate the hydrazido-DOTA derivatives to periodate-oxidized cT84.66 and ZCE025 were unsuccessful. When applied to cT84.66, the carbohydrate conjugation procedure caused a high degree of aggregation of the antibody. In addition to the problem of aggregation, both prelabeling and postlabeling attempts to modify cT84.66 with ^{90}Y and ^{111}In chelates resulted in low levels of radiometal incorporation. When the literature procedure for conjugation of ZCE025 with aminooxyacetyl desferrioxamine (*92*) was used for derivatization of that mAb with the hydrazido-DOTA compounds, no evidence for a successful reaction was obtained. However, the DOTA hydrazide analogs were reacted with oxidized ZCE025 at pH 6.0, as opposed to pH 4.0 in the case of the aminooxy BCA. Competing Schiff base formation with the antibody amino groups or the quench reagent 1,3-diaminopropan-2-ol may have prevented the coupling of the hydrazido-DOTA derivatives at pH 6.0. It is possible that conjugation at pH 4.0 or substitution of ethylene glycol for 1,3-diaminopropan-2-ol would lead to successful conjugation of oxidized ZCE025 with the hydrazide derivatives of DOTA.

One of the purposes for synthesizing the hydrazido-DOTA compounds and studying their reactions with carbohydrate-oxidized cT84.66 was to develop new reagents for site-specific conjugation of bioengineered "minibody" constructs. The 80-kDa cT84.66 minibody (*122*) allows new sequences for attachment of radiometal chelates, such as oligosaccharides or cysteine residues, to be engineered genetically into the C_H3 domain of the construct. Addition of glycosylation sites to the minibody would allow conjugation of DOTA hydrazide derivatives after carbohydrate oxidation of the mAb.

Leung and coworkers (*123*) were successful in engineering a unique glycosylation site into the framework-1 region of the light chain variable (Vκ) domain of the nonglycosylated, humanized anti-CEA mAb hMN-14. This approach allowed the F(ab')$_2$ fragment of the antibody to be conjugated efficiently with amino derivatives of DTPA. The conjugate labeled to high specific activity with ^{111}In and ^{90}Y without aggregation or loss of immunoreactivity. Reactivity and

stability to periodate oxidation are highly specific to individual glycoproteins. Thus, there is reason to expect that at least one of the carbohydrate-modified minibody constructs will exhibit efficient conjugation and radiometal labeling with the hydrazido-DOTA derivatives, while others may not. Furthermore, the glycosylation sites on the minibody will be placed on the exterior surface of the protein and will likely be more accessible to BCA conjugation and radiometal labeling.

Biodistributions

Figures 18-21 and Tables 8-11 (see Appendix) show that both the amide-linked cT84.66-DOTA conjugate and the cT84.66-MCDOTA conjugate, with its cleavable imide linker, demonstrate high tumor targeting in the LS174T nude mouse model. These results were consistent for both radiometals. At the 48 h time point, tumor uptake of the DOTA conjugate was between 3- and 5-fold greater than that of the normal tissue having the next highest accumulation (typically blood or liver). The MC-DOTA conjugate exhibited an approximate 7-fold difference between tumor and the highest normal tissue uptake at 48 h. Absolute magnitude of tumor uptake was between 50 and 70% ID/g for both conjugates. These values were comparable to those observed previously in the LS174T nude mouse model (65) for cT84.66 conjugated with a benzylisothiocyanate derivative of DTPA. Other xenograft data using the Lym-1 (25) and chimeric L6 (93) antibodies conjugated to DOTA derivatives have indicated maximum uptakes approaching only 17 and 18% ID/g, respectively. These lower values may be a result of differences in antibody-antigen affinity constants and/or xenograft models. Tumor masses were not specified in those earlier analyses; in these studies, the xenografts ranged from approximately 0.1 to 0.2 g at the 48 h time point.

Table 7 contains a summary of comparisons of the biodistribution data. It was seen that hepatic accumulation of ^{111}In was significantly greater than that of ^{90}Y when either BCA was coupled to cT84.66. Transchelation of indium by transferrin is one possible mechanism for

transport to the hepatocytes, but no evidence of this mechanism was found with either conjugate *in vitro* or *in vivo*. The kinetic stability studies of radiolabeled cT84.66-DOTA in human serum (*36*) showed that <1% of ^{111}In or ^{90}Y was converted to a low molecular weight species, possibly a result of hydrolytic (*25, 35*) or proteolytic cleavage of the chelate from the mAb. Even though MC-DOTA underwent a linker-specific cleavage reaction under physiological conditions, both released radiometals were found to associate with serum albumin and not with transferrin upon incubation in human serum at 37 °C, as described above.

Table 7. Summary of Biodistribution Comparisons

BCA or Radiometal	Number of common time points	Organ with significant difference (points/total)[a]	Times at which difference was significant with t-test	Uptake Result
DOTA	3	Liver (3/3)	48, 72, 96 h	^{111}In > ^{90}Y
MC-DOTA	7	Liver (N/A)[b]	N/A[b]	^{111}In > ^{90}Y
^{111}In	5	Blood (2/5)	18, 48 h	MC-DOTA < DOTA
		Kidney (2/5)	48, 96 h	DOTA < MC-DOTA
^{90}Y	2	Blood (2/2)	48, 96 h	MC-DOTA < DOTA

[a]Significant at $p < 0.05$.

[b]Significant difference was determined by concordance analysis.

Blood samples drawn from animals in this study were also analyzed by gel filtration HPLC. Radiolabeled mAb was the only radioactive species detected in the circulation of mice injected with cT84.66-DOTA (data not shown). Blood of animals receiving cT84.66-MCDOTA contained radiolabeled antibody and serum albumin, but the label associated with albumin cleared faster than the mAb (data not shown). It is possible that clearance of serum albumin played a role in hepatic uptake of radiometal from the MC-DOTA conjugate. However, the differences between ^{111}In and ^{90}Y were not dramatic and amounted to ≤5% ID/g increase with ^{111}In. Figure 23 shows

this clearly in the concordance analysis of cT84.66-MCDOTA. The difference between radiometal uptakes in hepatic tissues would have to be considered when estimating patient absorbed dose resulting from radioimmunotherapy. In that case, the indium biodistribution is used to predict the yttrium-induced absorbed dose. No other organ system studied showed such consistent disparity of uptake between the two radiolabels. A similar difference has been observed previously using DTPA benzylisothiocyanate as the BCA for ^{111}In and [90]Y (65).

For a given radiolabel, several differences were seen in these analyses with variation of the BCA. With indium, cT84.66-MCDOTA demonstrated less uptake in the blood at two of the five common time points. Renal accumulation, however, was found to be greater for the MC-DOTA conjugate at two of five time points. In the case of the [90]Y (Figure 24), blood clearance was increased by using the chemically labile MC-DOTA, a result similar to that found with [111]In. No significant differences in hepatic or bone uptakes were observed comparing ^{90}Y-labeled cT84.66-DOTA and cT84.66-MCDOTA.

Blood clearance kinetic analyses were consistent with biphasic curves for all combinations of radiometal and BCA (Table 6). The difference between the two half-times was almost two orders of magnitude, with the larger value being between 40 and 70 h. This $T_{1/2,2}$ was somewhat smaller than the comparable quantity observed by DeNardo et al. (93). This difference may not be significant, as no errors were quoted for their $T_{1/2,2}$ values. By comparing ^{90}Y data for the DOTA and MC-DOTA conjugates, it was shown that the latter BCA results in a generally lower blood clearance curve (Figure 24). This difference may have important consequences in bone marrow absorbed dose in a clinical situation.

The dominant source organ for bone marrow absorbed dose in patients cannot be predicted at this time. If it is assumed that murine data correspond to the human case, then it can be anticipated that both blood and bone will be substantial contributors. Both BCAs studied here exhibited substantially reduced bone uptake compared to the benzylisothiocyanato-DTPA chelate studied earlier (65). Thus, the use of a macrocycle can be generally justified for minimization of marrow dose arising from bone as a source organ. As noted above, skeletal uptake of yttrium was

comparable for both BCAs. If bone marrow radiation dose in human subjects proves to be dominated by circulating antibody, then selection of an optimal agent for RIT applications from these two BCAs may be accomplished on the basis of the murine blood clearance data. In that case, the statistically significant lower blood curves for cT84.66-MCDOTA could be a reason for selecting this conjugate for use in clinical trials.

REFERENCES

1. T. A. Waldmann, *Science (Washington, D.C.)* **252**, 1657 (1991).

2. O. A. Gansow, *Int. J. Radiat. Appl. Instrum. Part B Nucl. Med. Biol.* **18**, 369 (1991).

3. Y. Liu and C. Wu, *Pure Appl. Chem.* **63**, 427 (1991).

4. B. W. Wessels and R. D. Rogus, *Med. Phys.* **11**, 638 (1984).

5. W. Wolf and J. Shani, *Int. J. Radiat. Appl. Instrum. Part B Nucl. Med. Biol.* **13**, 319 (1986).

6. J. Schlom *et al.*, *Cancer Res.* **51**, 2889 (1991).

7. C. F. Meares, *Int. J. Radiat. Appl. Instrum. Part B Nucl. Med. Biol.* **13**, 311 (1986).

8. R. W. Kozak *et al.*, *Cancer Res.* **49**, 2639 (1989).

9. R. M. Sharkey, C. Motta-Hennessy, D. Pawlyk, J. A. Siegel, D. M. Goldenberg, *Cancer Res.* **50**, 2330 (1990).

10. C. F. Meares *et al.*, *Anal. Biochem.* **142**, 68 (1984).

11. D. J. Hnatowich *et al.*, *Science (Washington, D.C.)* **220**, 613 (1983).

12. D. J. Hnatowich, R. L. Childs, D. Lanteigne, A. Najafi, *J. Immunol. Methods* **65**, 147 (1983).

13. S. E. Halpern *et al.*, *Cancer Res.* **43**, 5347 (1983).

14. R. G. Buckley and F. Searle, *FEBS Lett.* **166**, 202 (1984).

15. R. J. Paxton *et al.*, *Cancer Res.* **45**, 5694 (1985).

16. M. W. Brechbiel *et al.*, *Inorg. Chem.* **25**, 2772 (1986).

17. D. A. Westerberg, P. L. Carney, P. E. Rogers, S. J. Kline, D. K. Johnson, *J. Med. Chem.* **32**, 236 (1989).

18. M. K. Moi, C. F. Meares, M. J. McCall, W. C. Cole, S. J. DeNardo, *Anal. Biochem.* **148**, 249 (1985).

19. M. K. Moi, C. F. Meares, S. J. DeNardo, *J. Am. Chem. Soc.* **110**, 6266 (1988).

20. J. P. L. Cox *et al.*, *J. Chem. Soc., Chem. Commun.* 797 (1989).

21. A. S. Craig *et al.*, *J. Chem. Soc., Chem. Commun.* 794 (1989).

22. D. Parker, J. R. Morphy, K. Jankowski, J. Cox, *Pure Appl. Chem.* **61**, 1637 (1989).

23. J. P. L. Cox *et al.*, *J. Chem. Soc. Perkin Trans. 1* 2567 (1990).

24. J. R. Morphy *et al.*, *J. Chem. Soc. Perkin Trans. 2* 573 (1990).

25. S. V. Deshpande *et al.*, *J. Nucl. Med.* **31**, 473 (1990).

26. M. K. Moi, S. J. DeNardo, C. F. Meares, *Cancer Res. (Suppl.)* **50**, 789s (1990).

27. C. F. Meares *et al.*, *Br. J. Cancer* **62**, Suppl. X, 21 (1990).

28. C. L. Ruegg *et al.*, *Cancer Res.* **50**, 4221 (1990).

29. P. M. Smith-Jones *et al.*, *Bioconjugate Chem.* **2**, 415 (1991).

30. S. J. Kline, D. A. Betebenner, D. K. Johnson, *Bioconjugate Chem.* **2**, 26 (1991).

31. T. J. McMurry, M. Brechbiel, K. Kumar, O. A. Gansow, *Bioconjugate Chem.* **3**, 108 (1992).

32. O. Renn and C. F. Meares, *Bioconjugate Chem.* **3**, 563 (1992).

33. A. Smith *et al.*, *Cancer Res.* **53**, 5727 (1993).

34. W. J. Kruper, Jr., P. R. Rudolf, C. A. Langhoff, *J. Org. Chem.* **58**, 3869 (1993).

35. M. Li and C. F. Meares, *Bioconjugate Chem.* **4**, 275 (1993).

36. M. R. Lewis, A. Raubitschek, J. E. Shively, *Bioconjugate Chem.* **5**, 565 (1994).

37. M. Li *et al.*, *Bioconjugate Chem.* **5**, 101 (1994).

38. M. F. Loncin, J. F. Desreux, E. Merciny, *Inorg. Chem.* **25**, 2646 (1986).

39. W. P. Cacheris, S. K. Nickle, A. D. Sherry, *Inorg. Chem.* **26**, 958 (1987).

40. K. Kumar, M. Magerstädt, O. A. Gansow, *J. Chem. Soc., Chem. Commun.* 145 (1989).

41. C. J. Broan *et al.*, *J. Chem. Soc. Perkin Trans. 2* 87 (1991).

42. E. T. Clarke and A. E. Martell, *Inorg. Chim. Acta* **190**, 27 (1991).

43. E. T. Clarke and A. E. Martell, *Inorg. Chim. Acta* **190**, 37 (1991).

44. M. Kodama, T. Koike, A. B. Mahatma, E. Kimura, *Inorg. Chem.* **30**, 1270 (1991).

45. M. W. Brechbiel *et al.*, *J. Chem. Soc., Chem. Commun.* 1169 (1991).

46. S. P. Kasprzyk and R. G. Wilkins, *Inorg. Chem.* **21**, 3349 (1982).

47. X. Wang *et al.*, *Inorg. Chem.* **31**, 1095 (1992).

48. C. Motta-Hennessy, R. M. Sharkey, D. M. Goldenberg, *J. Nucl. Med.* **31**, 1510 (1990).

49. B. E. Rogers *et al.*, *Bioconjugate Chem.* **7**, 511 (1996).

50. P. L. Jones, B. A. Brown, H. Sands, *Cancer Res. (Suppl.)* **50**, 852s (1990).

51. C. H. Paik *et al.*, *Int. J. Radiat. Appl. Instrum. Part B Nucl. Med. Biol.* **19**, 517 (1992).

52. B. E. Rogers *et al.*, *Cancer Res. (Suppl.)* **55**, 5714s (1995).

53. J. R. Duncan and M. J. Welch, *J. Nucl. Med.* **34**, 1728 (1993).

54. F. N. Franano, W. B. Edwards, M. J. Welch, J. R. Duncan, *Int. J. Radiat. Appl. Instrum. Part B Nucl. Med. Biol.* **21**, 1023 (1994).

55. C. F. Meares, M. J. McCall, S. V. Deshpande, S. J. DeNardo, D. A. Goodwin, *Int. J. Cancer Suppl. 2* 99 (1988).

56. C. H. Paik *et al.*, *J. Nucl. Med.* **30**, 1693 (1989).

57. R. W. Weber, R. H. Boutin, M. A. Nedelman, J. Lister-James, R. T. Dean, *Bioconjugate Chem.* **1**, 431 (1990).

58. Y. Arano *et al.*, *Bioconjugate Chem.* **7**, 628 (1996).

59. P. Gold and S. O. Freedman, *J. Exp. Med.* **121**, 439 (1965).

60. J. E. Shively and J. D. Beatty, *Crit. Rev. Oncol. Hematol.* **2**, 355 (1985).

61. J. M. Esteban, R. Paxton, P. Mehta, H. Battifora, J. E. Shively, *Hum. Pathol.* **24**, 322 (1993).

62. J. M. Esteban *et al.*, *Cancer* **74**, 1575 (1994).

63. R. Colomer, A. Ruibal, L. Salvador, *Cancer* **64**, 1674 (1989).

64. M. Neumaier *et al.*, *Cancer Res.* **50**, 2128 (1990).

65. L. E. Williams *et al.*, *Tumor Targeting* **2**, 116 (1996).

66. J. M. Esteban *et al.*, *Oncol. Reports* **2**, 237 (1995).

67. J. Y. C. Wong *et al.*, *J. Nucl. Med.* **38**, 1951 (1997).

68. P. Riva, G. Moscatelli, G. Paganelli, S. Benini, A. Siccardi, *Int. J. Cancer Suppl. 2* 114 (1988).

69. P. Lind *et al.*, *Int. J. Cancer* **47**, 865 (1991).

70. D. M. Hyams, J. M. Esteban, B. G. Beatty, P. M. Wanek, J. D. Beatty, *Arch. Surg.* **124**, 175 (1989).

71. R. R. Buras *et al.*, *Arch. Surg.* **125**, 660 (1990).

72. B. A. Morton, B. G. Beatty, A. P. Mison, P. M. Wanek, J. D. Beatty, *Cancer Res. (Suppl.)* **50**, 1008s (1990).

73. J. Y. C. Wong *et al.*, *Cancer Res. (Suppl.)* **55**, 5929s (1995).

74. R. E. Thiers, *Methods Biochem. Anal.* **5**, 273 (1957).

75. P. R. P. Salacinski, C. McLean, J. E. C. Sykes, V. V. Clement-Jones, P. J. Lowry, *Anal. Biochem.* **117**, 136 (1981).

76. J. E. Coligan, J. T. Lautenschleger, M. L. Egan, C. W. Todd, *Immunochemistry* **9**, 377 (1972).

77. H. S. Slayter and J. E. Coligan, *Cancer Res.* **36**, 1696 (1976).

78. K. Takenouchi, K. Watanabe, Y. Kato, T. Koike, E. Kimura, *J. Org. Chem.* **58**, 1955 (1993).

79. K. Takenouchi *et al.*, *J. Org. Chem.* **58**, 6895 (1993).

80. T. Wieland, E. Bokelmann, L. Bauer, H. U. Lang, H. Lau, *Ann. Chem. Liebigs* **583**, 129 (1953).

81. P. E. Dawson, T. W. Muir, I. Clark-Lewis, S. B. H. Kent, *Science (Washington, D.C.)* **266**, 776 (1994).

82. B. M. Trost and D. P. Curran, *Tetrahedron Lett.* **22**, 1287 (1981).

83. D. Willner *et al.*, *Bioconjugate Chem.* **4**, 521 (1993).

84. G. L. Ellman, *Arch. Biochem. Biophys.* **74**, 443 (1958).

85. P. W. Riddles, R. L. Blakeley, B. Zerner, *Anal. Biochem.* **94**, 75 (1979).

86. D. L. Kukis *et al.*, *Cancer Res.* **55**, 878 (1995).

87. J. B. Stimmel, M. E. Stockstill, F. C. Kull, *Bioconjugate Chem.* **6**, 219 (1995).

88. R. S. Greenfield *et al.*, *Cancer Res.* **50**, 6600 (1990).

89. G. R. Braslawsky, M. A. Edson, W. Pearce, T. Kaneko, R. S. Greenfield, *Cancer Res.* **50**, 6608 (1990).

90. C. M. Haskell, F. Buchegger, M. Schreyer, S. Carrel, J.-P. Mach, *Cancer Res.* **43**, 3857 (1983).

91. J. E. Shively, R. J. Paxton, T. D. Lee, *Trends Biochem. Sci.* **14**, 246 (1989).

92. S. Pochon *et al.*, *Int. J. Cancer* **43**, 1188 (1989).

93. S. J. DeNardo *et al.*, *J. Nucl. Med.* **36**, 829 (1995).

94. A. Harrison *et al.*, *Int. J. Radiat. Appl. Instrum. Part B Nucl. Med. Biol.* **18**, 469 (1991).

95. L. I.-K. Lin, *Biometrics* **45**, 255 (1989).

96. D. Z. D'Argenio and A. Schumitzky, *Comput. Prog. Biomed.* **9**, 115 (1979).

97. T. J. Atkins, J. E. Richman, W. F. Oettle, *Org. Syn.* **58**, 86 (1978).

98. A. Safavy, D. J. Buchsbaum, M. B. Khazaeli, *Bioconjugate Chem.* **4**, 194 (1993).

99. J. D. Gregory, *J. Am. Chem. Soc.* **77**, 3922 (1955).

100. C.-W. Wu, L. R. Yarbrough, F. Y.-H. Wu, *Biochemistry* **15**, 2863 (1976).

101. S. L. Betcher-Lange and S. S. Lehrer, *J. Biol. Chem.* **253**, 3757 (1978).

102. B. Lux and D. Gérard, *J. Biol. Chem.* **256**, 1767 (1981).

103. Y. Ishii and S. S. Lehrer, *Biophys. J.* **50**, 75 (1986).

104. M. A. Griep and C. S. McHenry, *J. Biol. Chem.* **265**, 20356 (1990).

105. M. A. Griep and T. N. Mesman, *Bioconjugate Chem.* **6**, 673 (1995).

106. M. Eisenhut *et al.*, *J. Nucl. Med.* **37**, 362 (1996).

107. H. S. Winchell, M. Pollycove, W. D. Loughman, J. H. Lawrence, *Blood* **23**, 44 (1964).

108. H. S. Winchell, M. Pollycove, A. C. Andersen, J. H. Lawrence, *Blood* **23**, 321 (1964).

109. M.-M. Le Mignon, C. Chambon, S. Warrington, R. Davies, B. Bonnemain, *Invest. Radiol.* **25**, 933 (1990).

110. R. W. Katzberg *et al.*, *Invest. Radiol.* **26**, S129 (1991).

111. B. S. Ashby, M. B. Cantab., *Lancet* **2**, 312 (1966).

112. A. P. van den Berg, J. L. Wike-Hooley, A. E. van den Berg-Blok, J. van der Zee, H. S. Reinhold, *Eur. J. Cancer Clin. Oncol.* **18**, 457 (1982).

113. J. L. Wike-Hooley, A. P. van den Berg, J. van der Zee, H. S. Reinhold, *Eur. J. Cancer Clin. Oncol.* **21**, 785 (1985).

114. F. Kallinowski and P. Vaupel, *Br. J. Cancer* **58**, 314 (1988).

115. L. E. Gerweck, J. G. Rhee, J. A. Koutcher, C. W. Song, M. Urano, *Radiat. Res.* **126**, 206 (1991).

116. G. R. Martin and R. K. Jain, *Cancer Res.* **54**, 5670 (1994).

117. K. Engin *et al.*, *Int. J. Hyperthermia* **11**, 211 (1995).

118. C. L. McCoy *et al.*, *Br. J. Cancer* **72**, 905 (1995).

119. L. E. Gerweck and K. Seetharaman, *Cancer Res.* **56**, 1194 (1996).

120. J. L. Wike-Hooley, J. Haveman, H. S. Reinhold, *Radiother. Oncol.* **2**, 343 (1984).

121. I. F. Tannock and D. Rotin, *Cancer Res.* **49**, 4373 (1989).

122. S.-z. Hu *et al.*, *Cancer Res.* **56**, 3055 (1996).

123. S.-o. Leung *et al.*, *J. Immunol.* **154**, 5919 (1995).

APPENDIX:

Tables of Mean Percent Injected Dose per Gram (% ID/g) with Standard Errors (SE) of ^{111}In- and ^{90}Y-Labeled cT84.66-DOTA and cT84.66-MCDOTA for All Tissues and Time Points Evaluated

Table 8. Mean percent injected dose per gram of tissue (% ID/g) for ^{111}In-labeled cT84.66-DOTA in LS174T tumor-bearing nude mice. Standard errors (SE) are given in parentheses; all data were corrected for radiodecay.

Organ	0 h	4 h	18 h	48 h	72 h	96 h
Blood	34.3 (6.9)	25.4 (2.8)	23.5 (4.8)	11.2 (0.2)	8.56 (2.2)	9.09 (1.3)
Liver	10.0 (0.7)	7.40 (0.8)	8.54 (1.3)	11.5 (1.6)	13.4 (2.4)	11.6 (2.0)
Spleen	6.00 (0.8)	6.16 (1.1)	7.11 (1.6)	5.91 (1.0)	8.06 (0.8)	7.82 (0.6)
Kidney	5.93 (1.5)	7.51 (0.2)	7.86 (1.6)	5.30 (0.3)	4.72 (1.1)	4.29 (0.3)
Lung	18.4 (1.5)	11.8 (1.6)	13.0 (3.4)	5.52 (0.4)	3.79 (1.2)	4.59 (0.5)
Bowel	1.30 (0.1)	2.70 (0.3)	2.20 (0.3)	1.50 (0.1)	1.19 (0.2)	1.14 (0.02)
Bone	2.30 (0.2)	3.05 (0.1)	3.32 (0.9)	1.86 (0.1)	1.64 (0.3)	1.66 (0.1)
Tumor	3.89 (0.1)	16.7 (2.0)	51.9 (10.6)	57.6 (6.7)	50.4 (6.0)	69.4 (2.6)
Carcass	2.28 (0.3)	3.00 (0.2)	3.10 (0.3)	2.60 (0.2)	1.60 (0.3)	2.10 (0.2)
Tumor mass (mg)	58 (4)	83 (26)	153 (28)	258 (51)	360 (44)	232 (45)
No. of animals	3	4	4	4	4	4

Table 9. Mean percent injected dose per gram of tissue (% ID/g) for ^{90}Y-labeled cT84.66-DOTA in LS174T tumor-bearing nude mice. Standard errors (SE) are given in parentheses; all data were corrected for radiodecay.

Organ	0.75 h	6 h	24 h	48 h	72 h	96 h
Blood	41.3 (6.2)	27.7 (1.12)	22.5 (1.1)	21.2 (1.7)	12.0 (1.0)	11.3 (1.0)
Liver	7.42 (0.9)	5.37 (0.2)	4.41 (0.3)	5.13 (0.3)	3.71 (0.3)	6.11 (0.9)
Spleen	5.74 (1.0)	5.20 (0.3)	5.63 (0.4)	7.82 (0.6)	7.82 (1.5)	6.12 (1.1)
Kidney	7.50 (1.0)	6.02 (0.3)	5.88 (0.6)	6.10 (0.2)	4.60 (0.2)	4.68 (0.4)
Bone	1.97 (0.4)	1.90 (0.5)	1.86 (0.1)	1.39 (0.3)	1.42 (0.3)	1.07 (0.1)
Tumor	7.57 (0.8)	17.2 (1.1)	57.4 (3.8)	65.9 (16.2)	55.0 (6.5)	64.0 (10.0)
Carcass	2.72 (0.1)	2.70 (0.1)	2.58 (0.1)	2.87 (0.1)	2.28 (0.1)	2.10 (0.1)
Tumor mass (mg)	79 (26)	45 (10)	64 (8)	74 (27)	71 (8)	85 (4)
No. of animals	4	4	4	4	4	4

Table 10. Mean percent injected dose per gram of tissue (% ID/g) for ^{111}In-labeled cT84.66-MCDOTA in LS174T tumor-bearing nude mice. Standard errors (SE) are given in parentheses; all data have been corrected for radiodecay.

Organ	0 h	4 h	12 h	18 h	48 h	96 h	120 h
Blood	34.9 (4.3)	21.1 (3.4)	25.3 (5.2)	12.4 (1.4)	9.98 (0.3)	8.16 (0.3)	2.00 (0.7)
Liver	8.22 (0.5)	7.44 (0.6)	7.31 (0.8)	5.93 (0.4)	9.54 (2.2)	7.56 (1.2)	10.9 (1.1)
Spleen	7.00 (0.7)	7.41 (0.5)	9.08 (1.1)	5.34 (0.5)	8.87 (1.6)	6.89 (1.0)	9.86 (1.9)
Kidney	9.04 (0.9)	7.74 (0.4)	9.42 (1.2)	7.05 (0.4)	7.63 (0.6)	6.83 (0.2)	4.64 (0.4)
Lung	19.0 (2.0)	16.8 (1.2)	12.7 (1.5)	9.84 (0.8)	6.73 (1.4)	3.98 (0.2)	1.35 (0.3)
Bowel	1.80 (0.3)	2.69 (0.2)	2.61 (0.3)	2.05 (0.1)	1.70 (0.2)	1.05 (0.1)	0.48 (0.1)
Bone	1.90 (0.3)	2.22 (0.1)	2.38 (0.2)	1.64 (0.1)	1.82 (0.1)	1.70 (0.2)	1.20 (0.1)
Tumor	3.44 (0.2)	24.3 (3.5)	43.5 (4.2)	45.8 (5.8)	67.8 (5.0)	48.8 (9.5)	38.5 (5.1)
Carcass	2.42 (0.1)	3.01 (0.1)	3.89 (0.4)	3.33 (0.2)	2.45 (0.2)	1.86 (0.1)	1.00 (0.2)
Tumor mass (mg)	46 (8)	120 (33)	110 (31)	140 (49)	196 (49)	180 (37)	372 (51)
No. of animals	5	5	5	5	5	5	5

Table 11. Mean percent injected dose per gram of tissue (% ID/g) for ^{90}Y-labeled cT84.66-MCDOTA in LS174T tumor-bearing nude mice. Standard errors (SE) are given in parentheses; all data were corrected for radiodecay.

Organ	0 h	4 h	12 h	18 h	48 h	96 h	120 h
Blood	34.7 (4.2)	20.2 (3.3)	24.1 (5.0)	14.4 (1.6)	8.83 (0.2)	6.93 (0.4)	1.70 (0.6)
Liver	8.86 (0.5)	8.25 (1.2)	9.87 (1.1)	4.53 (1.1)	7.75 (1.0)	8.42 (0.8)	9.30 (1.7)
Bone	1.91 (0.3)	1.97 (0.1)	2.17 (0.2)	1.44 (0.1)	1.51 (0.1)	1.28 (0.2)	0.95 (0.1)
Tumor	2.34 (0.3)	18.8 (5.4)	40.9 (4.2)	31.1 (4.8)	62.8 (3.6)	42.2 (7.9)	36.7 (3.8)
Tumor mass (mg)	46 (8)	120 (33)	110 (31)	140 (49)	196 (49)	180 (37)	372 (58)
No. of animals	5	5	5	5	5	5	5

BIBLIOGRAPHY

1.   Lewis, M. R., Bebb, G., Bui, A., Raubitschek, A., and Shively, J. E., Site-Specific Conjugation of a Maleimidocysteinyl-DOTA Derivative to Hinge Region Sulfhydryl Groups of an Anti-Carcinoembryonic Antigen Antibody [abstract]. 212th American Chemical Society National Meeting, Orlando, FL, August 1996.

2.   Wu, A. M., Williams, L. E., Yazaki, P. J., Sherman, M., Lewis, M. R., Shively, J. E., Wong, J. Y. C., and Raubitschek, A. A., Engineered Anti-CEA Fragments: Selection of Optimal Imaging Agents [abstract]. The Fourteenth International Conference on Advances in the Applications of Monoclonal Antibodies in Clinical Oncology, Santorini, Greece, May 1997.

3.   Lewis, M. R., Williams, L. E., Bebb, G. G., Clarke, K., Odom-Maryon, T. L., Raubitschek, A. A., and Shively, J. E., Evaluation of Macrocyclic Radiometal Chelates Conjugated to Hinge Region Sulfhydryl Groups of an Anti-Carcinoembryonic Antigen Antibody [abstract]. The Department of Defense Breast Cancer Research Program Meeting: Era of Hope, Washington, DC, October 1997.

4.   Yazaki, P. J., Sherman, M., Lewis, M. R., Shively, J., and Wu, A. M., Engineering and Expression of Site-Specific Cysteine Mutations for Radiolabeling an Anti-CEA T84.66 Minibody (scFv-CH3) [abstract]. Eighth Annual International Conference on Antibody Engineering, San Diego, CA, December 1997.

5.   Lewis, M. R., and Shively, J. E., Maleimidocysteineamido-DOTA Derivatives: New Reagents for Radiometal Chelate Conjugation to Antibody Sulfhydryl Groups Undergo pH-Dependent Cleavage Reactions. *Bioconjugate Chem.* 9: 72-86, 1998.

6.   Williams, L. E., Lewis, M. R., Bebb, G. G., Clarke, K. G., Odom-Maryon, T. L., Shively, J. E., and Raubitschek, A. A., Biodistribution of [111]In- and ^{90}Y-Labeled DOTA and Maleimidocysteineamido-DOTA Conjugated to Chimeric Anti-Carcinoembryonic Antigen Antibody in Xenograft-Bearing Nude Mice: Comparison of Stable and Chemically Labile Linker Systems. *Bioconjugate Chem.* 9: 87-93, 1998.

PERSONNEL

Michael R. Lewis   100% effort